EXPERIMENTAL INVESTIGATION OF UNBONDED MAGNETIC ABRASIVE POLISHING (UMAP) OF SILICON NITRIDE BALLS

By

ANAND UPLAONKAR

Bachelor of Engineering

P.D.A College of Engineering

Gulbarga University

Gulbarga, India

1999

Submitted to the Faculty of the
Graduate College of the
Oklahoma State University
in partial fulfillment of
the requirements for
the Degree of
MASTER OF SCIENCE
December, 2005

EXPERIMENTAL INVESTIGATION OF UNBONDED MAGNETIC ABRASIVE POLISHING (UMAP) OF SILICON NITRIDE BALLS

Thesis Approved:

Dr. Ranga Komanduri
Thesis Advisor

Dr. Hongbing Lu

Dr. R.D. Delahoussaye

Dr. A. Gordon Emslie
Dean of the Graduate College

SUMMARY

Development of new, harder, and tougher workmaterials has lead to the development of new machining processes and machine tools. One such material is silicon nitride (Si_3N_4) which falls under advanced ceramics group. Compared to bearing steel, silicon nitride has higher stiffness, higher operating temperature, and greater chemical stability. It also has higher hardness and lower density. Hence, silicon nitride balls are considered as suitable candidate for hybrid bearing applications which meets high-temperature and high speed operating conditions. However, its application has been limited due to expensive finishing cost and longer processing time. Hence, it becomes important to develop new polishing equipments and processes which can reduce the finishing costs and processing times.

In this investigation, a new experimental setup has been designed and a new process known as unbonded magnetic abrasive polishing (UMAP) was developed. The process works on the combination of underling principles of the following techniques 1) magnetic float polishing (MFP), 2) magnetic abrasive finishing (MAF), and 3) V-groove lapping.

UMAP process utilizes a mixture of loose iron particles and abrasives grits, known as, unbonded magnetic abrasive (UMA) and mixture of water and

glycerin as carrier fluid, know as, non-magnetic fluid (NMF) [Chang and Childs, 1998].

Most of the components utilized in UMAP apparatus were similar to that of MFP, except for 1) use of a lathe instead of a milling machine, 2) use of UMA instead of loose abrasive, 3) use of NMF instead of magnetic fluid, and 4) use of mechanical compression spring instead of magnetic buoyancy force to provide the desired polishing load.

UMAP consist of a polishing chamber with two inlet openings at 1.5 in. apart. It was mounted on a lathe using the four-jaw chuck. Polishing plate was placed inside the chamber. It was supported by the spring and rotated by the lathe head stock. Balls to be polished were loaded between the polishing plate and the spindle through the first inlet. Polishing spindle was rotated by an external motor mounted on the carriage of the lathe. Load was then applied by forcing spindle against the plate. The end of the chamber was sealed and the magnetic field was created around the small area know as the polishing zone. UMA, NMF along with a rust inhibitor were introduced in the chamber through second inlet of the chamber. Finally both the inlets were sealed with rubber corks.

Due to magnetic action, the mixture of UMA and NMF are concentrated at the polishing zone in such a way that loose abrasive grits are available to embed in the spindle. Polishing was carried out by the rotating spindle and the plate in opposite directions and at different speeds. Ball material was removed due to the

relative motion of the worksurface and the abrasive between the spindle and the plate.

An integrated approach is used for the development of UMAP technology involving 1) design and development of the experimental apparatus, 2) magnetic field analysis, 3) fundamental studies to determine optimum polishing condition, and 4) complete process modeling.

The UMAP equipment design started primarily with the understanding of design data provided for MFP by Raghunandan [1997]. It was important to generate uniform magnetic field around the working zone. To determine the lay out of magnets, FEM analysis of magnetic field was carried out using COMSOL 3.2 Multiphysics FEM software. Best magnetic flux distribution of 0.25 – 0.3 Tesla was obtained using 14 magnets of ½ in^3 each. N and S poles of magnets were arranged alternately on the inner surface of a 5-in. ID steel pipe with spacer a between them. Diameters of the polishing plate and the spindle were determined based on ball diameter and batch size. Finally, chamber length was decided depending on the spring dimensions.

Parametric tests were conducted to determine the effect of input parameters (magnetic field, spindle speed, plate speed, polishing duration, and abrasive type and size) on output parameters (material removal rate, sphericity and surface finish). Based on this experimental work, spindle speed, and wear on the shaft were identified as the key parameters effecting sphericity. Similarly, taper angel was found to be the key parameter effecting surface finish.

During polishing process a groove is formed on the bevel of the spindle. This groove plays an important role in improving sphericity and maintaining accuracy of alignment. Hence, this groove is kept intact until the batch of balls was completely polished. Sphericity value as low as 0.5 μm and surface finish value in the range of 10.4 -12.5 nm and average Material Removal Rate (MRR) of 1 μm/min/ball was achieved.

The methodology for finishing Si_3N_4 balls by UMAP consists of mechanical polishing followed by chemo-mechanical polishing. Boron carbide (B_4C), silicon carbide (SiC), and cerium oxide (CeO_2) are the abrasives used in this investigation [Jiang, 1998d].

Three distinct polishing patterns similar to MFP were identified. First stage known as the initial roughing stage emphasizes on the material removal rate (MRR) and sphericity improvement (range of 1-3 μm). Second stage was an intermediate semi-finishing stage to control sphericity and improve surface roughness. Finally the third stage known as finishing stage results in good surface finish and sphericity using chemo-mechanical action as proposed by Jiang*et. al.* [1998b].

ACKNOWLEDGEMENTS

I would like to express my heartfelt thanks to my advisor, Dr. R. Komanduri, for his guidance, encouragement, advice, and for financial support throughout my Master's program. I would like to show my sincere appreciation to Dr. H. B. Lu and Dr. R. D. Delahoussaye for serving on my graduate advisory committee. I would also thank Dr. N. Umehara for useful discussions.

This project was funded by a grant (DMI-0000079) from the Manufacturing Processes and Machines Program of the Division of the Design, Manufacture, and Industrial Innovation (DMII) of the National Science Foundation. The author thanks Drs. W. Devries, G. Hazelrigs, J. Cao, Delcie Durham of DMII and Dr. J. Larsen Basse of the Tribology and Surface Engineering Program for their interest in and support of this work.

I would like to thank Mr. Takiro Inoue for friendship and helpful conversations. Special thanks are due to Mr. Jerry Dale for his helpful discussions during design and fabrication of the apparatus. I would also like to extend my gratitude to Hariprasad, Lee, Madhan, Raju, Surya, Milind, Mallikarjun Mudiam, Sony and all the members of our research group for their support and friendship.

I am indebted to my parents, Mr. Shivasharanappa. T. Uplaonkar, Mrs. Vijaylaxmi, brother Vinod, sister Apporva and other members of uplaonkar family (Mrs. Ambabai, Mr. Shishupal, Mrs. Sharda and Ramu) and relatives who were always encouraging me. Without them, I would have not come this far. My sincere thanks are due to Mr. Sailesh Mishra for his support and friendship.

Finally, I would like to thank the Department of Mechanical and Aerospace Engineering for providing the opportunity to pursue my M.S. at Oklahoma State University.

TABLE OF CONTENTS

LIST OF TABLES

LIST OF FIGURES

CHAPTER 1

INTRODUCTION

1.1 BACKGROUND

Advanced ceramics provide high performance, cost-effective alternative solutions compared to traditional materials such as metals, polymers, and glass. In general terms, advanced ceramics offers unique and excellent properties that make them highly resistant to temperatures, bending, stretching, corrosion or wear. Their hardness, physical stability, high heat resistance, chemical inertness, biocompatibility, superior electrical properties make them one of the most versatile groups of materials in the world [Morgan Advanced Ceramics website]. Today, there are a wide range of advanced ceramics, including, alumina, zirconia, silicon nitride, silicon carbide, steatite, cordierite and many, many more - each with their own particular performance characteristics and benefits.

The demand for improved service life and higher thrust-to-weight ratio of rolling contact bearing elements for high-speed or high DN conditions (where DN is a severity indicator and is equals the bearing bore diameter in millimeters times shaft rotational speed in rpm) [Reddecliff and Valori, 1976], high-temperature and corrosive environment applications has been sharply increasing in the last two decades.

Advanced ceramics have come up as alternative materials that can overcome the drawbacks of traditional bearing ball materials, such as AISI 52100 or M50 high-speed steel.

Among all the advanced ceramics, silicon nitride (Si_3N_4) has become an exceptional candidate for bearing application due to its numerous superior properties. These properties include higher elastic modulus (higher stiffness), higher hardness and wear resistance, lower density, higher thermal and chemical resistance, creep resistance, higher fracture toughness compared to other advanced ceramics, oxidant resistance, not wetted by molten metals, and reduced need for lubrication [Morgan Advanced Ceramics website]. Table 1.1 [Katz and Hannoosh, 1987, Jaing, 1998] provides a detailed comparison of properties and failure modes of silicon nitride with other advanced ceramics and conventional bearing steel materials. An advanced ceramic is not suited for bearing races due to its low tensile strength but due to its higher compressive strength. It is found suitable for bearing balls. Also, it was found to be inappropriate to use all ceramic bearing due to difference in the thermal expansion coefficient between the ceramic inner race and the metal driven shaft. Hence steel bearing races with ceramic balls make a good combination, so as to avoid the possibility of micro welding or adhesive failure between the two. Since ceramic balls and steel race are of different metallurgy, the possibility of adhesion can be eliminated.

Among the advanced ceramics, ZrO_2 and Si_3N_4 have a close fracture toughness value, but Si_3N_4 is 45% less dense that ZrO_2. Hence, HIP- Si_3N_4 wins

over ZrO_2 as far as bearing balls material is concerned. When compared with the bearing steel, Si_3N_4 is 60% less dense and its higher modulus and hardness makes it suitable material for ball bearings. Due to its lower density, a Si_3N_4 ball reduces the gyroscopic slip and centrifugal loading on the outer steel race.

Table 1.1 - Properties of Some Advanced Ceramics and Bearing Steel [after Katz and Hannoosh, 1987, Jaing, 1998]

	Si_3N_4	B_4C	SiC	Al_2O_3	ZrO_2	Bearing Steel
Density g/cm^3	3.24	2.52	3.06	3.78	5.9	7.85
Young's Modulus GPa	314	448	410	360	200	200
Hardness (Hv10kg) GPa	16	28	24	22	12.5	7
Flexural Strength MPa	700	300	450	240	500	2500
Fracture Toughness MNm$^{-3/2}$	7	3	4.5	4.9	8	20
Therm. Exp. Coef. 10^{-6}/ºC	3.2	5.8	4.6	8	9.8	11.6
Therm. Conductivity W/mºK	32	26	85	25	38	40
Maximum Work Temp. ºC	1100	1750	1700	1200	950	200
Corrosion Resistance	High	High	High	High	High	Moderate
Failure Mode	Spalling	Fracture	Fracture	Fracture	Spalling	Spalling

Many researchers have reviewed and reported several advantages of silicon nitride hybrid bearings (SNHB) over steel bearings, by comparing their properties and test data's.

Due to SNHB's high-speed and high-temperature operating capability, it finds wide applications in machine tool spindles, aircraft accessories/aerospace (generators, gyros, gearboxes, turbine engines, radar, weapon systems, satellites), industrial machinery (turbomolecular pumps, diesel fuel injection pumps, textile machines, woodworking machinery, food processing equipment

drilling equipment) and medical equipment (dental drills, centrifuges, X-ray tubes) [Jaing, 1998]

To summarize SNHB meets the requirements of higher efficiency, higher reliability, higher accuracy, higher speed, greater stiffness, longer life, lower friction, corrosion resistance, marginal lubrication, and less maintenance action as compared to traditional bearing [Wang *et al.*, 2000]. As cost effective and eco-friendly processing grows, the use of permanently lubricated and sealed bearings will also increase, and many of these are likely features of Si_3N_4 balls [Katz, 1999].

1.2 SILICON NITRIDE FINISHING TECHNIQUE

Abrasive machining, such as grinding, lapping, and polishing are the techniques presently used for finishing of silicon nitride (Si_3N_4) for hybrid bearing applications [Chandrasekar and Farris, 1997]. In grinding, Si_3N_4 balls are loaded between abrasive bonded grinding wheel on the top and V-groove block at the bottom (both in contact with Si_3N_4 balls) are rotated at relatively high-speed in opposite directions. Where as in the case of lapping and polishing, balls located in a mixture of loose abrasives, suspended in the form of slurry or paste and loaded in-between flat or beveled spindled on the top and V-groove block or float at the bottom, respectively. Rotational speed of the lapping or polishing spindle is varied depending on the load applied either by hydraulic or mechanical pressure, in each case. The polishing process is applied after grinding or lapping to obtain smooth surface finish, because it is more flexible than grinding or lapping.

Buijs and Korpel-vanHouten [1993] and Chandrasekar and Farris [1997] concluded that material removal mechanism in brittle materials by the above processes resembles a 3-body abrasion. Here, abrasive acts like sharp sliding indenters that are relatively active mechanically on the Si_3N_4 surface to remove material. Two main mechanisms of material removal have been associated with ceramics. They are brittle fracture due to crack systems oriented both parallel (lateral) and perpendicular (radial/median) to the surface, and chemically assisted wear in the presence of a reactant that is enhanced by the mechanical action (tribochemical reaction). The relative role of each of the two mechanisms in a particular finishing process can be related to the load applied to an abrasive particle, the sliding speed of the particle and the presence of a chemical reactant. These material removal mechanisms also cause damage to the near surface in the form of microcracks, residual stresses, plastic deformation, and surface roughness which together determine the strength and performance of the finished component.

1.2.1 V-GROOVE LAPPING AND ITS LIMITATIONS

V-Groove lapping is an abrasive method, traditional used for finishing of steel bearing balls. With the advent of hybrid bearings for stringent operating conditions, this method was extended further for the finishing of silicon nitride balls after grinding. The process uses high-loads (~ 10 N per ball), low polishing speeds (~ 50 rpm), and expensive diamond abrasive. The principle of the process is shown in Figure 1.1. The balls are in 3-point contact running in the V-groove. They balls revolve around the pad, at the same time they rotate

continuously, and glide and roll relatively against the contacting surfaces of the pad [Yuan *et al.*, 2002]. Due to lower speeds, the process sometime takes 12 - 16 weeks to finish ceramic balls from the as-received condition. Thus, long processing time and use of expensive diamond abrasive result in high processing costs. More over the hard and expensive diamond abrasive used creates a number of surface defects, such as scratches, pits, and microcracks on the balls. This is due to the fact that harder abrasive is used in combination with high-load and low polishing speeds. Nucleation sites for cracks are generated due to the presence of surface imperfection on the harder and brittle ceramics, resulting in catastrophic failure by large brittle fracture.

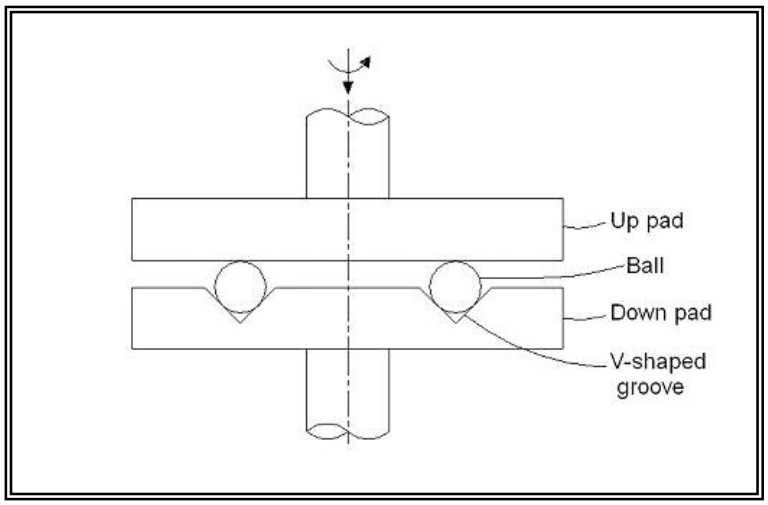

Figure1.1 Schematic of conventional V-groove lapping apparatus [after Yuan *et al.*, 2002]

In order to overcome the limitations of lapping process it was necessary to develop a new 'gentle' polishing technique to reduce the surface damage. The approach used here was magnetic field assisted polishing, known as Magnetic Float Polishing (MFP).

1.2.2 MAGNETIC FIELD ASSISTED FINISHING METHODS

In 1897 [Kann, 1897] reported the use of metallic abrasive material for grinding and polishing of glass and stone in presence of a magnetic field. During World War II [Coats, 1940] in U.S. introduced magnetic field assisted polishing technique to finish inner surface of the gun barrels. This technique was later used in the former U.S.S.R by Baron [1975] and in Bulgaria by Mekedonski *et al.* [1974]. They used MAF to finish difficult-to-machine and non-magnetic materials of large size. Japanese researchers in the 1980's [Takazawa *et al*., 1983; Tani and Kawata, 1984; Shinmura *et al*., 1990; Kato and Umehara, 1990] improved this technique and utilized it for finishing various workmaterials to obtain good surface finish. In the 1990's Komanduri's group in US and Childs's group in UK have advanced this technology and worked towards taking this technology for industrial applications.

Magnetic field assisted polishing (MFAP) is a process in which, either permanent or electro magnets are used to generate magnetic field to orient abrasive particles along the field direction. Depending on the abrasive carrying medium it is classified into two categories, namely, magnetic float polishing (MFP) and magnetic abrasive finishing (MAF). Figure 1.2 shows the detailed classification of the magnetic field assisted polishing processes.

Magnetic abrasive finishing has been applied by a number of researchers [Takazawa et al, 1983, 1985; Shinmura et al, 1990, 1993; Agrawal, 1994; Fox et al., 1994; Thomas, 1997; Chang et al., 2001] to finish both magnetic and non-magnetic materials and to finish both internal and external surfaces of a cylinder.

In this investigation, principles of both categories have been combined to finish silicon nitride balls with a permanent magnets and a concentric shaft.

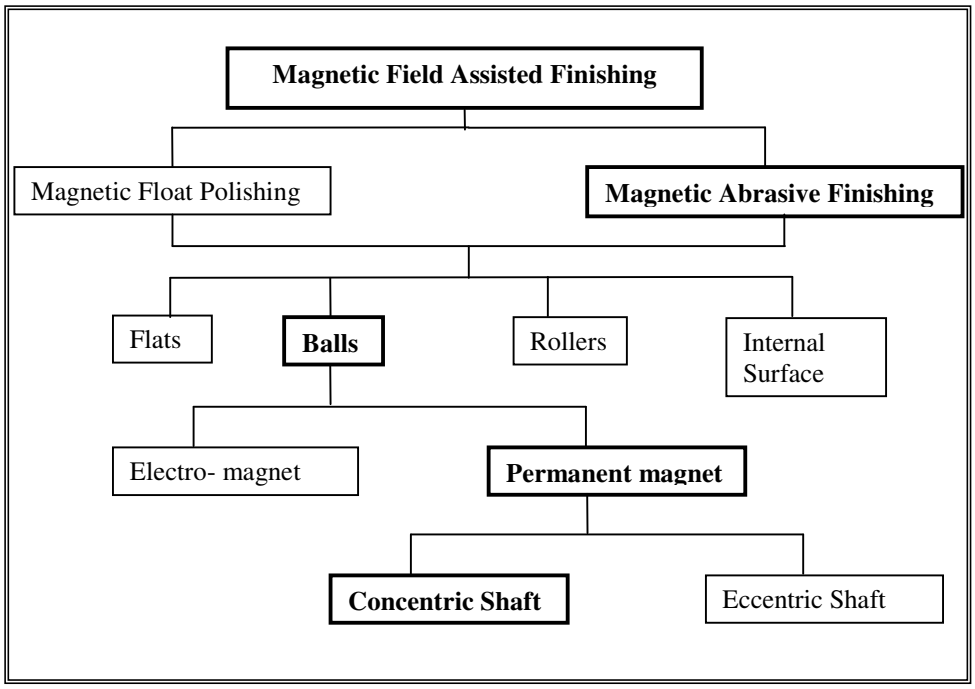

Figure 1.2 Classification of magnetic field assisted finishing

1.2.2.1 MAGNETIC FLOAT POLISHING (MFP)

MFP is a 'gentle' polishing technique based on magneto-hydrodynamic behavior of a magnetic fluid that can levitate all non-magnetic materials suspended in it. MFP uses low-loads (~ 1 N per ball), high-speeds (~ 2000 rpm for 2.5 in. diameter shaft in the small batch apparatus and ~ 400 rpm for 12.2 in. diameter spindle or the top shaft in the large batch apparatus), and abrasives, such as boron carbide, silicon carbide, and cerium oxide. Figure 1.3 is a schematic of the magnetic float polishing apparatus. In MFP, balls supported by acrylic polishing float are placed in a cylindrical nonmagnetic chamber containing magnetic fluid and abrasive mixture. This chamber is placed on a set of magnets.

Magnetic fluid is a colloidal dispersion of extremely fine (<100 Å) iron oxide particles in a carrier fluid, such as water or kerosene and surfactants. Surfactant is used to prevent the agglomeration of non oxide or iron particles. Due to the magnetic field, iron oxide particles are attracted down towards the area of higher magnetic field and an upward buoyant force is exerted on the non-magnetic float, abrasive particles, and balls forcing them towards the area of lower magnetic field. The beveled drive shaft which is concentric to the chamber is loaded to exert the desired force on the balls. Material is removed due to relative movement of balls and abrasives under the action of the magnetic buoyancy force, when the shaft rotates. An actual polishing time of about 20 hours is adequate to finish a batch from the as-received condition [Komanduri *et al.*, 1999b].

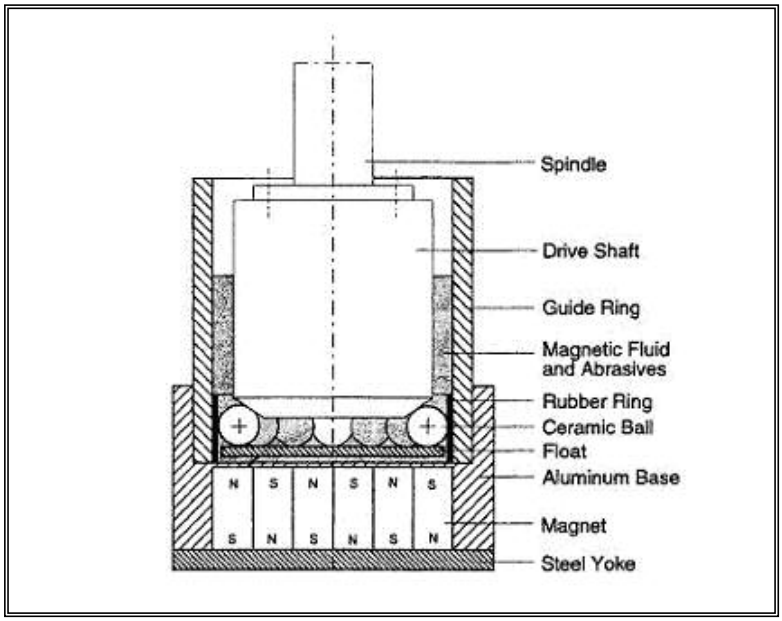

Figure 1.3 Schematic of the magnetic float polishing apparatus for finishing advanced ceramic balls [after Jiang and Komanduri, 1998c]

1.2.2.2 UNBONDED MAGNETIC ABRASIVE POLISHING (UMAP)

Magnetic abrasive finishing is a technique in which magnetic brush is formed in the presence of a magnetic field inducing finishing pressure between the abrasive and the workpiece. Either permanent or electromagnet is used to generate the required field. Magnetic brush is formed between the magnetic N and S poles along the direction of the magnetic force, by the combination of magnetic abrasive grains to each other magnetically. The workpiece such as a roller or a cylinder is held in between a processing field. By rotating the workpiece at high-speed and vibrating magnets or workpiece axially, relative motion between workpiece and abrasive brush under the influence of magnetic force leads to the surface or edge finishing [Shinmura, 1989].

To date magnetic abrasive finishing has be on employed for finishing of flat, cylindrical or rollers objects. In the present investigation, efforts have been made to implement this principle for finishing of spherical objects. By now it is clear that application of ceramic bearing has been limited due to the high-cost involved in polishing silicon nitride balls. Conventional lapping process uses expensive diamond abrasive and long processing time (6 - 16 weeks) resulting in high processing costs. On the other hand MFP has come up as an alternative and matured technology which, not only uses less expensive abrasive but also reduces the surface damage on the balls. The only setback with magnetic float polishing is the cost of magnetic fluid and extensive setup time.

Figure 1.4 shows the apparatus used for unbonded magnetic abrasive polishing (UMAP) of balls. A mixture of abrasive, iron particles, glycerin, de-

ionized water and a rust inhibitor are mixed in desired proportion and introduced into the chamber. The chamber, includes a spring holder and two inlet openings, is mounted onto the lathe head stock using the 4-jaw chuck. Silicon nitride balls to be polished are loaded between the spring loaded acrylic polishing plate and beveled spindle. Thus load is applied on the balls by forcing the spindle mounted on the lathe carriage against the polishing plate supported by the mechanical spring. Now, the balls are in three point contact, namely, with the plate, the spindle and the urethane liner fixed to the chamber inner surface. Magnets fixed around the chamber develops magnetic field with a gradient in the radial direction. The flux generated develops a magnetic brush at the working zone. Magnetic brush helps in concentrating the unbonded magnetic abrasive mixture at the working zone thus increasing the material removal rate; so they are available to be embedded in the spindle.

Spindle is rotated at 850 rpm driven by an external motor mounted on the carriage and the acrylic polishing plate is rotated at 32 rpm using the lathe spindle. The polishing action occurs by rotating the balls in-between the polishing plate and the spindle in presence of loose abrasive grits suspended by iron particles

In the present study, unbonded magnetic abrasive technology is developed using permanent magnets to generate magnetic abrasive brush and a compression spring as loading compliant system. Concentric shaft has been used in this study.

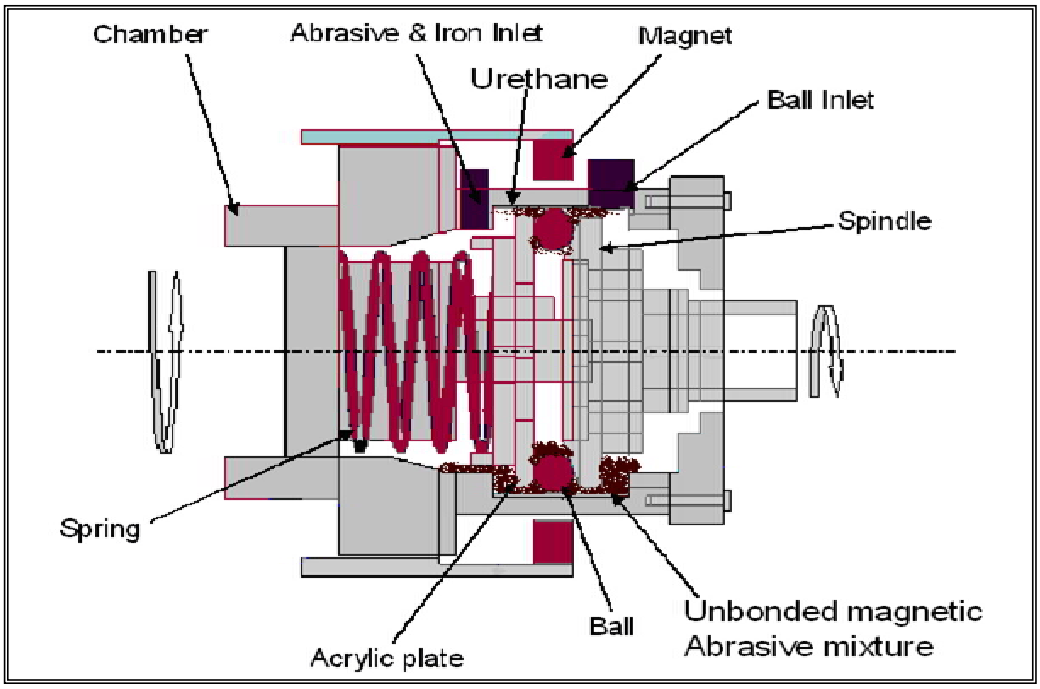

Figure 1.4 Schematic of the unbonded magnetic abrasive polishing apparatus for finishing silicon nitride balls

1.3 WORKMATERIAL, ABRASIVES AND IRON POWDER

1.3.1 WORKMATERIAL

Workmaterial used is silicon nitride which has a decomposition temperature of ~1900 ˚C and is synthetic, covalently bonded material. Si_3N_4 is made of two hexagonal structures; Namely, β-Si_3N_4 and α- Si_3N_4 phases the first structure is more elongated than the later and c-axis length of α is close to two times that of β. A-phase is a energy rich metastable form, but becomes unstable and converts to β phase at high-temperature [Ziegler *et al*, 1987]. Table 1.2 show mechanical and thermal properties of hot pressed silicon nitride.

Traditional sintering cannot be used for the production of dense and compact silicon nitride products, because of its high degree of covalence. Hence, sintering aids are used to create a dense product. Different methods used for the

manufacturing of silicon nitride are reaction bonded sintering, hot pressing, and hot isostatic pressing (HIP'ing).

Workmaterial used in the present study is hot-isostatic pressed silicon nitride (HIP'ed Si_3N_4) NBD 200 from Norton Advanced Ceramics. HIP'ing process involves high-pressure (> 300 MPa) [Raghunandan, 1997] isostatic compression at 1700 ˚C, which leads to uniform material properties. Also, this leads to more uniform and fine grained structure. Further, densification is enhanced to obtain fully dense product with smaller amount of sintering aids. Milled Si_3N_4 and MgO or Y_2O_3 powder either in alcohol or water are mixed with binders to improve formability in later operations. The milled slurry is then spray dried to make a flowable, compactable powder. The powder is then pressed into blanks using uniaxial or isostatic methods. The "green" ball blanks are then air-fired to remove binders and HIP'ed at extremely high-temperatures (>1700 ˚C) and pressures (> 300 MPa) to optimize densification and microstructure [Saint Gobain Ceramics website]. The chemical composition and typical properties of NBD-200 Si_3N_4 ball are given in Tables 1.3 and 1.4.

Table 1.2 Properties of silicon nitride [after Ziegler *et al*, 1987]

Crystal Structure	
α- Si_3N_4	a-axis 0.775-0.777 nm c-axis 0.516-0.569 nm
β-Si_3N_4	a-axis 0.759-0.761 nm c-axis 0.271-0.292 nm
Theoretical Density	
α- Si_3N_4	3.16-3.19 g/cm3
β-Si_3N_4	3.19-3.20 g/cm^3
Co-efficient of thermal expansion	2.9-3.6 x 10^{-6} / ˚C

Table 1.3 Chemical composition of NBD-200 Si_3N_4 balls [after Hah *et al.*, 1995]

Mg	Al	Ca	Fe	C	O	Si_3N_4
0.6 - 1.0	≤ 0.5	≤ 0.04	≤ 0.17	≤ 0.88	2.3 - 3.3	94.1 - 94.7

Table 1.4 Mechanical and thermal properties of Si_3N_4 balls [after Hah *et al.*, 1995]

PROPERTY	**VALUE**
Flexural Strength, MPa	800
Weibull Modulus	9.7
Tensile Strength, MPa	400
Compressive Strength, GPa	3.0
Hertz Compressive Strength, GPa	28
Hardness, Hv (10kg), GPa	16.6
Fracture Toughness, K_{1c}, $MNm^{-3/2}$	4.1
Density, g/cm^3	3.16
Elastic Modulus, GPa	320
Poisson's Ratio	0.26
Thermal Expansion Coefficient at 20-1000˚C, / ˚C	2.9×10^{-6}
Thermal Conductivity at 100˚ C, W/m-K	29
Thermal Conductivity at 500˚ C, W/m-K	21.3
Thermal Conductivity at 1000˚ C, W/m-K	15.5

1.3.2 ABRASIVES

Following are the abrasives used in the present study.

- Boron carbide (B_4C)
- Silicon carbide (SiC)
- Cerium oxide (CeO_2)

To be specific B_4C (500 grit) and SiC (600 grit) abrasives are larger than ~ 10 μm, and grouped under coarser abrasive list used during initial runs to obtain high material removal rate (MRR) and reasonable improvement in sphericity. Relatively finer abrasive (larger than ~ 5 μm) such as B_4C (1500 grit) and SiC (1200 grit) abrasives are used to obtain better roundness, control diameter, and

surface finish of the balls. Extremely fine abrasives which are less than ~ 1 μm, such as SiC (8000 grit) and SiC (10,000 grit) are used to achieve good surface finish. Finally, CeO_2 abrasive (larger than ~ 5 μm) is used to obtain superior finish through chemo-mechanical polishing. Table 1.5 gives the properties of the abrasive used in the present study. All the abrasives except CeO_2 were obtained from Saint-Gobain CeO_2 abrasive was obtained from Aldrich Chemicals.

Table 1.5 Properties of the abrasives used [after Jiang, 1998d]

Abrasive	Density g/cm^3	Knoop Hardness kg/mm^2	Elastic modulus GPa	Melting point $^{\circ}C$
B_4C	2.52	3400	450	2450
SiC	3.2	2500	420	2400
CeO_2	7.13	625	165	2500

Chemo-mechanical polishing (CMP) process is used to finish hard and brittle materials to obtain mirror-like surface. In CMP a chemical reaction is instigated due to threshold pressure and temperature at the contact zone between the abrasive and the workmaterial in presence of water. Possibility of surface damage is eliminated or minimized by using abrasive which are generally softer than the workmaterial. The reaction products formed due to tribo-chemical reaction are subsequently removed by the mechanical action of the abrasive. Figure 1.5 describes the CMP action.

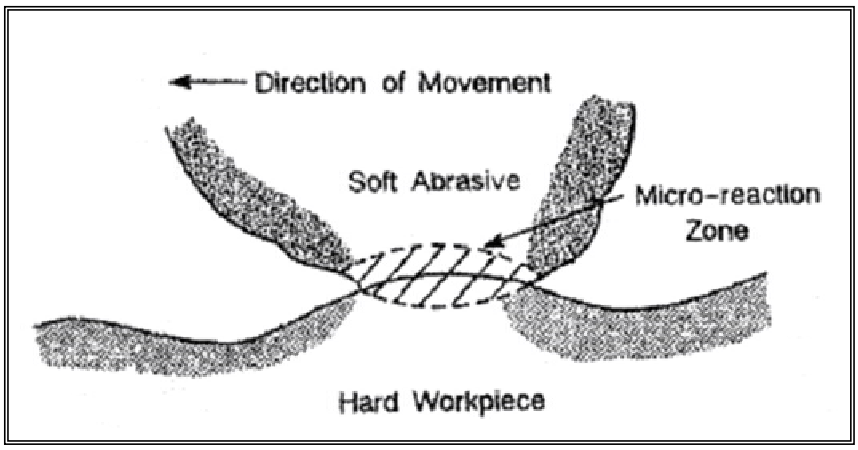

Figure 1.5 Schematic of the chemo-mechanical action between abrasive, workmaterial, and environment
[after Yasunaga *et al.*, 1978, Komanduri *et al.*, 1997]

1.3.3 IRON POWDERS

In case of unbonded magnetic abrasives, iron particles act as a medium to concentrate abrasives in the polishing zone. Iron particle size used in this study varies from 5 μm to 297 μm. Three different types of iron particles were used in this study. Table 1.6 gives general properties and Table 1.7 gives description of the each powder. The iron powders were obtained from Atlantic Equipment Engineers.

Table 1.6 Properties of iron powder used
[Atlantic Equipment Engineers website]

IRON, $_{26}$ $Fe^{55.847}$	
Melting Point °C	1536
Density g/Cm^3	7.87
Brinnell Hardness	82-100
Crystal Structure	body centered cubic

Table 1.7 Iron powder descriptions
[Atlantic Equipment Engineers website]

Name	Description	Purity %	Particle Size (μm)
FE-102	Iron metal powder, (electrolytic)	99.9	> 44
FE-112	Iron metal powder, (hydrogen reduced)	99.8	44 - 149
FE-114	Iron metal powder, (hydrogen reduced)	99.8	149 - 297

1.4 OUTLINE

Chapter 2 deals with a brief review of literature on MAF, ball lapping and MFP processes. The problem statement and approach taken in the design and development of UMAP technology has been covered in Chapters 3 and 4. Chapter 5 presents various steps taken to analysis magnetic field using COMSOL 3.2 Multiphysics FEM software. Chapter 6 provides details of the equipment design, fabrication, assembly, installation, and alignment of all the components of UMAP apparatus. Test procedure and methodology involved in finishing ceramic balls using UMAP technique is presented in Chapter 7. The discussion of results obtained by the experimental investigation is covered in Chapter 8. Finally, Chapter 9 presents conclusions of this study and outlines future work.

CHAPTER 2

LITERATURE REVIEW

The present study involves development of new polishing technology (without using expensive magnetic fluid) by combining the salient features of magnetic abrasive finishing (MAF), magnetic float polishing (MFP) and V-groove lapping. Hence, a brief review of literature on MAF, ball lapping and MFP is given.

2.1 MAGNETIC ABRASIVE FINISHING

An initial study on magnetic abrasive finishing was reported in the former USSR by Kargalov [1939] to finish the inner surface of a rotating tube with alternating magnetic field. Coats [1940] illustrated this technology in the United States to clean the inside of a drum. The main principle used in this method was that the magnetic abrasive under the influence of a magnetic field is aligned in the direction of the magnetic field. If the rotating workpiece is introduced in this abrasive, the magnetic force exerted by the magnetic abrasive on the workpiece causes the polishing action. Japanese researchers [Takazawa *et al*., 1983; Shinmura *et al*., 1986, 1987, 1990] further extended this technology to finish external and internal surfaces using both permanent magnets and electro magnets.

Takazawa *et al.* [1983] used MAF to finish cylindrical ferromagnetic workpiece. Figure 2.1 shows a schematic of this process. Here the magnetic abrasive grains are combined to each other magnetically between magnetic N and S poles along the lines of magnetic force, forming a magnetic brush between the workpiece and each pole. The workpiece is then given a revolution, feed and vibration in the axial direction. Finishing of the surface and the edge are carried out by the magnetic brush. In this instance the workpiece is also magnetic and the magnetic force acts on the top of the brush between the workpiece and the abrasive grain. As a result abrasive grains are pressed against the worksurface by an infinitesimal cutting force Px and performs cutting [Takazawa *et al*., 1983].

When a non-ferromagnetic workpiece is used, the resistance of the magnetic flux path increases due to low permeability of a nonmagnetic workpiece compared to that in a vacuum. This is in contrast to a ferromagnetic material which may have a magnetic permeability several thousand times higher than that in a vacuum. For this reason, under similar conditions, magnetic flux density is significantly higher in the case of ferromagnetic workpiece. A general representation of magnetic flux paths in the case of ferromagnetic and non-ferromagnetic materials similar to the electric field theory is shown in Figure 2.2. Notice that not only the distribution of magnetic flux differs, but the gradients are much higher in the case of the ferromagnetic workpiece. The higher flux densities along with the higher flux gradients results in higher forces. Hence, higher finishing pressure is generated in the case of the ferromagnetic workpiece. In the

described MAF process considered here, a bonded type of magnetic abrasive was used.

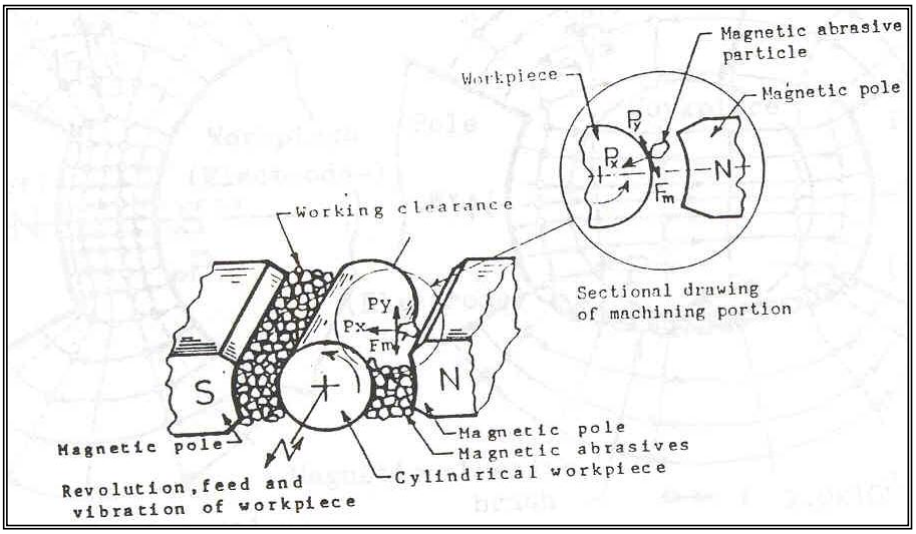

Figure 2.1 Arrangement for finishing ferromagnetic cylindrical workpiece with axial vibration [after Shinmura and Aizawa, 1989]

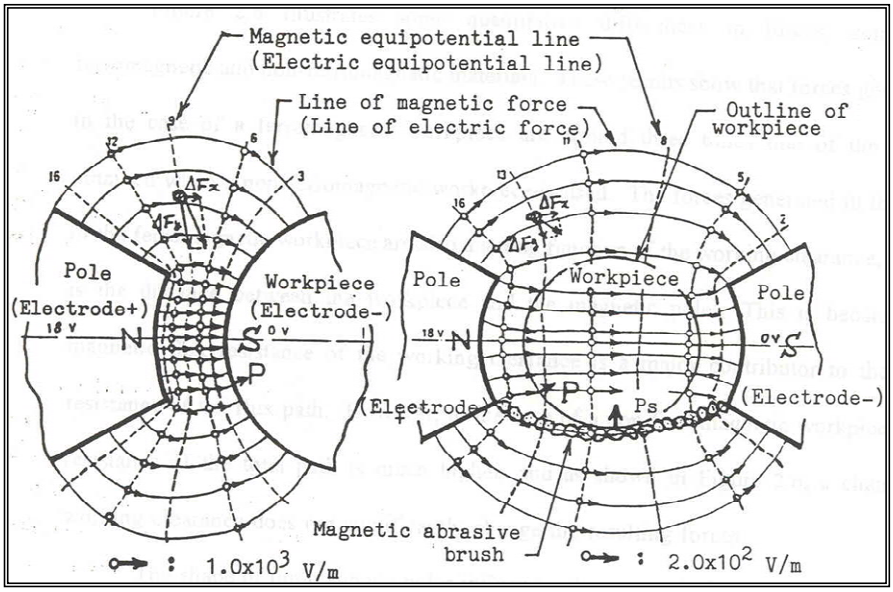

Figure 2.2 Two dimensional magnetic field distributions simulated by electric field distributions [after Shinmura, 1990]

Fox *et al.* [1994] demonstrated finishing of non-magnetic rollers using both bonded and unbonded magnetic abrasives. Bonded abrasive consist of sintered product of iron particles (80 – 400 μm) and abrasive, whereas unbonded type is a mixture of iron particles and abrasive grits. They also used zinc stearate as a dry lubricant and also used SAE 30 oil as liquid lubricant along with the magnetic abrasive. Figure 2.3 shows the plot comparing surface finish and material removal rate of bonded and unbonded type abrasives. It was concluded that relatively high material removal rate can be achieved with unbonded type as compared to the bonded type. The bonded type abrasive yields very good surface finish, whereas the unbonded type results in rougher surface.

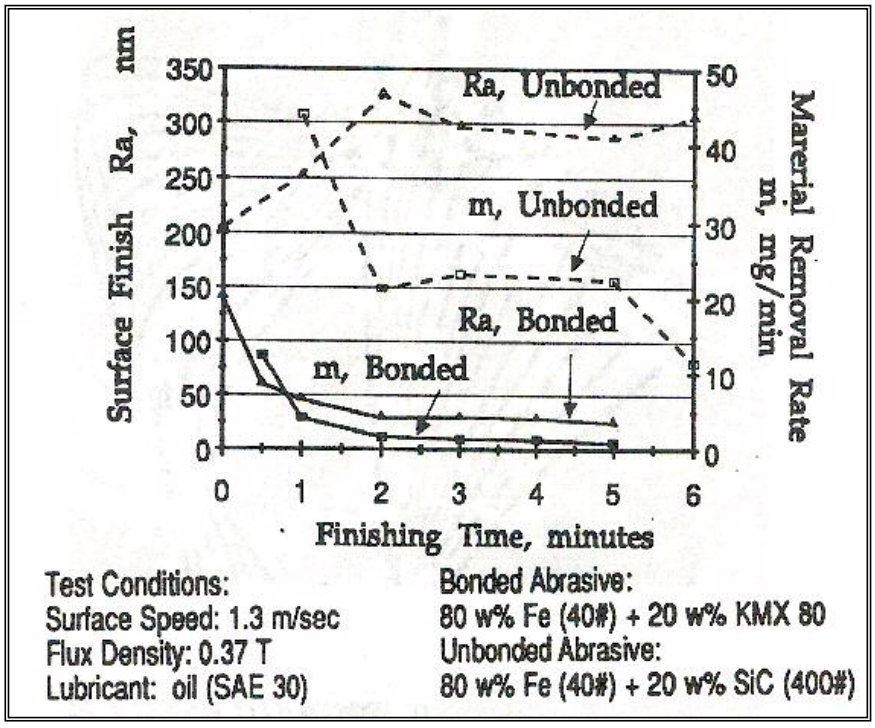

Figure 2.3 Variation of surface finish and material removal rate with finishing time for bonded and unbonded magnetic abrasive [after Fox, 1994]

Chang *et al.* [2002] successfully demonstrated the use of unbonded magnetic abrasive with SAE30 lubricant to finish worksurface to a value of 0.05 μm R_a. Figure 2.4 show a two dimensional magnetic field distribution and magnetic force acting on iron particles in a cylindrical MAF process. The magnetic force not only concentrates the iron particles in the working gap where the magnetic field strength is superior, but also prevents them from splashing due to workpiece rotation. Chang *et al.* used steel grit and iron grit as magnetic particles and concluded that steel grit is better suited for magnetic abrasive finishing [Chang *et al* , 2002].

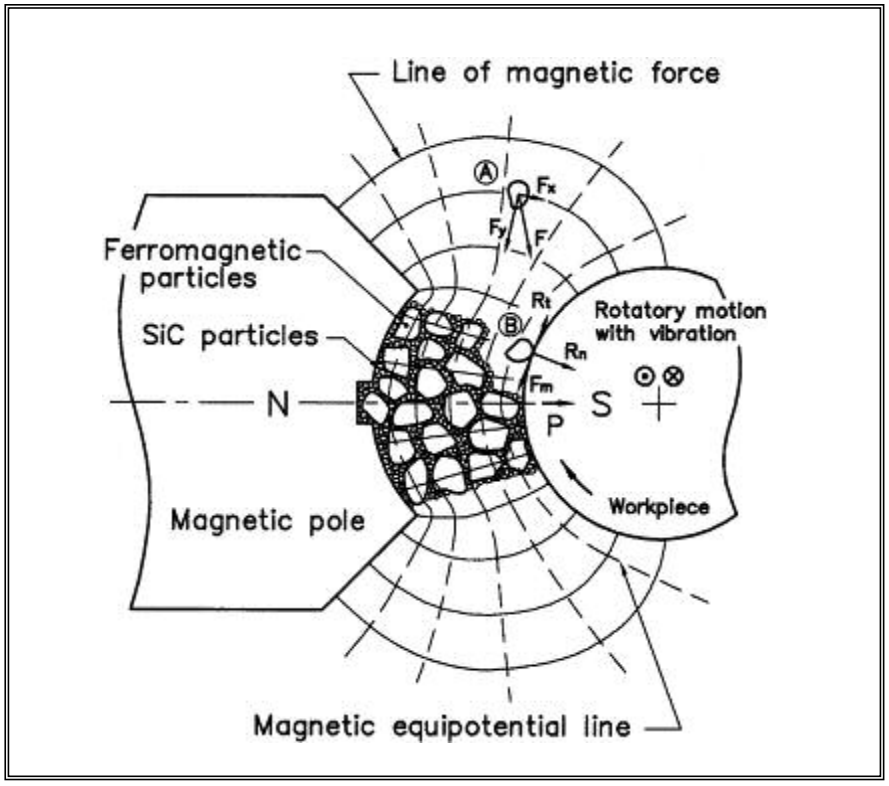

Figure 2.4 Schematic of magnetic field distribution and magnetic force acting on ferromagnetic particles [after Chang *et al.*, 2002]

2.2 BALL LAPPING

A number of machines were developed to finish spherical objects to obtain good sphericity and surface finish. However, finishing of spherical blanks requires precise and controlled removal, such that sphericity can be further improved. This was possible by proper rolling of the balls during grinding and subsequent polishing. The balls were normally loaded between two plates that have relative rotational motion. In most of the apparatus, plates are arranged horizontally. However, in some cases vertical and inclined arrangements can be seen. Some of the important parameters of the lapping process include load on the plate, rotational speed, type and volume of the abrasives, workmaterial to be finished, and abrasive carrier or slurry medium.

London [1990] reported an apparatus for low-stress polishing of spherical objects. The apparatus consists of two plates parallel to each other with a clearance between them to place spherical objects to be polished. Figure 2.5 shows the polishing device used by London. The top plate is a transparent plate made of ceramic material so that it can be monitored by viewing. Radial concave grooves are provided on the top plate in order to mix the balls during polishing. Rotation of the bottom plate produces the required polishing action. Magnets were mounted on the top plate to restrict the motion of balls out of the polishing zone. Thus, it limits the path of travel as the bottom plate rotates. The magnets also help in keeping the balls within the polishing chamber. In this apparatus ferromagnetic balls are polished by glycol mixed with fine diamond powder acting as abrasive slurry.

The polishing load used was of several hundred grams. The rotational speeds of the polishing plates were in the range of 5 – 60 rpm. One polishing batch consisted of 500 – 3000 balls, depending upon the ball blank diameter. The polishing action takes place on the balls which are larger in diameter and continuous until all the balls are polished to the same diameter and sphericity. This polishing process can be carried out round the clock with less operator's attention. Therefore, average time taken to finish a batch of balls varies from the 10 to 23 days.

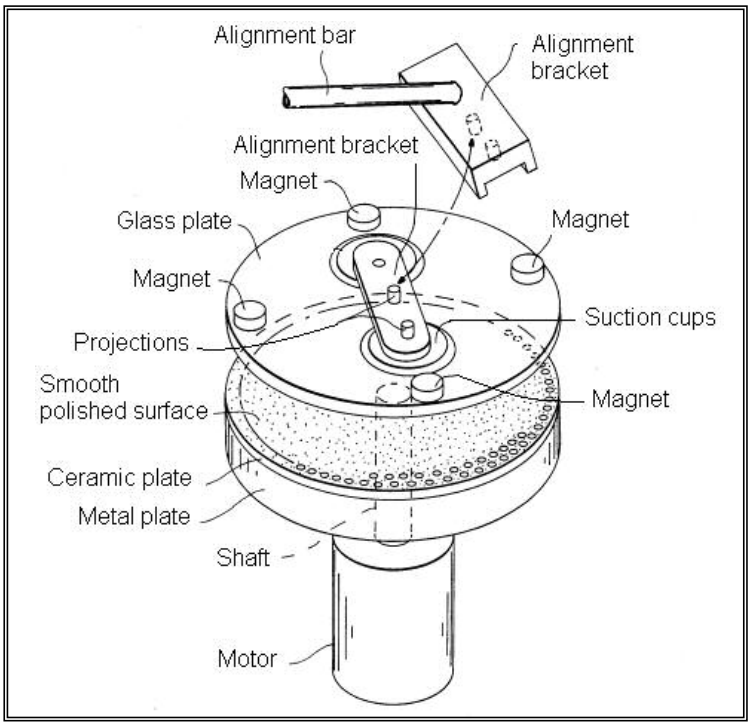

Figure 2.5 Schematic of the lapping apparatus [after London, 1990]

Figure 2.6 shows the ball lapping machine mounted along horizontal axis. Stationary lapping plate facilitates loading of balls and abrasive slurry into the grooves. Turn table rotates causing the balls to be lapped. This horizantal

arrangement poses serious disadvantages, namely, 1) improper circulation of the balls, 2) accumulation of abrasive slurry and wears debris on the lower side of the groove, 3) temperature of the lapping fluid increases due to the heat generated by the rotating spindle, This leads to a change in concentricity of the groove further degrades the sphericity and surface finish of the balls. 4) Adverse loading occurs. These issues were considered in a modified version of lapping machine developed by Sato [1994].

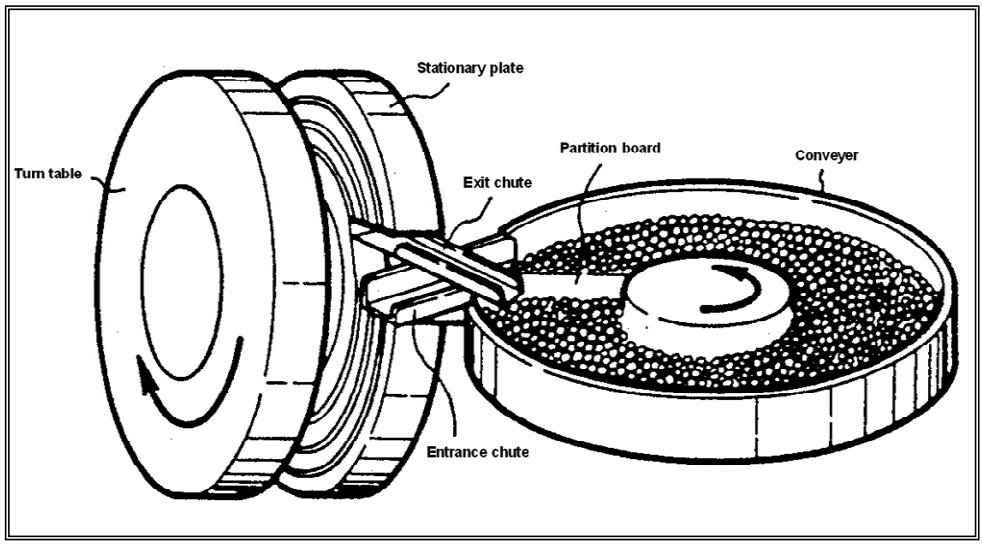

Figure 2.6 Schematic of horizontal ball lapping machine [after Sato, 1994].

Modified lapping machine is shown in Figure 2.7 where the plates are tilted at an angle during polishing process. The plates stay horizontal while loading and unloading the balls. The stationary plate is mounted on a central shaft and rotating plate on a sleeve. Supports for both the plates were provided from the same side, which avoids the plates getting heated up due to spindle rotation, thereby maintaining concentricity and parallelism of the grooves on both discs. The abrasive particles and the wear debris drop out from the space

between the discs preventing their agglomeration. Thus no scratching occurs and ball rolls uniformly without any hindrances.

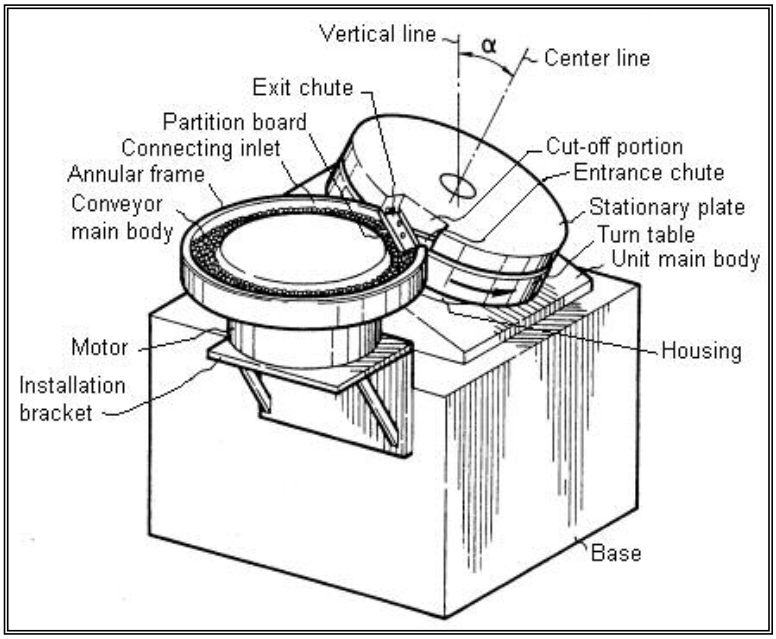

Figure 2.7 Perspective view of the ball lapping machine [after Sato, 1994]

Kang *et al.* [2000] developed a new eccentric lapping machine as shown in Figure 2.8 for finishing advanced ceramic balls. Lapping machine consisted of a flat surface plate on top and an eccentric V-groove plate at the bottom, as shown in Figure 2.9. The top is held stationary and the bottom V-groove plate is rotated eccentrically. The spring loaded unit was used to apply load on the top plate. Ceramic balls were loaded between these plates and were lapped along with a mixture of diamond paste and lubricating fluid. Aggressive lapping tests were conducted on ½ in. silicon nitride ball blanks with high-speed and high-load. Initially, the material removal rate increased with the lapping load reaching a maximum, 68 μm/h, at a load of 4.37 kg/ball. Beyond 4.37 kg/ball removal rates started to decrease with increase in load.

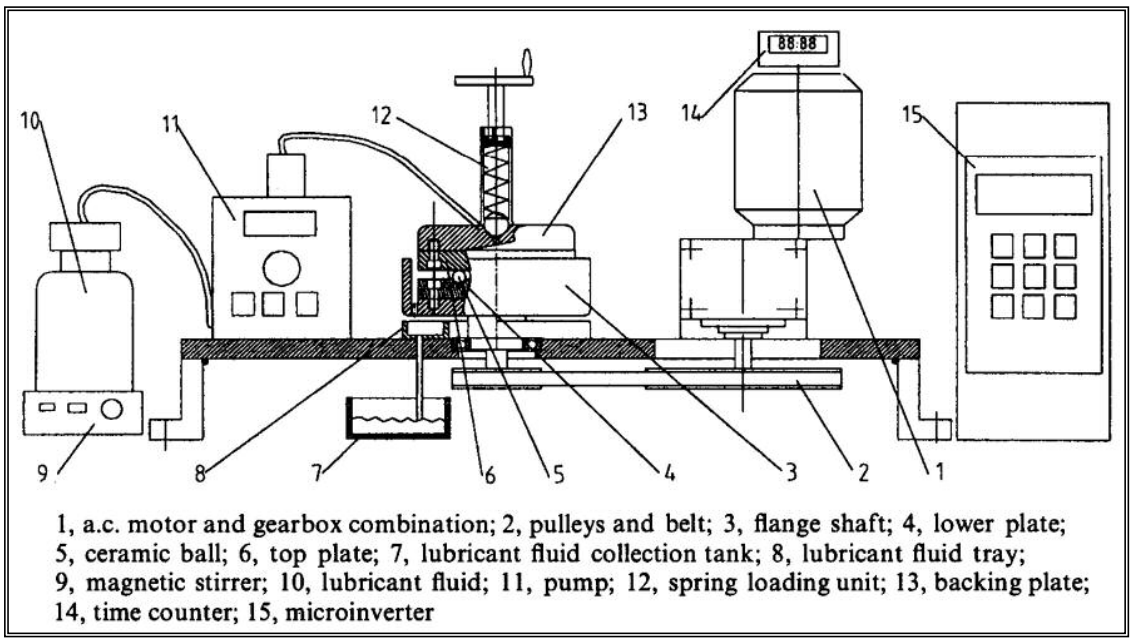

Figure 2.8 Schematic of the eccentric lapping machine [after Kang *et al.*, 2001b]

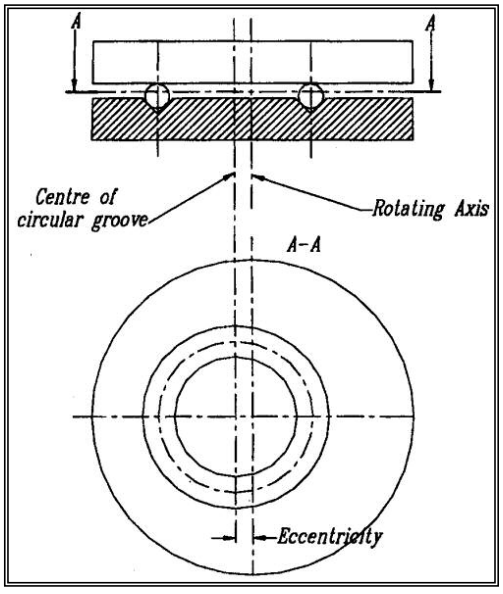

Figure 2.9 Flat surface and eccentric V-groove lapping [after Kang *et al.*, 2001b]

At 10.87 kg/ball load, 20 μm/h removal rates and a sphericity of 3 - 4 μm (with some balls measuring 6 μm) was achieved. It was concluded that at higher loads balls roll inappropriate resulting in a decrease in the material removal rate

and poor sphericity. Optical microscopy inspection and dye penetrant test confirmed that. Balls lapped at 10.87 kg/ball incurred surface spalls and sub-surface damage. In contrast, balls lapped at 4.37 kg/ball load had no substantial surface or sub-surface damage. Tests were also conducted at 270 rpm and 500 rpm. Balls lapped at 500 rpm incurred surface spalls, whereas, no evidence of lapping induced damage (except for C-cracks) was observed at 270 rpm [Kang *et al.*, 2000].

Taguchi method confirmed optimum lapping condition to be high-load, high-speed, high paste concentration, and 60 μm diamond particles [Kang *et al.*, 2001a]. Further analysis showed that lapping load was the most significant parameter accounting for 50 % of the total, followed by lapping speed (31 %). The particle size and paste concentration only accounted for 12 % and 7 %, respectively [Kang *et al.*, 2001a].

The role of lapping plates on the lapping and polishing process was conducted by Kang *et al.* [2001b]. Forthe initial step of lapping to obtain high MRR cast iron lapping plates were found to be appropriate. However, during polishing, which is categorized as second step, steel plates were found suitable to achieve roundness, surface finish, dimensional and geometric accuracies. It was found that surface condition of the V-groove on the lower plate has a significant influence on the sphericity and material removal rate, and the surface condition of top plate has more influence on final surface roughness [Kang *et al*, 2001b].

Following were the test conditions used for eccentric lapping to obtain high MRR.

- 65 mm diameter circular V-groove with 90° V-groove angle,
- 15 ball blanks of diameter 13.4 mm
- 8 mm eccentricity

The maximum material removal rate was achieved under the following conditions: average lapping load of 4.37 kg/ball, a lapping speed of 169 rpm, a diamond abrasive size of 60 μm, and a diamond paste concentration of 1 g/30 ml. Material removal rate of 68 μm/h for ball blank was achieved, which is 15 times higher than conventional concentric lapping. The ball roundness of 0.4 - 1.1 μm was obtained at the lapping step. In the polishing step, the average load varied from 1.1 to 1.5 kg/ball, the speed was 94 rpm and the diamond particle sizes varied from 0.25 to 1 μm. The polished ball surface roughness value, Ra, was 3 nm and ball roundness was in the range of 0.08 - 0.09 μm, which is above grade 5 of precision bearing ball specification.

Kang *et al.* [2005] measured surface residual stresses of lapped balls under different lapping loads and found that lapping load had less effect than the previous hot isostatic pressing process. Rolling contact fatigue tests were conducted on balls lapped at nominal loads of 43 and 107 N/ball. No failure occurred on the ball lapped at 43 N per ball after 138 $x10^6$ stress cycles.

The ball lapped at 107 N per ball failed after 13.3 x 10^6 stress cycles with a shallow spall with a flat bottom inside. They suggested that lapping load for

advanced ceramic balls in the conventional concentric lapping can be doubled from 20 to 40N per ball without degrading the surface quality of lapped balls.

2.3 MAGNETIC FLOAT POLISHING (MFP)

In MFP, the workpiece, abrasive, and float are acted upon by the magnetic levitation force. This causes the abrasives and the workpiece to be pushed against the polishing shaft that is driven at high-speeds. Material removal is caused by the relative movement of the workpiece and the polishing shaft. The force exerted by the abrasive and the shaft to the workpiece are extremely small and highly controllable. This method is very useful in finishing hard and brittle materials of any geometry- flat, cylindrical, tapered, spherical. [Kato and Umehara, 1990; Umehara, 1990; Childs, *et al*., 1994, 1995; Komanduri, *et al*., 1996; Bhagvatula and Komanduri, 1996; Umehara and Komanduri, 1996; Raghunandan and Komanduri, 1997; Raghunandan, 1997 a, b; Jiang and Komanduri, 1997 a, b, c; Jiang, 1998] they have also applied this process for finishing non-magnetic workpieces of various shapes and sizes.

Research on MFP to finish ceramic components both roller and balls was carried out by three different groups 1) In Japan, by Kato's group, 2) In UK by Childs 3) In USA, by Komanduri's group. Recently this technology was extended to finish large size and large number of ball at Oklahoma State University, Stillwater, Oklahoma [Kirtane, 2004].

Tani and Kawata [1984] were the first to use MFP. They were however, able to finish only soft materials, such as acrylic resin. The removal rates were

low (2 μm/min) due to very low polishing forces applied on the soft material. Silicon carbide abrasive (size: 4 μm) was used.

Umehara and Kato [1987] made a major breakthrough in polishing of ceramic balls by introducing the concept of a float, hence, the name magnetic float polishing (MFP). This float resulted in more uniform distribution of the polishing force on balls. The difficult part of MFP study was to describe the ball motion and the mechanism of material removal during polishing. Umehara and Kato [1990] identified that polishing time, polishing load, polishing speed, abrasives grain size, and abrasive concentration were the primary polishing parameters of the MFP process.

In 1994 and 1995 [Childs *et al.*, 1994b] developed a kinematic model of the ball motion during MFP of ceramic balls, as shown in Figure 2.8, thus developed it to calculate the sliding speeds and to estimate the wear coefficient.

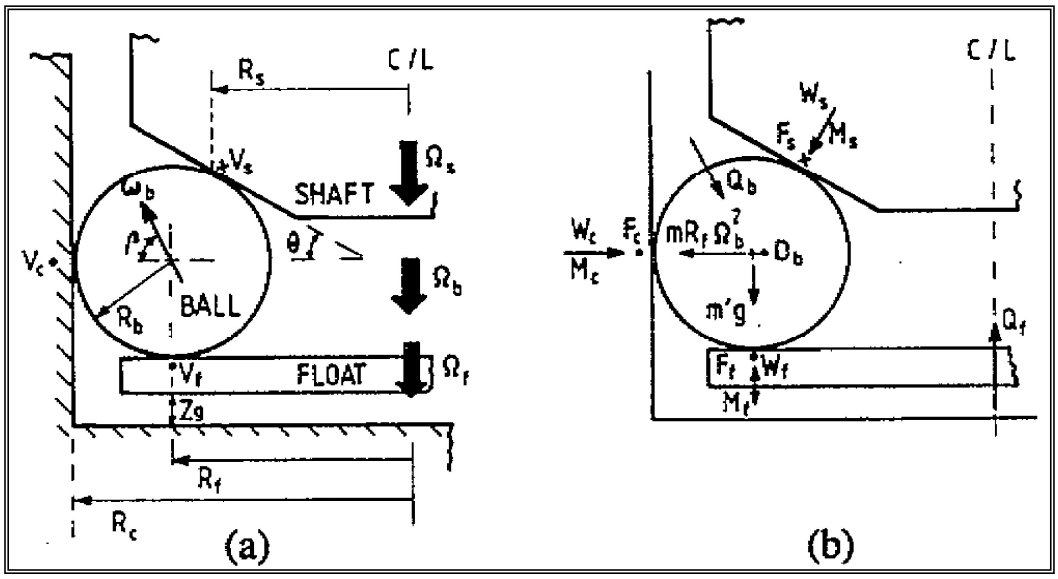

Figures 2.8 (a) Cell geometry and motions (b) contact loads, spin moments, and friction forces [after Childs *et al.*, 1994b]

Figure 2.8(b) shows the contact loads W_c, W_s and W_f, the spin moments M_c, M_s and M_f and the friction forces F_c, F_s and F_f. The Figure also shows the fluid drag moments Q_b and Q_f acting on the ball and float, the centrifugal force $mR_f\Omega_b^2$ acting on the ball, and a drag force D_b acting normal to the plane of the figure due to motion through the fluid.

From the analysis of the motion produced, the following equations were obtained:

$V_c = R_f\,\Omega_b - R_b\,\omega_b \sin\beta$

$V_s = R_s\,\Omega_s - R_f\,\Omega_b - R_b\,\omega_b \cos(\beta-\theta)$

$V_f = R_f\,\Omega_b - R_b\,\omega_b \cos\beta - R_f\,\Omega_f$

If there is no sliding at this three-point contact, the following relationship can be established between the ball circulation speed and the float rotation speed.

$$\alpha = \frac{\Omega_b}{\Omega_f} = \frac{R_s + R_f \dfrac{\Omega_f}{\Omega_s}\cos\theta}{R_f(1+\cos\theta+\sin\theta)}$$

Where

R_b = ball radius

θ = chamfer angle on the shaft

R_c = container's inner radius.

$R_f = R_c - R_b$ = radius at which the ball contacts the float.

$R_s = R_f - R_b \sin\theta$ = radius at which ball contacts the shaft.

z_g = distance between lower surface of the float to the bottom of the cell

Ω_s = angular speeds of the shaft.

Ω_b = ball circulation speed around the guide ring.

Ω_f = angular speed of the float.

ω_b =ball spin angular velocity ,

β = angle between the horizontal and the spin axis of the ball.

V_c = sliding speed at the contact point between ball/guide ring.

V_s = sliding speed at the contact point between ball/shaft.

V_f = sliding speed at the contact point between ball/float.

Childs *et al.* [1994b] concluded that high material removal rates were found due to large skidding velocities between the balls and the drive shaft. Load acting on the balls was found to be proportional to the removal rate. Similarly, removal rate was proportional to the skidding velocity at the drive shaft. Based on wear co-efficient study they concluded that abrasive get embedded in the shaft leads to material removal by two-body abrasion. They found that there is an optimum fluid viscosity for getting high material removal rates in MFP process. If the viscosity is too low, skidding does not occur between the balls and drive shaft. On the other hand, if the viscosity is too large, although skidding occurs, there is a reduction in the abrasive efficiency.

Raghunandan [1997] designed an experimental apparatus to study ball circulation speed with spindle speed and compared the experimental data with analytical solution. Zhang *et al.* [1996] developed a dynamic model for the MFP of the ceramic balls. They found the material removal rate is higher, when larger diameter portions of balls enter the contact area. This was due to a higher polishing load acting on that portion of the ball. Further, Zhang *et al.* [1997] investigated the motion of the ball during polishing and the various forces acting

upon it. They believed that if the polishing action is uniformly distributed over the ball surface, good sphericity can be obtained. To study these effects, they developed an eccentric polishing apparatus. This would facilitate uniform contact track distribution resulting in proper feed motion of the ball for polishing.

Jiang and Komanduri [1997] established three stage polishing process to finish silicon nitride balls to meet ASTM standards. They are 1) Initial roughing stage where the hard and coarser abrasives, such as B_4C and SiC are used to remove maximum material with minimum surface and subsurface damage; 2) An intermediate semi-finishing stage, where material removal rates are reasonable and sphericity and final size are closely monitored; 3) Final finishing stage, where material removal rates are negligible and emphasis is on the diameter, sphericity and surface finish.

Jiang and Komanduri [1998] optimized the MFP process using the Taguchi method. An orthogonal array was used for the tests. The three process parameters identified were polishing force, abrasive concentration in the slurry, and polishing speed. They found that polishing force was the most significant factor for the overall surface finish. Optimum process conditions for polishing were obtained. Within the range of parameter evaluated, the Taguchi experimental design indicated that a high level of polishing force (1.4 N/ball), a low level of abrasive concentration (5%), and a high level of polishing speed (7000 rpm) are optimal for improving surface finish, both R_a and R_t. Using 1 μm size abrasive, surface finish of 15 nm R_a and 150 nm R_t were obtained. CMP using CeO_2 further improved the surface finish to 2 nm R_a.

Hou and Komanduri [1998] carried out thermal analysis of MFP of ceramic balls was carried out by. Hou and Komanduri proposed a model to evaluate minimum flash temperatures and flash durations during polishing. This facilitated in determining whether sufficient temperatures were generated to initiate chemo-mechanical polishing. Area of contact between the balls and abrasives, where the material removal takes place, was taken as the area heat source. This heat source was approximated to a moving disc heat source with a parabolic distribution of heat intensity.

Kirtane [2004] and Lee [2005] reported that groove formed on the polishing spindle or cup helps in improving sphericity significantly but suggested to machine the groove off before finishing stage in order to obtain surface finish.

2.4 NON-MAGNETIC FLUID GRINDING

Chang and Childs [1998] addressed the costs associated with magnetic fluid grinding and developed an apparatus to polish silicon nitride balls without the magnetic fluid. They used a non-magnetic viscous fluid (glycerin – water mixture); and mechanical (coil or shim) springs to achieve complaint float. The drive shaft was replaced with a resin bonded diamond grinding wheel. Further they prevented float rotation by keys. Figure 2.9 shows the modified apparatus for non-magnetic fluid grinding. Three different glycerin-water ratios, 75:25, 50:50 and 25:75 were considered for the study and were named A, B, and C fluids, respectively. Friction coefficient of each of these were measured a pin-on-disc machine. For fluid A and B, $\mu = 0.08$, for C it was 0.11. Absolute viscosity (mPa) at 22 ˚C for fluid A was reported as 43.60, for B it was 7.9 and for C as 2.33. The

viscosity of the magnetic fluid used in MFP was reported to be 40 mPa, which is between the viscosity values of A and B.

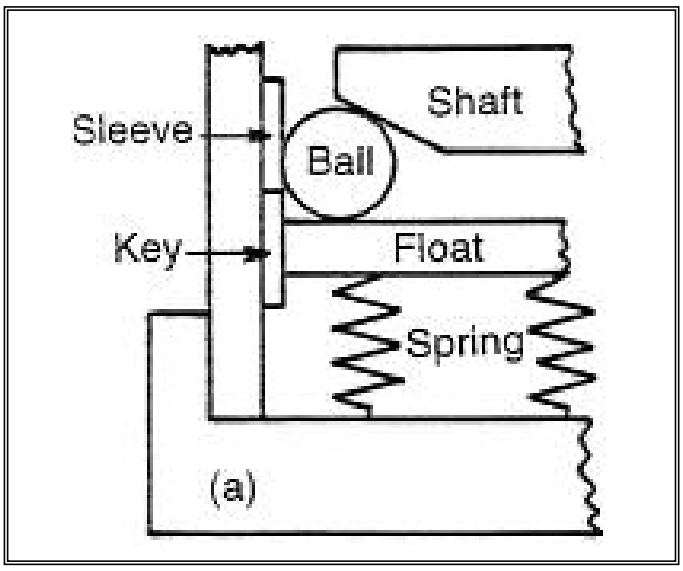

Figure 2.9 Schematic of the non-magnetic fluid grinding
[after Chang and Childs, 1998]

From this study, they concluded that magnetic fluid grinding can be realized with a cheaper fluid and yet high material removal rates (up to 5.3 μm/min) can be obtained. They also reported that out of roundness was reduced from 16 μm to 3 μm in 60 min using a shim as a complaint float and fluid B. In addition, the reduction of removal rate with time that has usually occurred in MFP has not occurred [Chang and Childs, 1998]. However, the expense of a pre-manufactured resin-bonded grinding shaft was the disadvantage associated with this method. Also surface defects were reported

CHAPTER 3

PROBLEM STATEMENT

As stated in the literature review (Chapter 2) it is clear that silicon nitride balls for bearing application has been successfully polished to meet industry standards using lapping and magnetic float polishing. But still advanced ceramic bearing have not been able to replace the conventional steel bearings. The reason being the high cost of machining or polishing. In case of MFP, the influence of the groove on sphericity was proved to be advantageous. However, re-machining of groove during initial and final polishing runs and setup for every polishing run were still laborious and time consuming. Further Chang and Childs [1998] have made an effort to modify the MFP apparatus and use it for non-magnetic fluid grinding (NFG). A high material removal rate (MRR), up to 5.3 μm/min and 3-4 μm sphericity was reported. However, acceptable surface finish accept was not addresses in their work. To overcome the long processing time and expensive abrasive costs in case of lapping and costly magnetic fluid and laborious alignment in case of MFP, a new method to finish silicon nitride balls taking the advantage of above mentioned technologies was developed. A sphericity of 1-2 μm, surface finish better than 15 nm and material removal rates in the range of 0.75 – 1.25 μm/min/ball were set as target in this investigation.

If this target is achieved, a new apparatus will be available for finishing silicon nitride balls.

This would set a base for future studies to finish silicon nitride balls in an economical way for bearing applications to meet ASTM standards.

Hence, it is the aim of the present study to design and processing develop an apparatus and methodology for finishing silicon nitride balls in an economical way. Thus, the following tasks were undertaken to accomplish the objective.

1. Understand the principles of magnetic abrasive finishing, magnetic float polishing, and lapping processes and design a new apparatus based on the advantages of all these process.
2. To use an integrated approach involving design of apparatus, identifying optimum polishing conditions, and process modeling to develop the technology.
3. To model all the components of equipment using 3-D modeling software, select the material for each parts, machine them *in-house*, assemble, install and align.
4. To design and fabricate lathe carriage attachment, in order to mount D.C. motor to provide an external drive to the polishing spindle.
5. Magnetic field analysis using COMSOL 3.2 Multiphysics FEM software to determine the layout of ½ in^3 magnets to achieve maximum radial magnetic flux density and intensity.
6. Designfixture for fabricating acrylic polishing plate to precise dimensions.
7. To identify the parameters involved in the polishing process.

8. Basic understanding of the finishing process to establish a connection between different parameters, such as material removal rate, roundness and surface finish. This includes study of factors effecting material removal, out-of roundness and surface finish.
9. Study the effect of groove formed on the bevel of the spindle during all the stages of the polishing process.
10. To provide details regarding the polishing of one batch of balls starting from the as-received condition to the final shape and size. This would provide a condition for finishing silicon nitride balls by this technology, serves as a benchmark to compare with current technologies, and aid in analyzing costs involved in producing one batch of balls for future studies.

CHAPTER 4

APPROACH

4.1 INTRODUCTION

Magnetic fluid is the basic ingredient in the MFP process, in which the fluid performs three functions [Childs and Moss, 2001].

1. It causes viscous drag on the ball that result in sliding between the ball and shaft.
2. In presence of magnetic field, it creates a very compliant loading system of the balls on the shaft.
3. It levitates the non-magnetic loose abrasive grits in the fluid, so as to be available for embedding in the shaft.

The high cost of magnetic fluid has been the biggest setback for this technology. Therefore, efforts were made in this study to develop a cost effective solution to finish silicon nitride balls by combining the principles of magnetic abrasive finishing, magnetic float polishing, and lapping. This method was named as unbonded magnetic abrasive polishing (UMAP).

The first step in developing the UMAP technology is to find an alternative non-magnetic viscous fluid which can replace magnetic fluid. In 2001, Childs and Moss reported that mixture of glycerin and water can be used as non-magnetic viscous fluid. It was shown that a non-magnetic viscous fluid provides the same viscous drag on the balls as the magnetic fluid.

Measured a wear co-efficient, K of 0.17 [Chang and Childs, 1998]. Further a compression spring can be used to generate flexible support to the float. Third function of the magnetic fluid was realized using unbonded magnetic abrasive to concentrate abrasive in the polishing zone under the action of the magnetic field. These abrasives are available for embedding in the spindle.

Vertical arrangement of the apparatus has been the common feature among lapping, MFP, and NFG. These apparatus were mounted on precision milling machines. If the present apparatus was to be built on the vertically milling machine, gravitation force would have posed serious challenge in achieving abrasive concentration in the polishing zone. In order to overcome the problem associated with vertical arrangement, a new horizontal apparatus was developed. To mount the apparatus, a lathe was used as the machine tool instead of milling machine.

In a lapping process, V-groove is provided on one or both the plates to obtain good sphericity. However, during the course of polishing in UMAP process, a groove was formed due to abrasive wear on the polishing spindle. This serves the same purpose of improving sphericity of balls.

In order to develop the UMAP technology, a systems approach consisting of combination of current ball polishing principles, magnetic abrasive principles, experimental and analysis work as shown in Figure 4.1 was used. This consisted of addressing the following concepts.

- Good understanding of the V-groove lapping, MAF, and MFP
- Equipment and fixture design

- Process parameter modeling
- Experimental study
- Magnetic field analysis (discussed in Chapter 5)

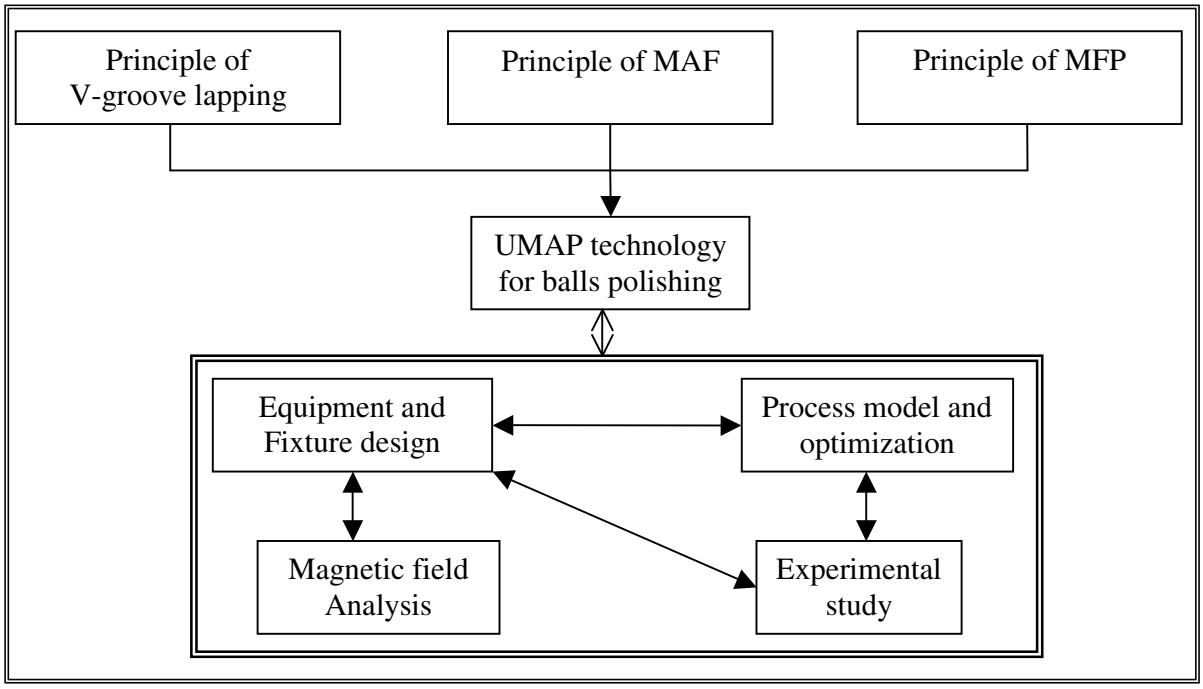

Figure 4.1 Steps involved in the development of UMAP of balls technology

Once principles of lapping, MAF and MFP were understood, the equipment and fixture were designed, fabricated and mounted on lathe. Next step was to carry out magnetic field analysis to obtain best magnetic field, by arranging ½ in^3 rare earth neodymium magnets in different ways. Then, experimental study was carried out to determine the load and the speeds required to obtain high MRR, sphericity, and finish. Once basic parameters were identified, equipment design was modified and polishing methodology was established using the present technology. Following is the description of the

various stages involved in the development of UMAP methodology for finishing Si_3N_4 balls.

4.2 GEOMETRIC DESIGN OF COMPONENTS

The primary design issue was to determine the geometry of various components, such as chamber, acrylic polishing plate, and spindle. Formulae listed in Table 4.1 were used to calculate the dimensions of each component. Approximate chamber inner diameter is obtained from direct measurement of average ball diameter to fit N balls.

In the present study 0.5 in. balls were chosen, Hence 0.5 in. magnet width was satisfactory to generate the required magnetic field. Raghunandan [1997] reported that magnetic flux density depends on the thickness of magnet. It was also shown that, when thickness of magnet is increased, the magnetization on the surface increases until the thickness equals two times the width [Raghunandan, 1997]. Beyond this point, no significant increase is obtained. Therefore ½ in^3 magnets were used in the present investigation.

Table 4.1 List of formulae for basic design
[after Raghunandan, 1997].

Minimum ball radius	r_{bmax} (given)
Maximum ball radius	r_{bmin} (given)
Average ball diameter	$D = r_{bmax} + r_{bmin}$
Number of balls	N (depends on chamber & ball dia.)
Chamber inner radius	R_c (given)
Chamber outer radius	$R_{couter} = R_c$ + (0.4 to 0.6 in.)
Acrylic polishing plate	$R_{Plate} > R_c - r_{bmax}/2$
Chamfer angle	θ (given)
Shaft outer radius	$R_{souter} > R_c - (1 + \sin(\theta))r_{bmax}$
Spring outer radius	$R_{SpringOuter} \approx 0.75\ R_{Plate}$
Shaft inner radius	$R_{sinner} < R_c - (1 + \sin(\theta))r_{bmax}$
Magnet width	$W \leq 2\ r_{bmin}$

4.3 PROCESS PARAMETER STUDY

This section deals with identifying the basic process parameters and various steps involved in process optimization. Figure 4.2 summarizes the important parameters useful for the development of process. Some of the important process parameters of interest are the spring loading compliance, abrasive size and type, polishing plate speed, spindle speed, liner joint, magnetic powder size, and viscosity of non-magnetic fluid. It should be noted that there are large number of parameters and the account of their mutual influence on one another was outside the scope of present study. For example, viscosity of non-

magnetic fluid was reported as 0.17 [Childs and Moss, 2001], but on addition of magnetic particle the viscosity will change. Such cross influencing parameters were not included.

Childs [1995] and Raghunandan [1997] classified MFP as 3-body polishing model because loose abrasives were held between polishing pad and the worksurface. UMAP process works on the same principle as MFP. Hence, UMAP can be categorized into 3-body polishing model. Material removal can be described in terms of 2-body or 3-body abrasion. Specifically, polishing falls into 3-body abrasion category while grinding falls into 2-body abrasion. Further, researchers have assumed that the material removal occurs due to indentation fracture, scratching, plastic deformation, chemo-mechanical action, or combination of these mechanisms. Therefore, by choosing process parameters similar to that of MFP; high material removal, good sphericity, and surface finish can be achieved.

The first step was to identify the polishing parameters that can be closely linked to make meaningful descriptions. For example, magnetic field analysis helps to define the dimensions of the magnets and their arrangement.

Number of balls in a batch can be determined by initial geometric analysis of the ball diameter and chamber dimensions. Similarly, material removal behavior can be studied by knowing physical and chemical properties of the workmaterials, and the abrasive particles. Interaction of balls with various elements in contact accounts for the ball-motion study. Further, flash temperatures during polishing facilitates for chemo-mechanical polishing. The

thermal analysis related to surface finish was already addressed by Hou and Komanduri [1998a, b, c]. Accuracy and alignment of apparatus can be directly related to the sphericity of the finished balls.

In this investigation, magnetic field analysis was carried out using COMSOL FEM tool to determine the parameters associated with the magnetic aspects. Also, ball motion mechanism has been assumed to be the same as the one reported by Childs *et al* [1994a]. Experimental studies were conducted to identify the effect of various process parameters on polishing performance. Specifically, various factors effecting sphericity were analyzed. Suitable experiments were performed to find out the effect of magnetic field on the removal rates. Similarly, influence of spindle bevel on surface finish of balls was determined. This knowledge based extensive experimentations have helped in identifying the optimum polishing parameters to achieve the desired outputs.

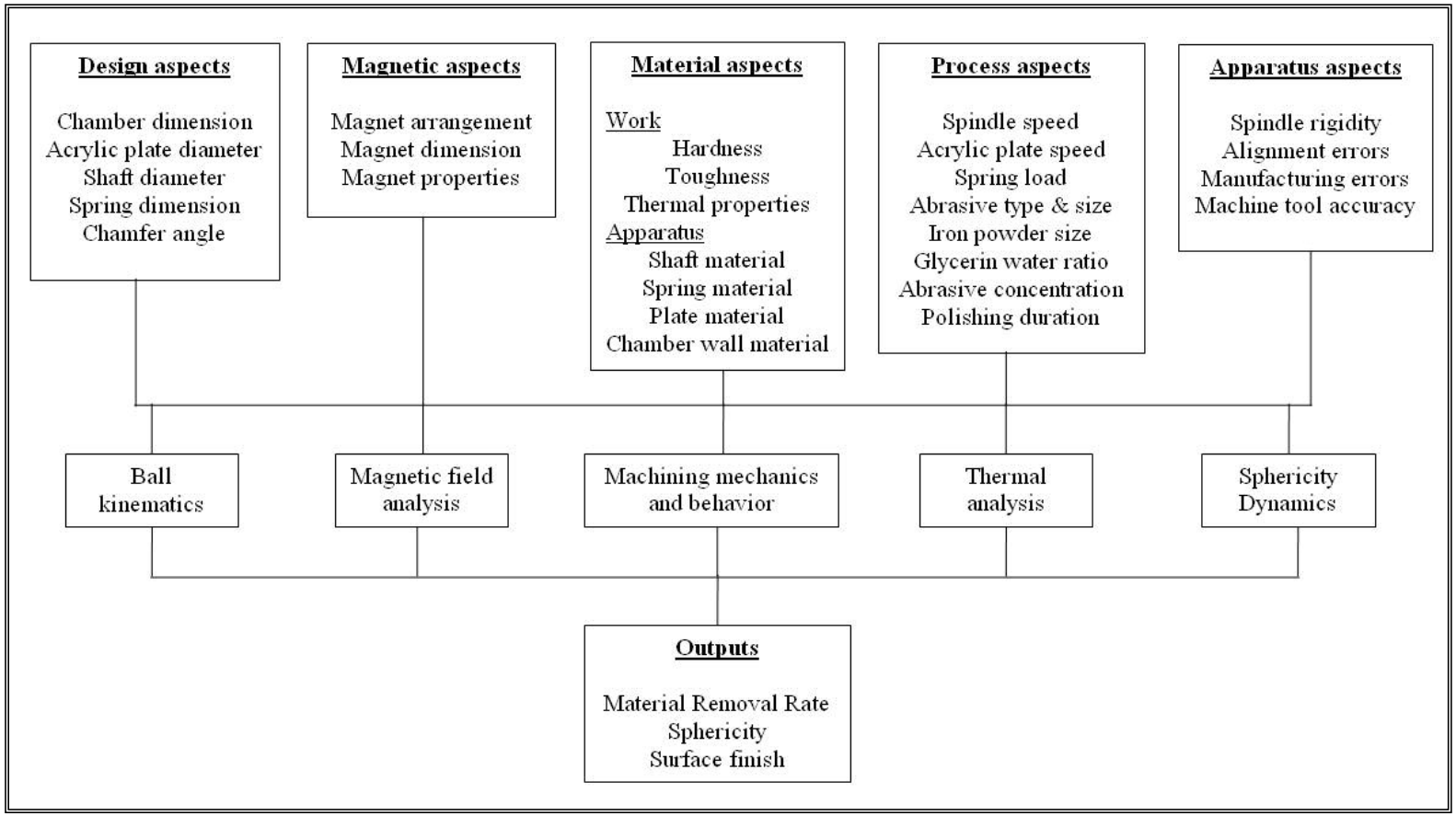

Figure 4.2 Process parameters analysis of UMAP

4.4 EXPERIMENTAL STUDY

This section discussion various experimental conditions involved UMAP. Table 4.2 shows the details of typical test conditions used in this study. The emphasis was to determine the material removal rate, sphericity and surface finish values.

Table 4.2 Polishing conditions

Workmaterial	HIP – Silicon Nitride
Magnetic abrasive	Mixture of abrasive and magnetic powder
Abrasives	B_4C, SiC, CeO_2
Abrasive size	1 – 40 μm
Magnetic powder	Fe
Magnetic powder size	< 44 to 297 μm
Abrasive to Magnetic powder ratio	0.4 : 1 to 0.5 : 1
Carrier fluid (Non-magnetic Fluid)	Mixture of glycerin, de-ionized water and rust inhibitor
Vol. of glycerin in each run	15 – 20 ml
Vol. of water in each run	20 – 30 ml
Magnetic abrasive to carrier fluid ratio	1 : 2
Polishing duration	90 – 180 minutes
Magnet	Rare earth Nd-Fe-B (Neodymium Magnet) Dimension : ½ X ½ X ½ in^3
Load	2 – 6.5 N/ball
Speeds	600 – 1000 rpm
Machine tool	Lathe

4.5 COMPLETE PROCESS DESIGN

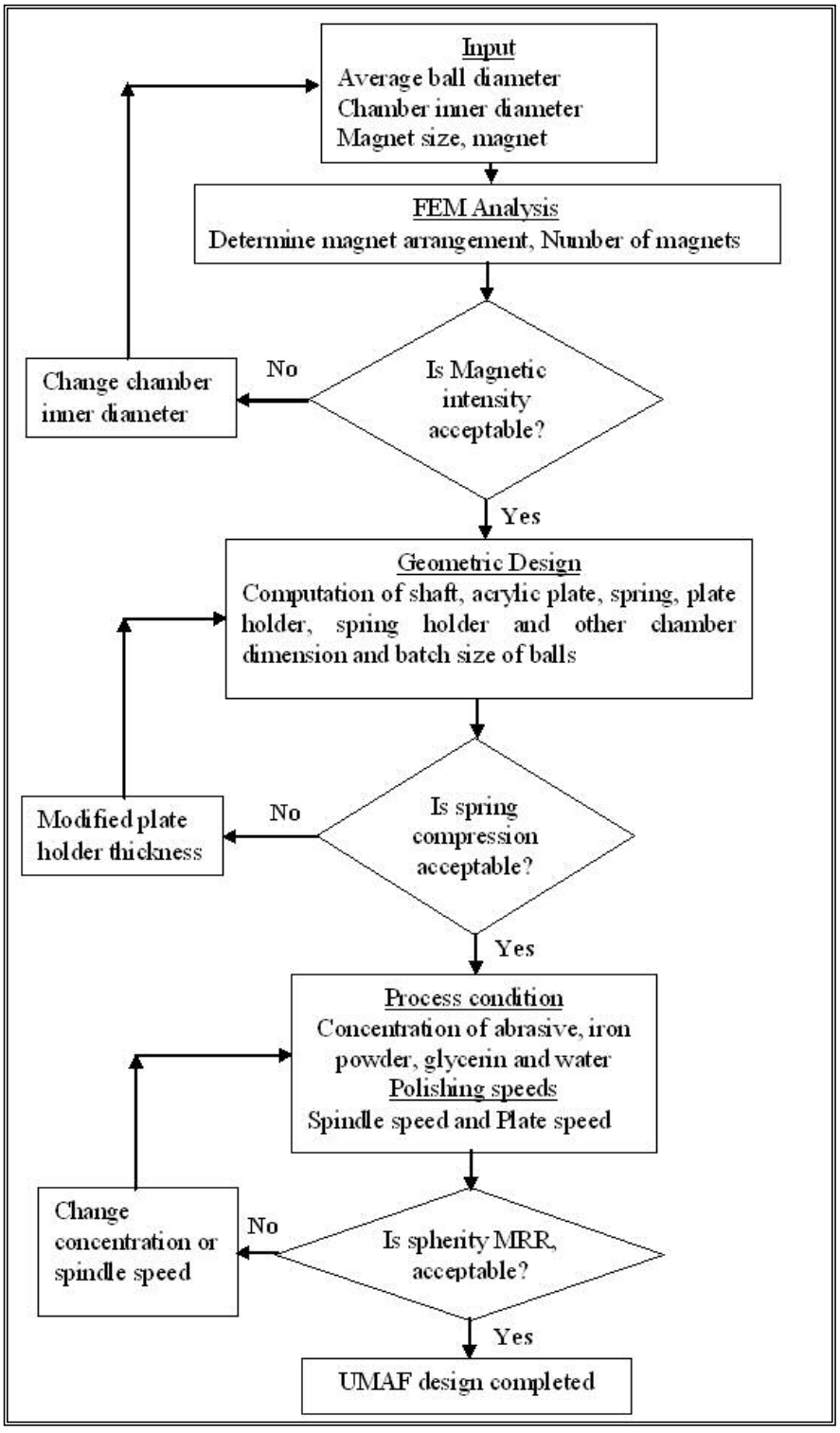

Figure 4.3 Flow chart for the development of UMAF Process design

The output from the last three sections can be further processed to design a complete model for UMAP technology. Figure 4.3 sows the flow chart indicating the steps involved in the complete design of UMAP process these steps are listed in the following:

1. Process starts with inputs, which includes average ball diameter to be processed, chamber ID and size of magnet.
2. Multiple FEM analysis (discussed in Chapter 5) was carried out to determine the number of magnets required and their arrangement to generate uniform and strong magnetic field.
3. If magnetic flux obtained was not acceptable then chamber ID was modified.
4. Chamber inner diameter was modified to obtain required magnetic flux density. This will prevent magnetic abrasive dispersion or scattering
5. Next, basic dimensions of the components are calculated using formulae given in table 4.1.
6. Plate holder thickness is directly proportional to the load applied. Therefore, appropriate plate holder thickness has to be chosen to obtain the required load. If the plate holder thickness is not sufficient to generate required loading on the balls, additional plates of required thickness has to fixed to the plate holder along with acrylic polishing plate.
7. Then tests runs are carried out with approximate unbonded magnetic abrasive slurry and speeds.
8. If material removal rate (MRR) is low, then abrasive slurry concentration, speed and load were varied until the desired MRR is obtained.

9. If sphericity is bad at a given speed, experiments have to be conducted at different speeds. However, it is important to identify the maximum speed at which apparatus is stable.
10. Once all the parameters and polishing conditions are identified modeling is completed.

Process involves some of the hidden parameters such as ball kinematic, different magnet size, iron powder size, viscosity which are not included in this study.

CHAPTER 5

MAGNETIC FIELD ANALYSIS

Experimental or manual determination of magnetic intensity can take considerable time. Hence, finite element analysis is efficient tool to aid in the simulation of different arrangements of the magnets. In order to determine the flux density and field intensity in the working zone using ½ in^3 magnets. Figure 5.1 is the flow chart indicating the steps involved in the magnetic analysis.

The objective of FEA was to develop ways to increase the magnetic field intensity in the polishing zone. Material properties, dimension description and placement decide the accuracy of the analysis. Commercially available COMSOL 3.2 Multiphysics FEM software was used for magnetic field analysis in this investigation.

COMSOL Multiphysics is a powerful interactive environment for modeling and solving different types of scientific and engineering problems based on partial differential equations (PDEs). This software extends conventional models for one type of physical model into multiphyscal models that solve coupled physical phenomena—and do so simultaneously. Accessing this power does not require an in-depth knowledge of mathematics or numerical analysis. The built-in physics

make it is possible to build models by defining the relevant physical quantities—such as material properties, loads, constraints, sources, and fluxes—rather than by defining the underlying equations. COMSOL Multiphysics then internally compiles a set of PDEs representing the entire model. COMSOL 3.2 provides CAD import modules for importing CAD data using all popular formats: Parasolid®, SAT®, STEP, IGES, CATIA® V4, CATIA® V5, Pro/ENGINEER®, Autodesk Inventor®, and VDA-FS [COMSOL Multiphysics user's guide].

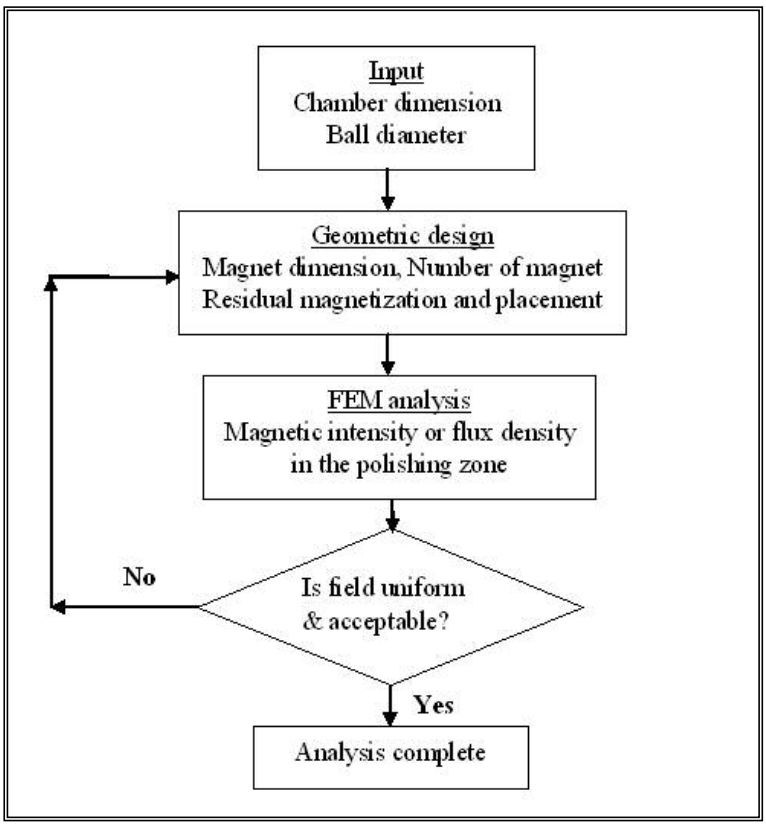

Figure 5.1 Flow chart for the magnetic field analysis

Normal method for a FEA can be described in four steps.

1. Model building
2. Specifying material properties

3. Obtaining solution

4. Reviewing the results

5.1 MODEL BUILDING

The 3-D model of the arrangement of magnets on the inner surface of either magnetic or non-magnetic pipe was created using Pro-E. 3-D model was converted to 2-D CAD file. Next, initiate COMSOL 3.2 > 2D > Application modes > COMSOL multiphysics > Electromagnetics > Magnetostatics and CAD file was imported. Then the objects were split in such way that each magnet and pipe can be identified as different entities. A square boundary was generated around the model. Its property was considered as that of air (μ_r=1). A common modeling session is followed to establish general outline of modeling.

In this study, four models have been analyzed to obtain the optimum solution. Table 5.1.1 gives the details of each analysis. The dimensions of each component have been maintained constant in all four models. However, number of magnets and property of the pipe was varied. Figure 5.1.1 shows the schematic of first model, in which 24 magnets of 0.5 in^3; with steel pipe of 5.1 in. ID and 6 in. OD has been used.

Table 5.1.1 Details of the models used for FEA analysis of magnetic field

Analysis number	Pipe Type	Number of magnets
1	Magnetic(steel)	24
2	Magnetic(steel)	14
3	Magnetic(steel)	12
4	Non-Magnetic(μ_r=1)	14

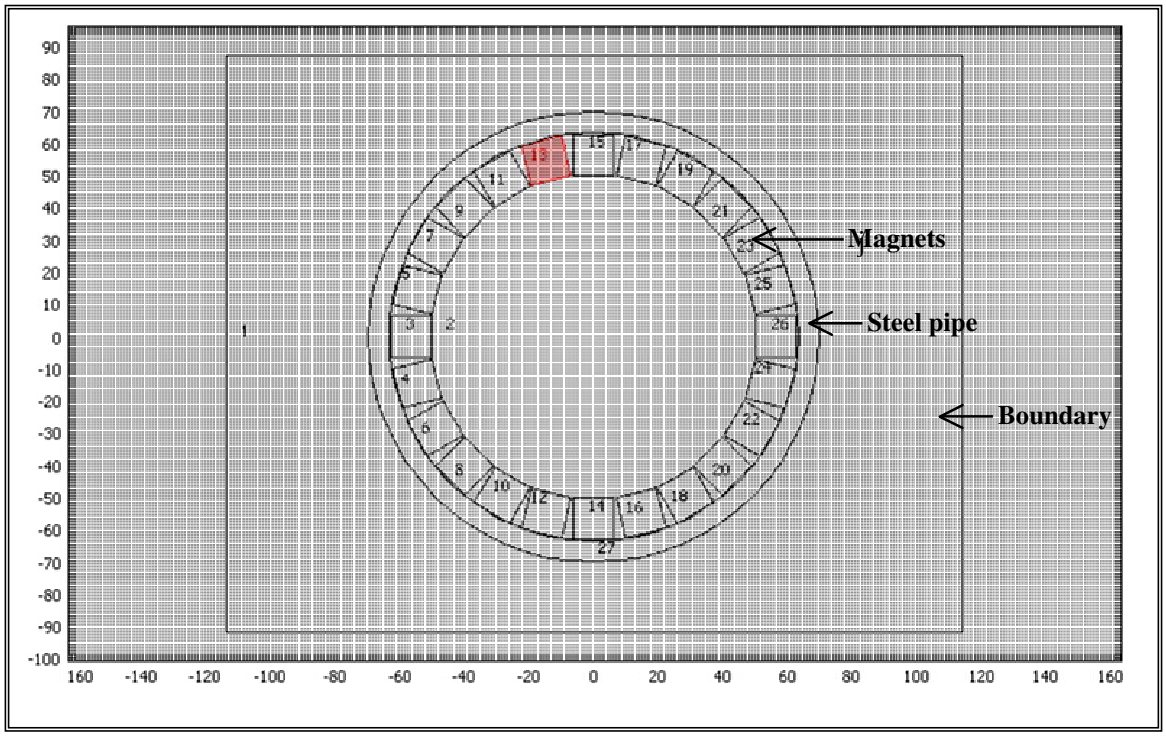

Figure 5.1.1 Schematic of thefirst model generated by COMSOL

5.2 SPECIFING MATERIAL PROPERTIES

The model consisted of following regions.

- Magnet
- Magnetic saturable material (steel pipe)
- Air
- Non-magnetic (plastic cubes)

The material properties (relative permeability, μ_r) of air and nonmagnetic regions were taken as 1 and for magnetic material it was taken as 800. Property of magnet depends on its remanent flux density. In the present model, magnets are arranged in the radial direction. Hence, the remanent flux has to be resolved into horizontal and vertical components, depending on the angular orientation.

Table 5.2.1 gives the values of the vertical and horizontal components. Figure 5.2.2 show the profile of resultant magnetization direction. This confirms that vertical and horizontal component values assigned to each magnet listed in Table 5.2.1 are correct. Arrows pointing towards the center indicates the N pole and arrow away from center indicates the S pole.

Table 5.2.1 Values of resolved remanent flux density

Number of Magnets	Angle (θ degrees)	Vertical component (SIN(θ) x Br)	Horizontal component (COS(θ) x Br)
1	0	0	1.25
2	15	0.323524	1.207407
3	30	0.625	1.082532
4	45	0.883883	0.883883
5	60	1.082532	0.625
6	75	1.207407	0.323524
7	90	1.25	7.66E-17
8	105	1.207407	-0.32352
9	120	1.082532	-0.625
10	135	0.883883	-0.88388
11	150	0.625	-1.08253
12	165	0.323524	-1.20741
13	180	1.53E-16	-1.25
14	195	-0.32352	-1.20741
15	210	-0.625	-1.08253
16	225	-0.88388	-0.88388
17	240	-1.08253	-0.625
18	255	-1.20741	-0.32352
19	270	-1.25	-2.3E-16
20	285	-1.20741	0.323524
21	300	-1.08253	0.625
22	315	-0.88388	0.883883
23	330	-0.625	1.082532
24	345	-0.32352	1.207407

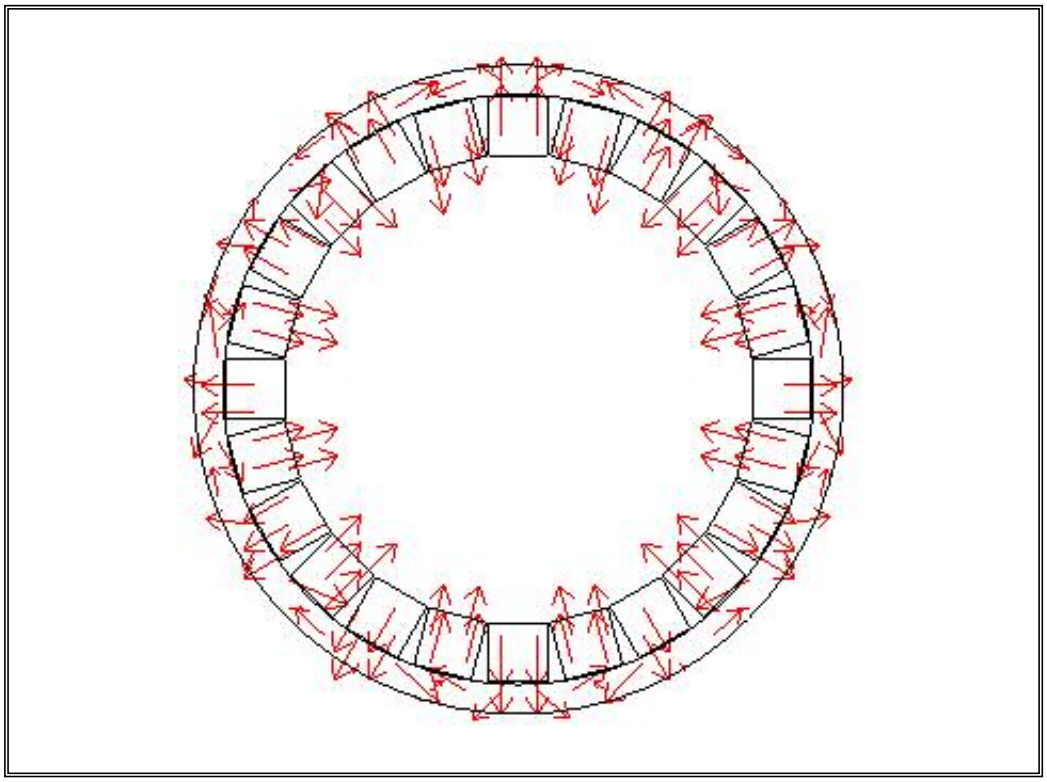

Figure 5.2.2 Schematic showing resultant magnetization direction

5.3 OBTAINING SOLUTION

This section present the sub-domain setting and postprocessor which are needed in order to obtain the desired results. Once the model has been built and material properties have been assigned, the next step involves setting up pre-processing properties. This includes properties, such as mesh parameters, mesh statistics (degrees of freedom, boundary elements), element type, analysis type, variables, boundary settings, subdomain settings and solver settings. But, in the case of COMSOL 3.2 suitable properties is assigned by the software itself depending on the multiphysics model selected. Default element and analysis type assigned are Lagrange-quadratic and static, respectively.

Figure 5.3.1 show the default mesh generated for this model. Fine mesh was generated in and around the magnet. Progressively coarser mesh was generated as we move away from the magnet. Figure 5.3.2 shows the surface profile of magnetic flux density distribution. The color code indicates the value of the flux density. Minimum and maximum values of the color codes can be varied in the post processor, but after a number of iterations these values were set to $1x10^{-9}$ to 0.5 Tesla or ($1x10^{-8}$ - 5 KGauss), respectively. Figures 5.3.3 and 5.3.4 show the plot of flux density and intensity with radial length from the center, respectively.

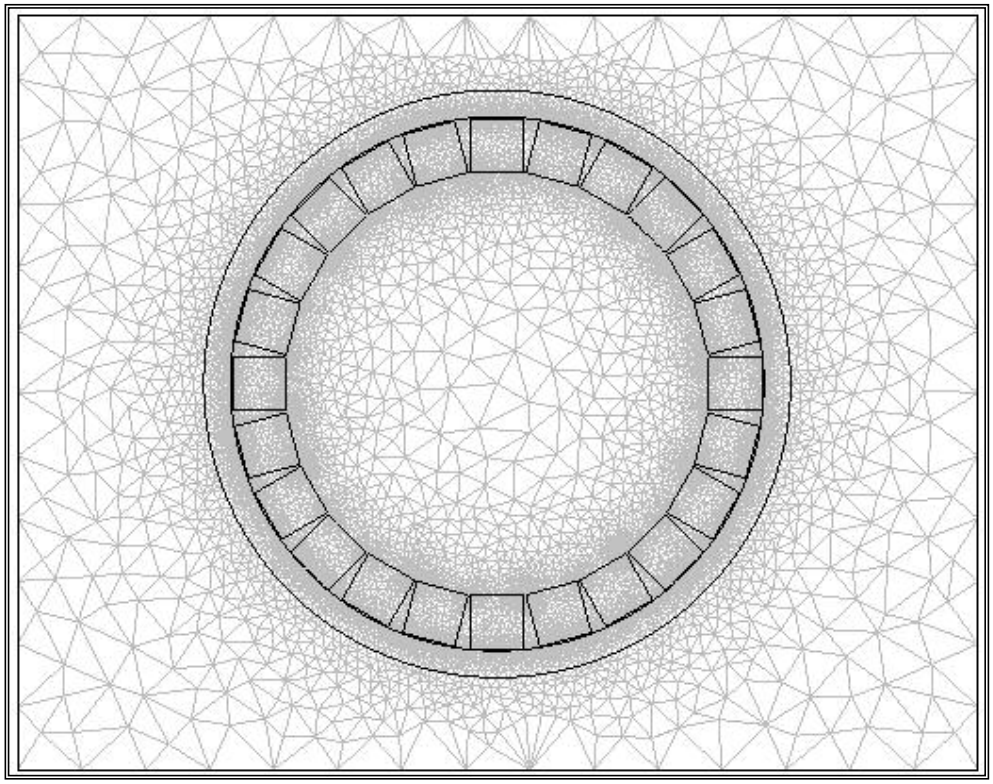

Figure 5.3.1 Schematic showing the mesh distribution

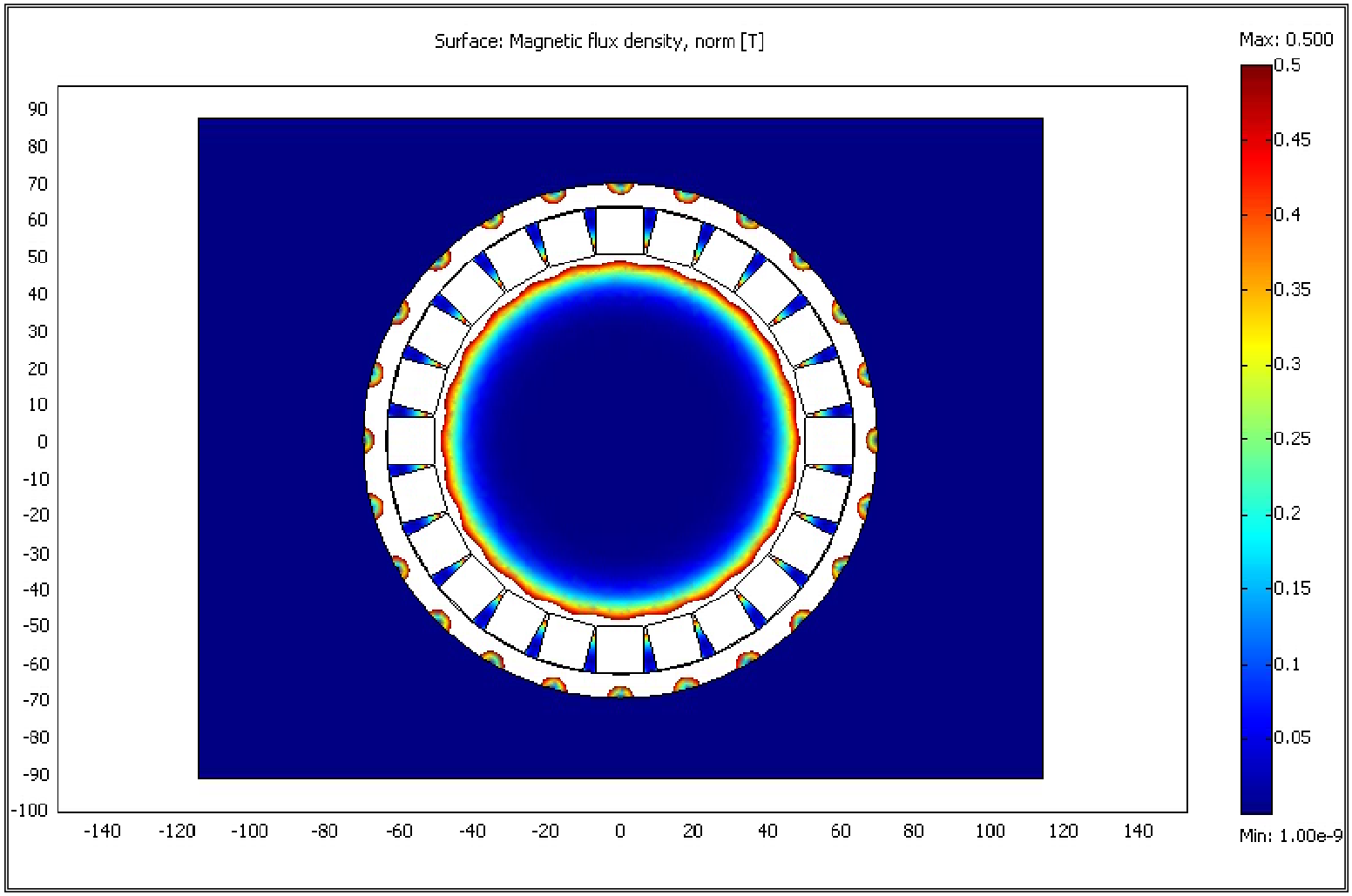

Figure 5.3.2 surface plot of magnetic flux density for first model with 24 magnets and a steel pipe

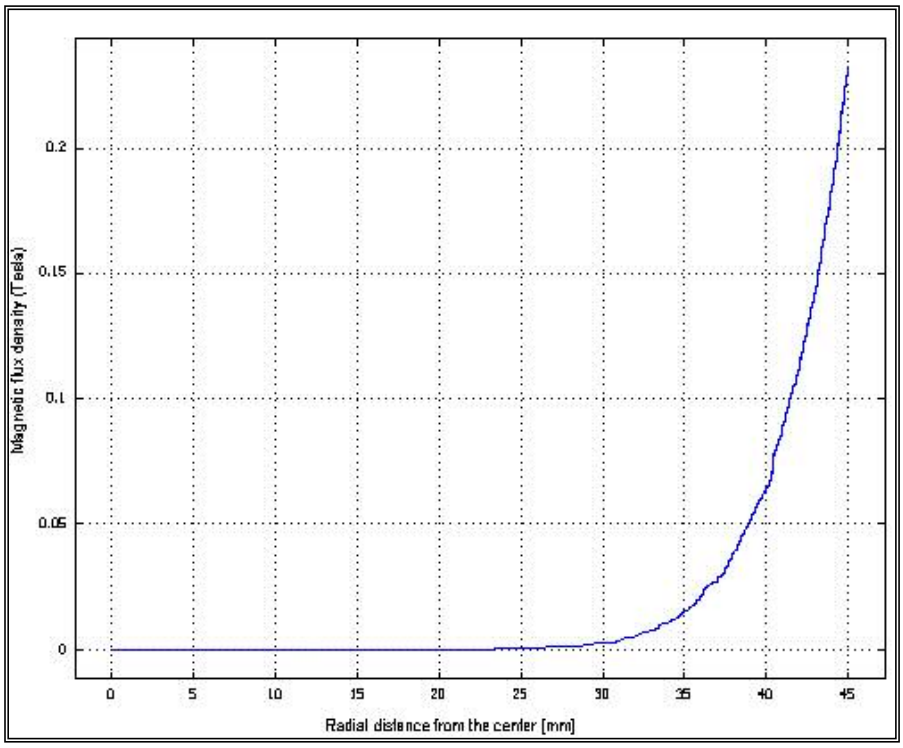

Figure 5.3.3 Magnetic flux density plot for the first model with 24 magnets

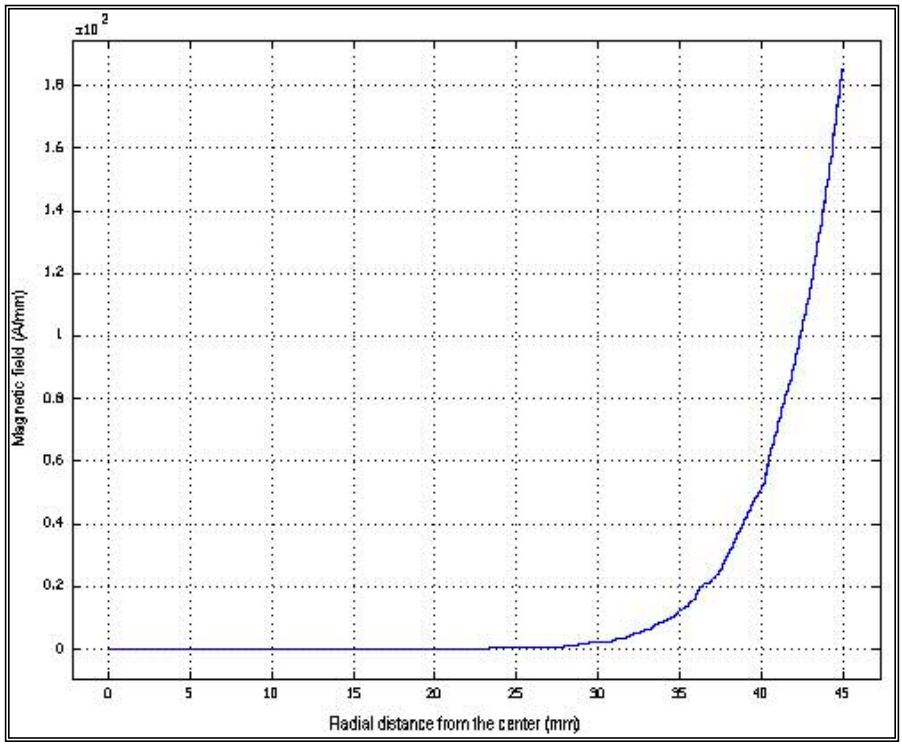

Figure 5.3.4 Magnetic field plot for the first model with 24 magnets

In order to compare the results and decide on the best arrangement similar results were generated for rest of the three models. Therefore similar surface plots and graphs were generated.

Figures 5.3.5 - 5.3.7 show the surface plot, flux density graph and magnetic field graph for model-2, which includes steel pipe and 14 magnets, respectively.

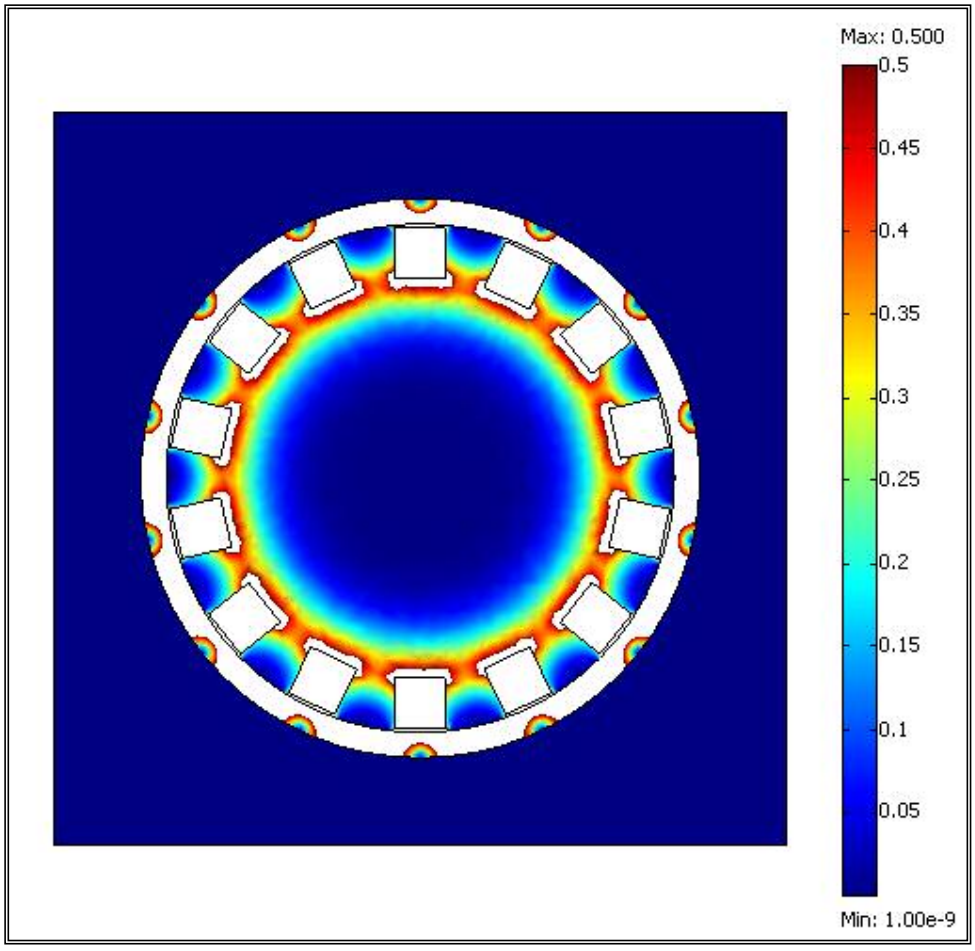

Figure 5.3.5 Surface plot of magnetic flux density for second model with 14 magnets and a steel pipe

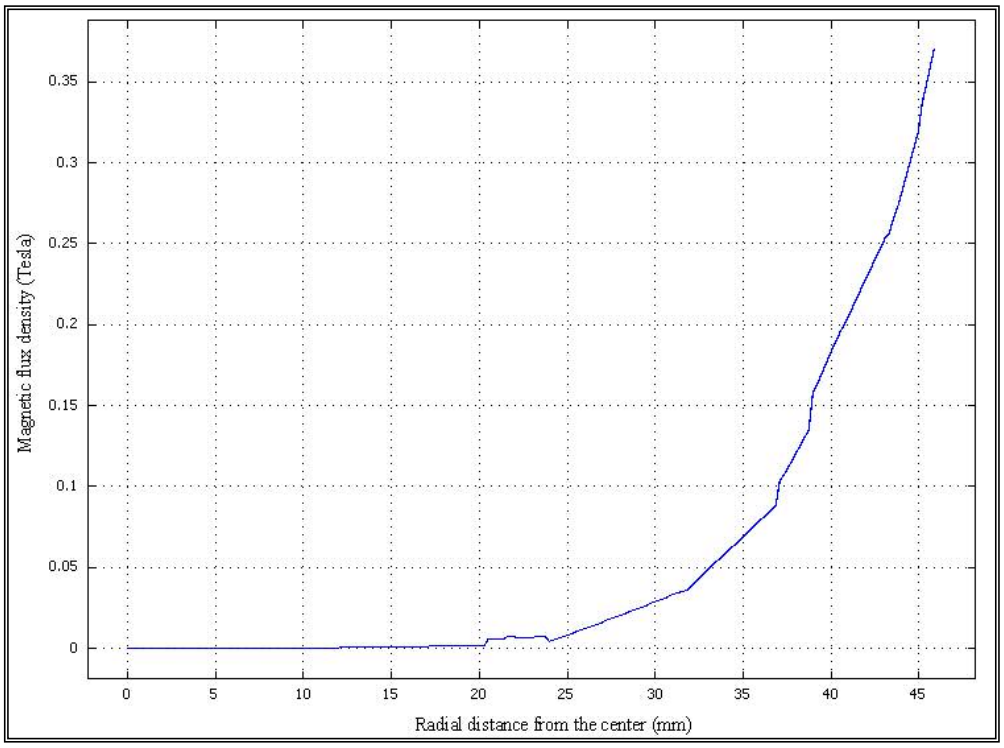

Figure 5.3.6 Magnetic flux density plot for the second model with 14 magnets

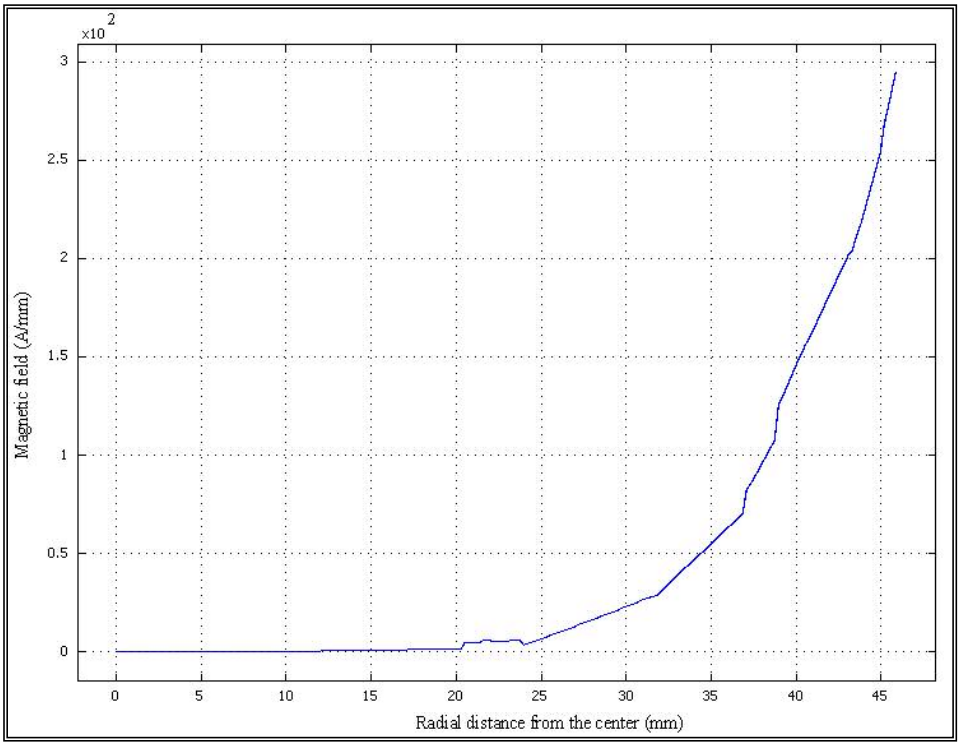

Figure 5.3.7 Magnetic field plot for the second model with 14 magnets

Similarly, Figures 5.3.8 - 5.3.9 show the surface plot, flux density graph and magnetic field plot for model -3, which includes steel pipe and 12 magnets, respectively.

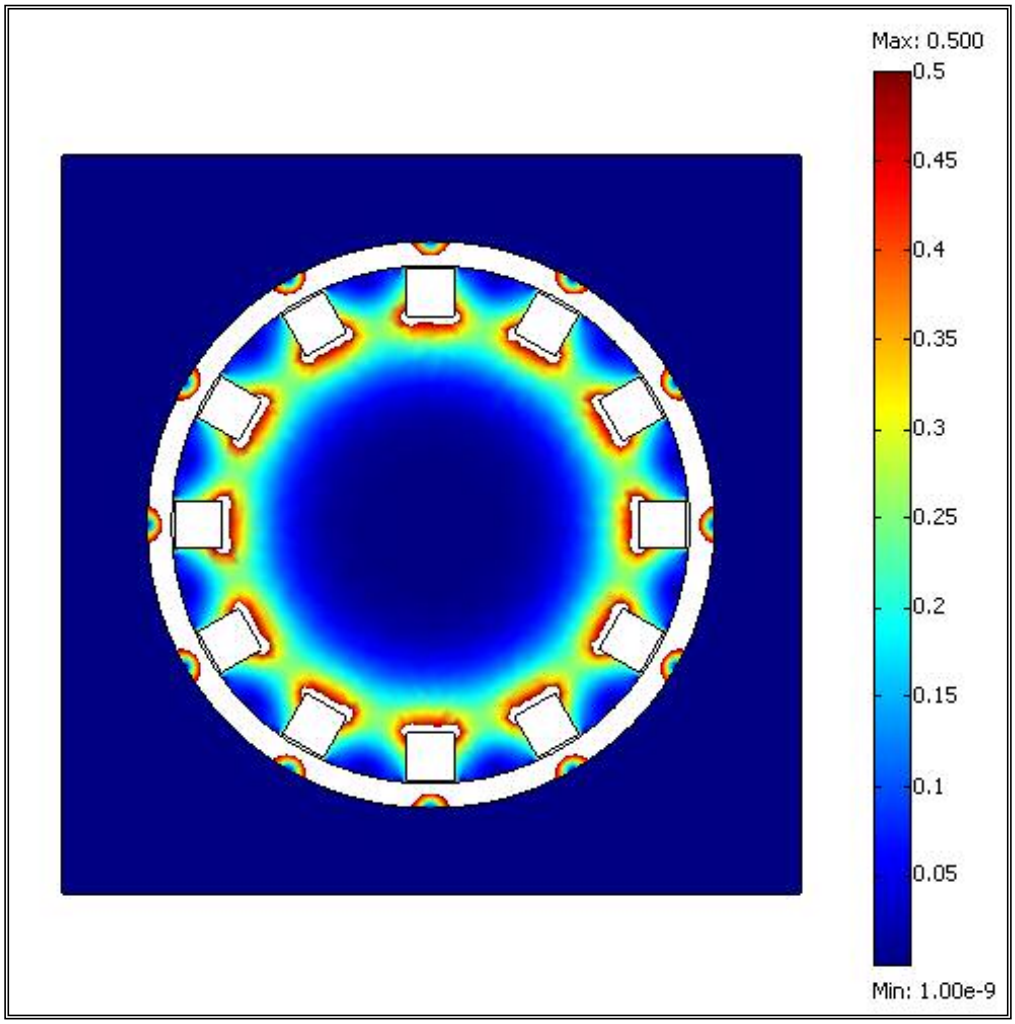

Figure 5.3.8 Surface plot of magnetic flux density for third model with 12 magnets and a steel pipe

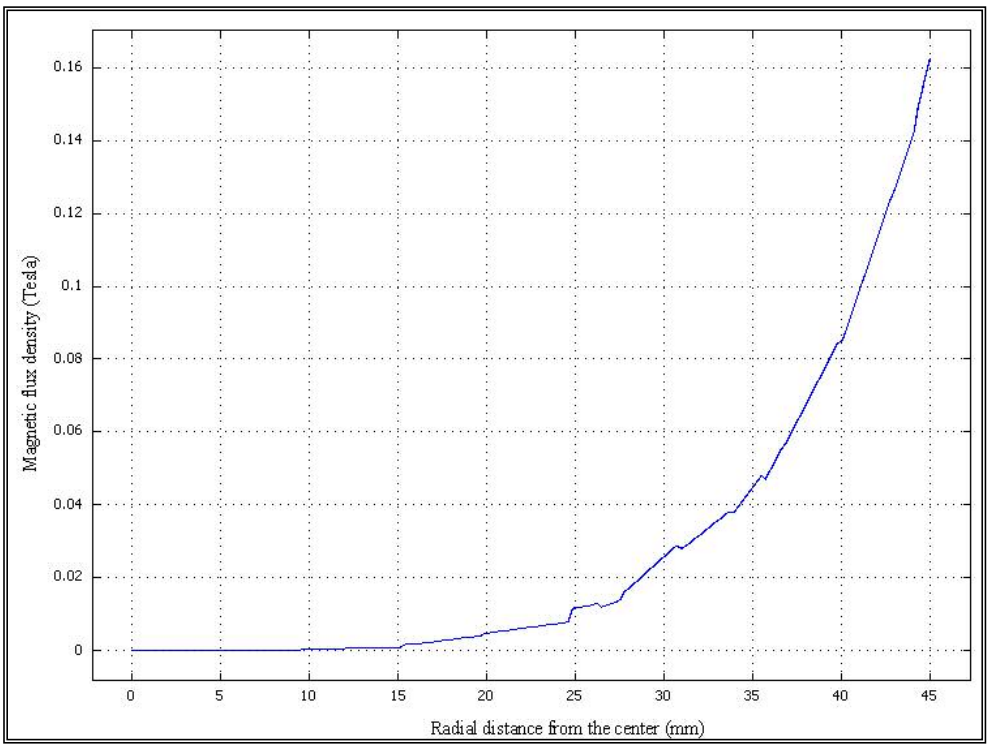

Figure 5.3.9 Magnetic flux density plot for the third model with 12 magnets

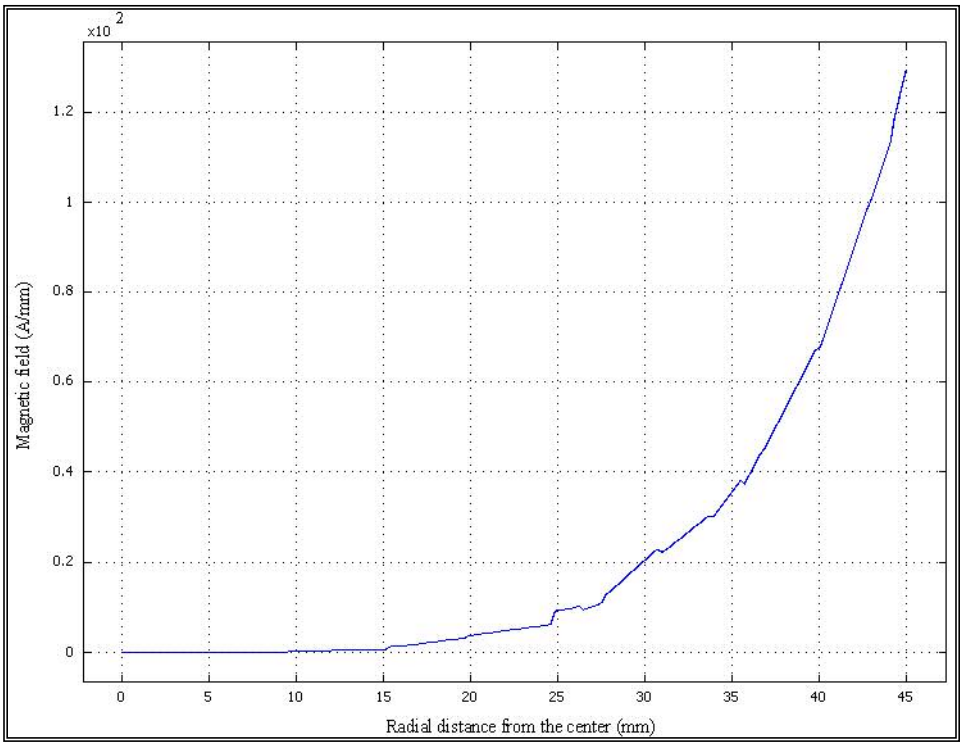

Figure 5.3.10 Magnetic field plot forthe third model with 12 magnets

Finally, Figures 5.3.11 - 5.3.13 show the surface plot, flux density graph and magnetic field plot for fourth model, with a non-magnetic pipe and 14 magnets, respectively.

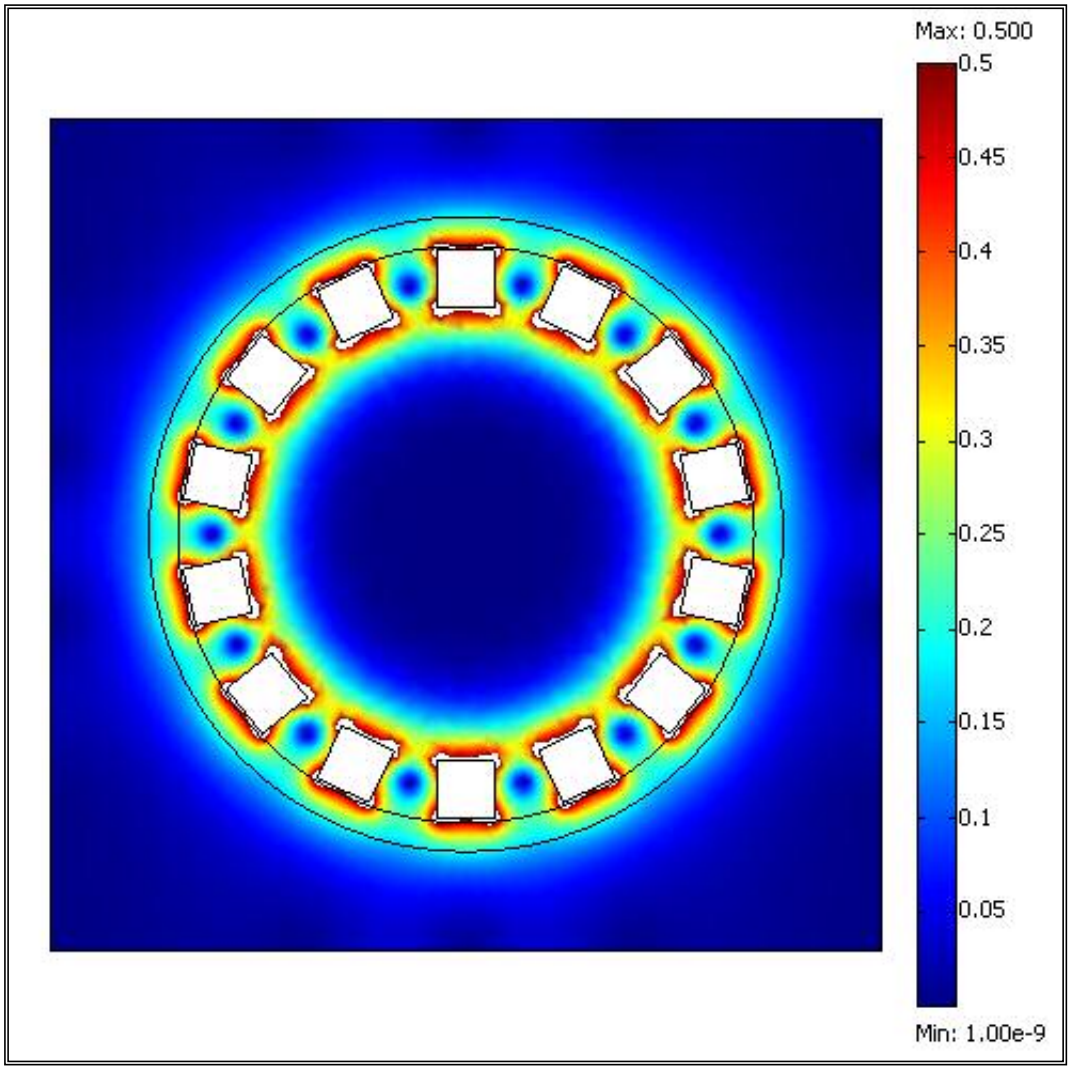

Figure 5.3.11 Surface plot of magnetic flux density for fourth model with 14 magnets and a non-magnetic pipe

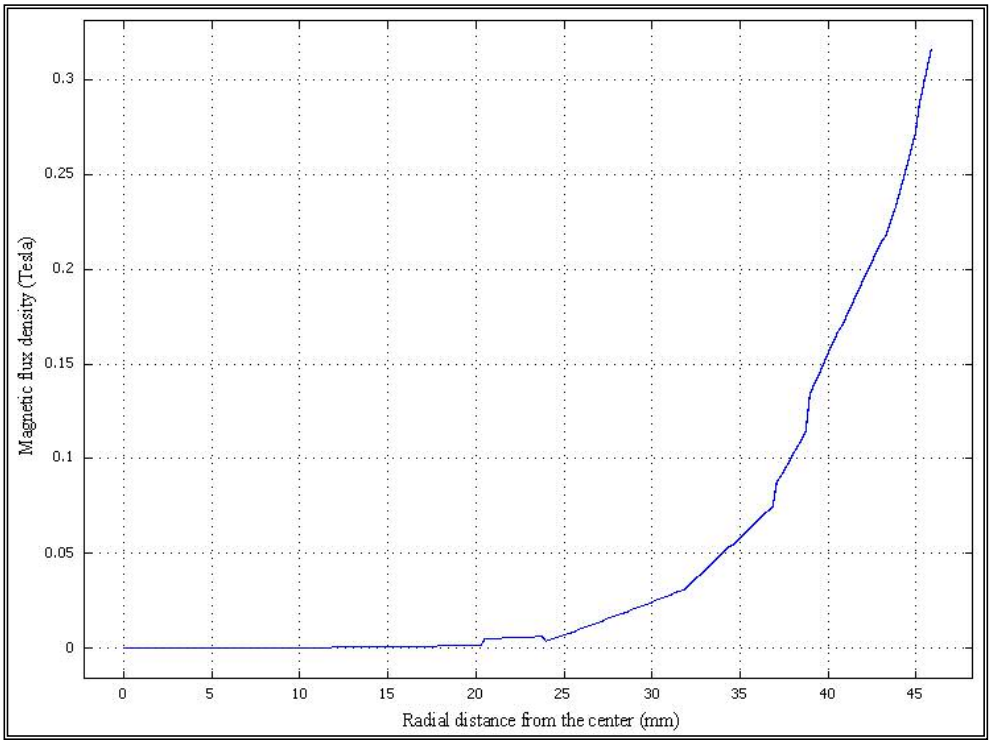

Figure 5.3.12 Magnetic flux density plot for the fourth model with 14 magnets and a non-magnetic pipe

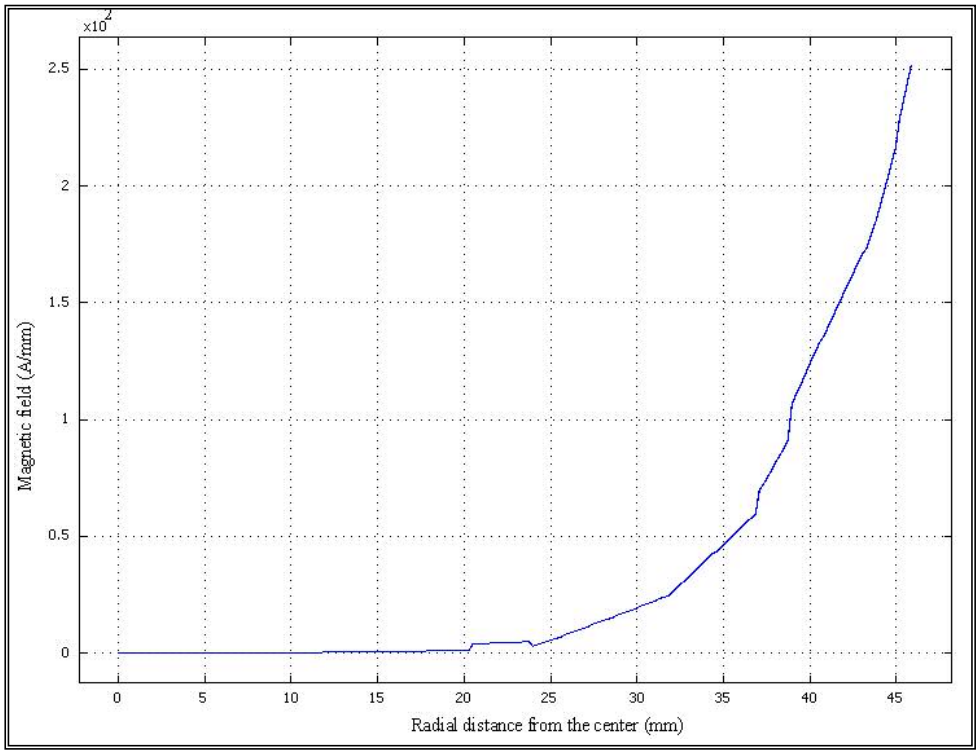

Figure 5.3.13 Magnetic field plot for the fourth model with 14 magnets and a non-magnetic pipe

5.4 REVIEWING THE RESULTS

The objective of this section is to draw conclusions based on the results presented in the previous section. A comparison is required to meet the objective. Table 5.4.1 gives the results of all the four models.

Table 5.4.1 Comparison of results generated by all the 4 models

Model No.	Magnetic flux density (Tesla at 45 mm)	Magnetic field (A/mm at 45 mm)	Flux density Surface plot
1	0.23	1.85×10^2	Partially uniform
2	0.35	2.5×10^2	Uniform
3	0.16	1.3×10^2	Uniform
4	0.27	2.2×10^2	uniform

By analyzing the results obtained, it was concluded that model two generates maximum value of flux density and normal magnetic field as compared to other three layouts. Also, it generates uniform magnetic flux density. Hence, the second layout with 14 magnets arranged around 5 in. ID steel pipe was used for this investigation.

CHAPTER 6

UNBONDED MAGNETIC ABRSIVE POLISHING APPARATUS

This Chapter provides details of the equipment design, *in-house* fabrication, assembly, installation and alignment of the components. Figure 6.1 shows the 3-D sectional view of the apparatus and Figure 6.2 shows the full and exploded view of the apparatus. The apparatus was designed and *in-house* machined for the present study. It should be noted that the final design of all the components was the outcome of multiple design iteration.

6.1 COMPONENTS

Major components of UMAP system are listed below:-

- Machine tool
- Chamber accessories
    - Non-magnetic Chamber
    - Spring holder
    - Acrylic polishing plate
    - Plate holder
    - Chamber cover
    - Urethane liner for wear prevention
- Spindle
    - Non-magnetic 304 stainless steel spindle

    - Spindle carrier
- Spindle drive attachment
    - Lathe carriage attachment
    - Motor and adjustable speed drive
- Spring
- Magnet layout

6.1.1 MACHINE TOOL

Machine tool used in the study was KENT USA KLS-1740 Gear headed Lathe with 12 speeds, varying from 32 to 1800 rpm. In order to mount the chamber accurately a 4-jaw chuck was used on the lathe.

6.1.2 CHAMBER ACCESSORIES

Chamber assembly forms an essential part of the apparatus. It includes chamber, spring holder, polishing plate, plate holder, and chamber cover. In the following paragraphs each of these components are explained in detail with schematics and dimensions.

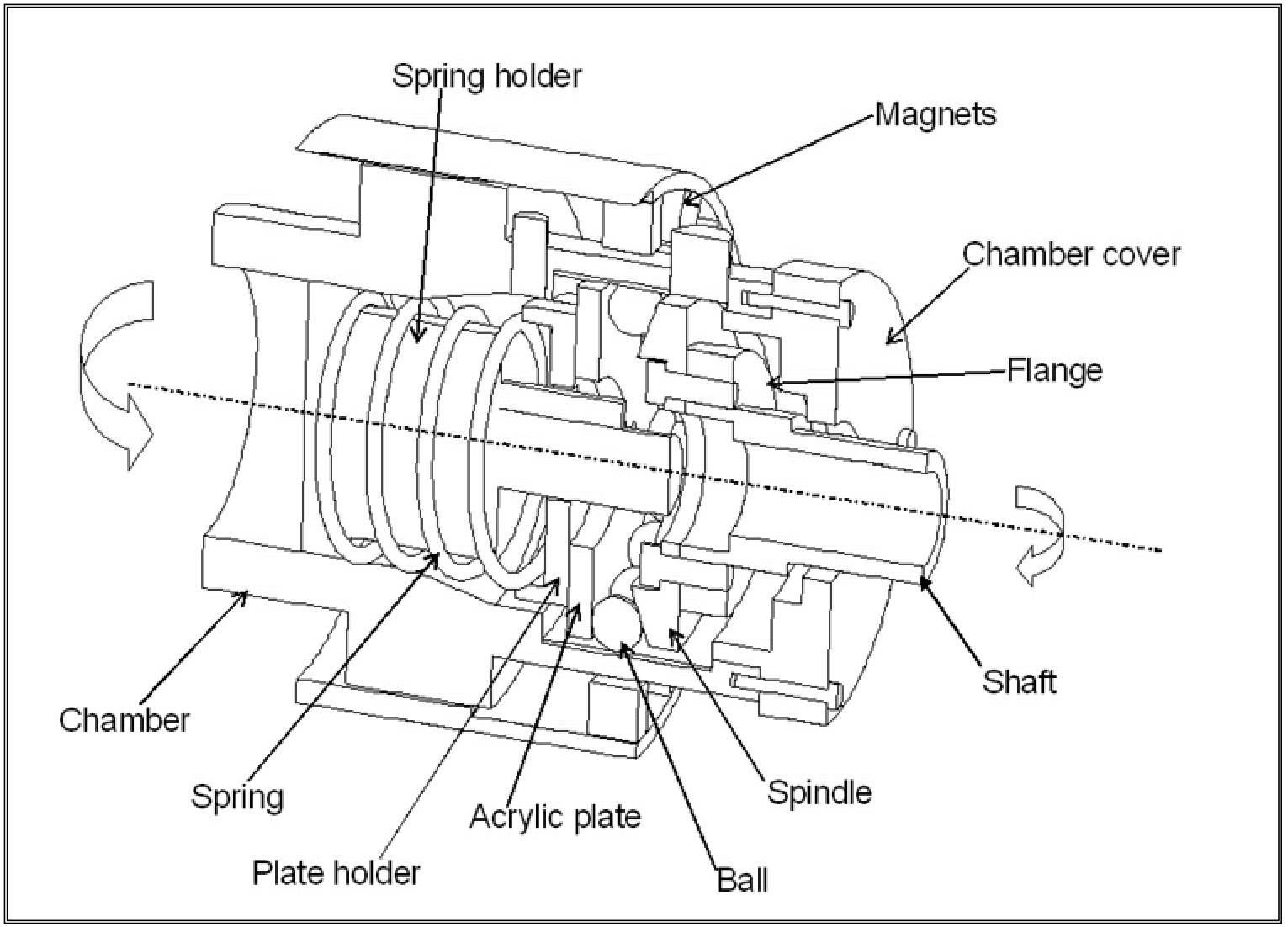

Figure 6.1 3-D cut sectional view of UMAP apparatus

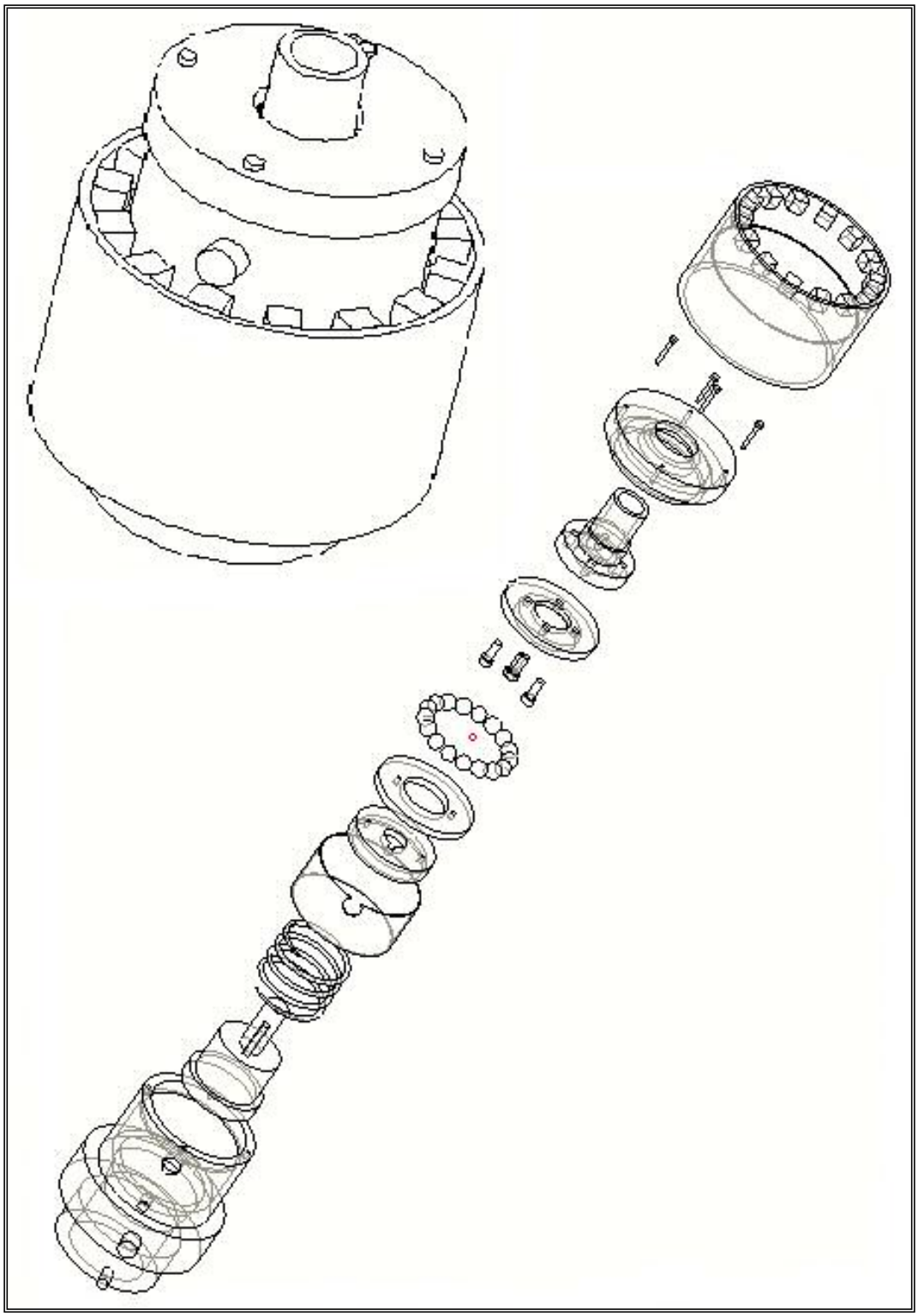

Figure 6.2 Full and exploded view of the UMAP apparatus

1. Non-magnetic chamber

The non-magnetic chamber forms the back bone of the apparatus. Aluminum, being non-magnetic and easier to machine, were used for chamber fabrication. Ball diameter to be polished and spring length was the key considerations for chamber design. Ball diameter and number of balls decides chamber inner diameter and spring length was used to determine its working length. Figure 6.1.1 is a multiview schematic showing drawing of the polishing chamber with dimensions.

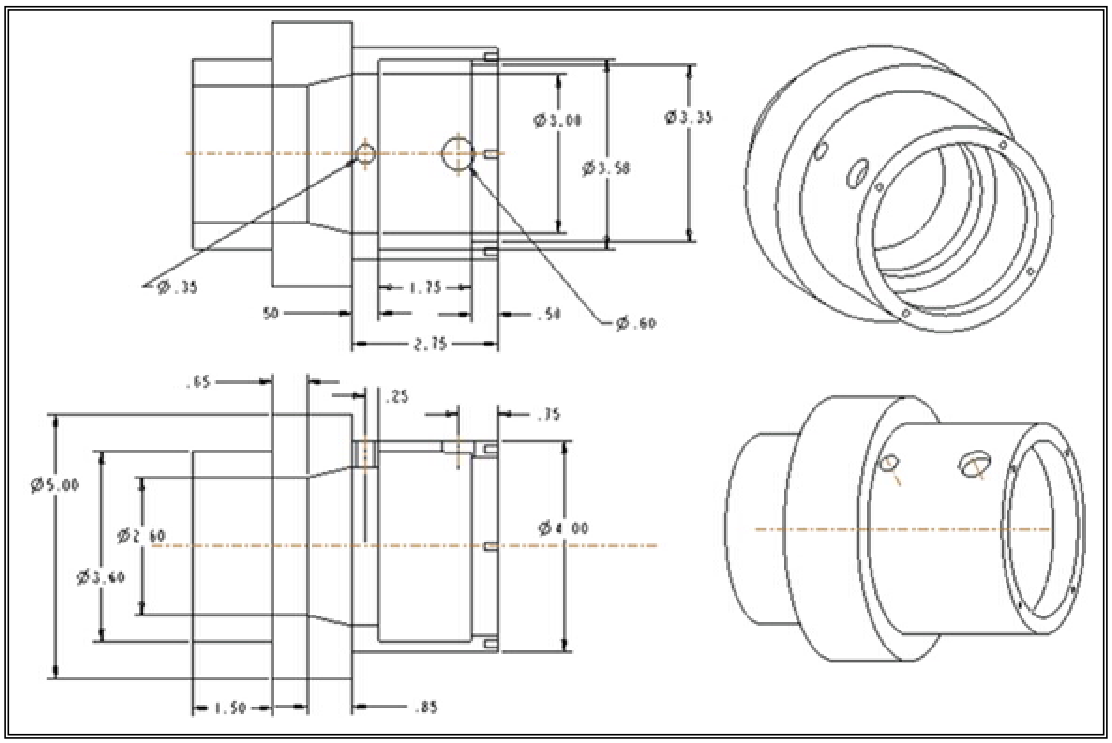

Figure 6.1.1 Multiview drawing of chamber with dimensions

2. Spring holder

Spring holder was co-axially pressure fitted to the polishing chamber. Spring holder serves two purposes; 1) It supports the spring coaxially with chamber and spindle 2) It locks the acrylic polishing plate holder, in order to

rotate the acrylic polishing plate and plate holder at the speed of chamber. Figure 6.1.2 gives details of spring holder.

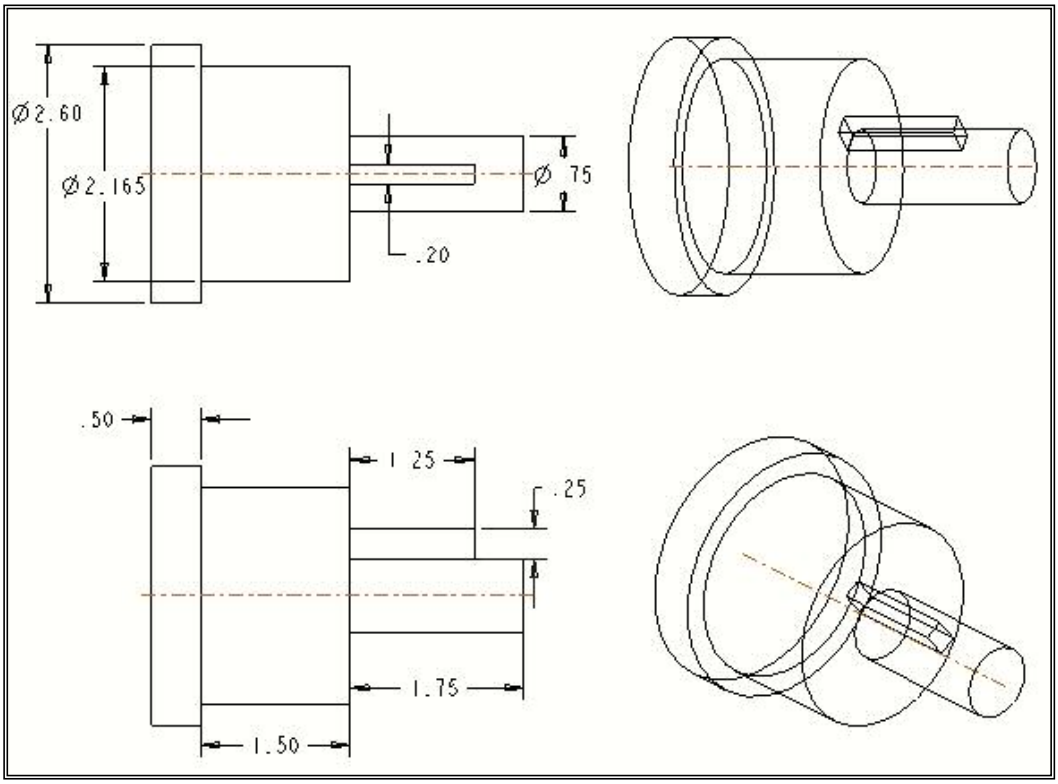

Figure 6.1.2 Multiview drawing of spring holder with dimensions

3. Acrylic polishing plate

Acrylic plate serves the same purpose as float in MFP, the only difference being the loading method. In MFP, loading was accomplished by magnetic levitation force. This force provides flexible support to the float and the balls inside the chamber. In UMAP, plate was screwed to plate holder, which was supported by a spring fixed on the spring holder. On compressing the spring, plate holder gets itself locked to the key provided on the spring holder. Plexiglas was used as the polishing plate material. Figures 6.1.3 and 6.1.4 show the

drawings of the acrylic polishing plate and photograph of the fixture used to machine the polishing plate, respectively.

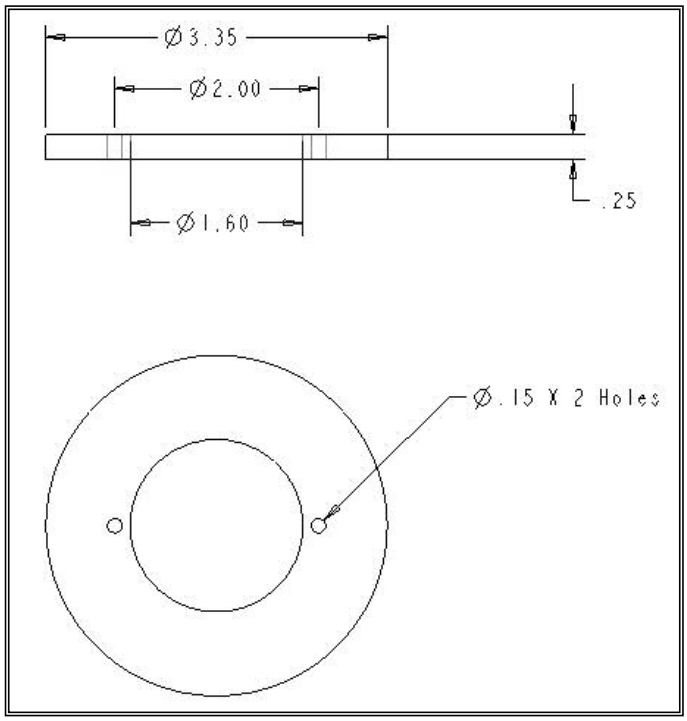

Figure 6.1.3 Multiview drawing of acrylic polishing plate with dimensions

Plexiglas sheet was initially cut approximately to circular shape on a band saw machine and mounted on a fixture. It was then machined to the required outer diameter. Two holes were drilled at 2 in. apart so as to screw it on to the plate holder. Finally, central opening of 1.6 in. diameter was machined. Careful machining was carried out to obtain smooth machined edges. This is possible only by machining at very low-speed. Care was taken to avoid any scratches on the surface of the plate.

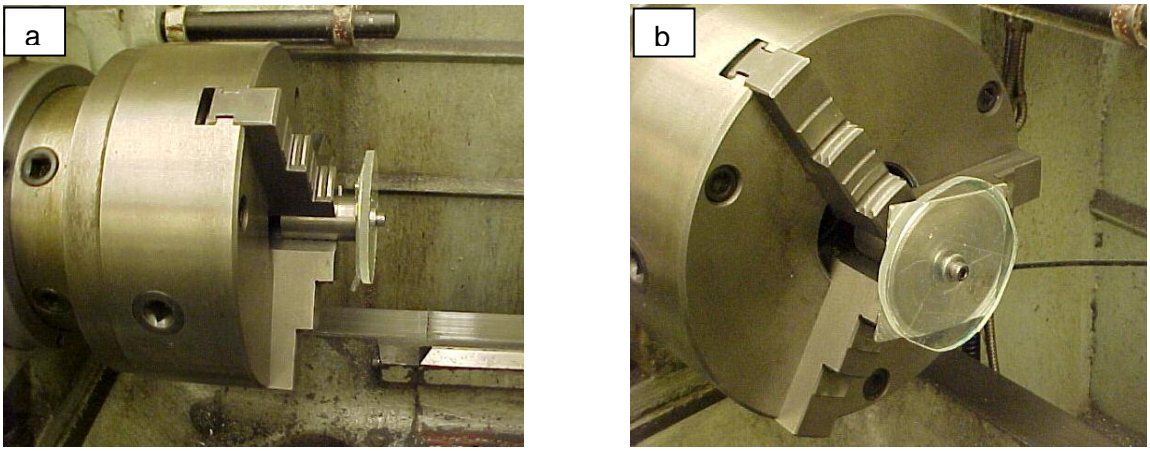

Figures 6.1.4 (a) Side view and (b) front view of the fixture used to machine acrylic polishing plate mounted on lathe

4. Plate holder

Figure 6.1.5 shows detailed drawings of the plate holder with dimensions.

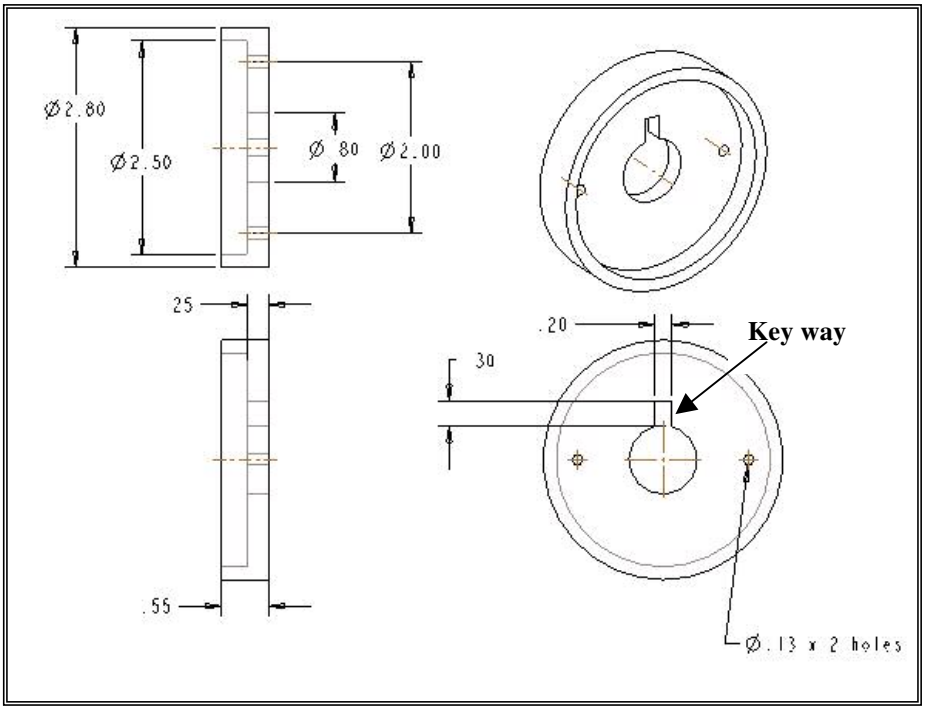

Figure 6.1.5 Multiview drawing of plate holder with dimensions

The Function of the plate holder is to support and transfer uniform spring load to the acrylic polishing plate, while rotating with the chamber. By maintaining the holder's ID equal to spring's OD, possible bending of the spring can be prevented. Key way provided on the plate holder gets itself locked with the key on the spring holder. This arrangement allows the plate holder to rotate in the same direction as the chamber.

5. Chamber cover

Once the balls are loaded between the spindle and the plate, the spindle is forced against the spring to establish desired load. Before magnetic abrasive and non-magnetic fluid were introduced into the chamber, open end of the chamber was closed and tightly covered. Figure 6.1.6 show the schematic of chamber cover.

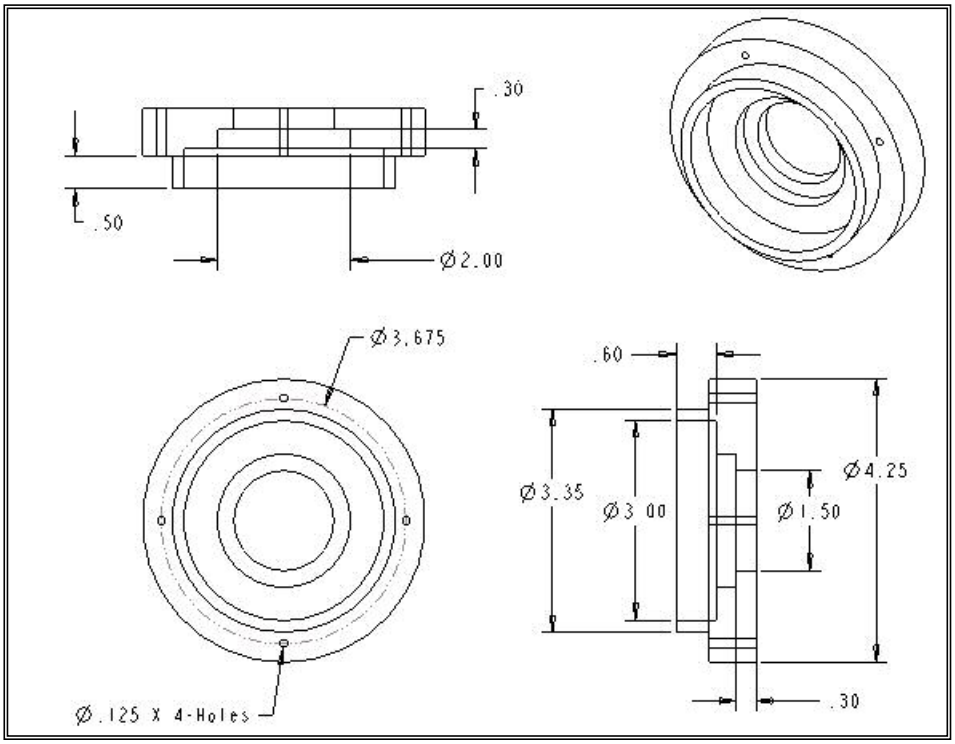

Figure 6.1.6 Multiview drawing of chamber cover

6. Urethane liner for ware prevention

Polyurethane rubber layer was used to prevent abrasive wear of soft aluminum chamber walls during the polishing process. Liner with a Shore A, hardness of 90 and thickness of 0.04 in. was used in the study. This liner was replaced with new one after each polishing run. Since the polishing chamber does not need recoating, the process becomes faster and cheaper to implement.

6.1.3 SPINDLE

Figure 6.1.7 is a drawing showing the spindle dimensions. Non-magnetic, Type 304 stainless steel (SS) bar was used as polishing spindle. SS bar was machined to the required shape of a cup with inner and outer diameters calculated using the formulae given in Section 4.1. The open edge was beveled at ≤ 25° and 4 - holes were drilled on the closed end of the cup in order to fix it to the flange. The most important aspect of the spindle was its dynamic balancing and alignment with the flange. At speeds of 650 – 1000 rpm, any unbalance can cause vibrations and quickly degrade the ball sphericity. However, minor misalignment between spindle and flange was taken care of by the groove formed on the spindle during the polishing process. This groove was maintained until the batch of balls was finished. Hence, there is no need to re-machine the spindle after each polishing run, there by reducing the cost and time involved in re-machining spindle; this can add up to 30 – 45 minutes saving for each run. Figure 6.1.8 is a drawing of the flange. The aluminum flange is press fitted to the drive shaft.

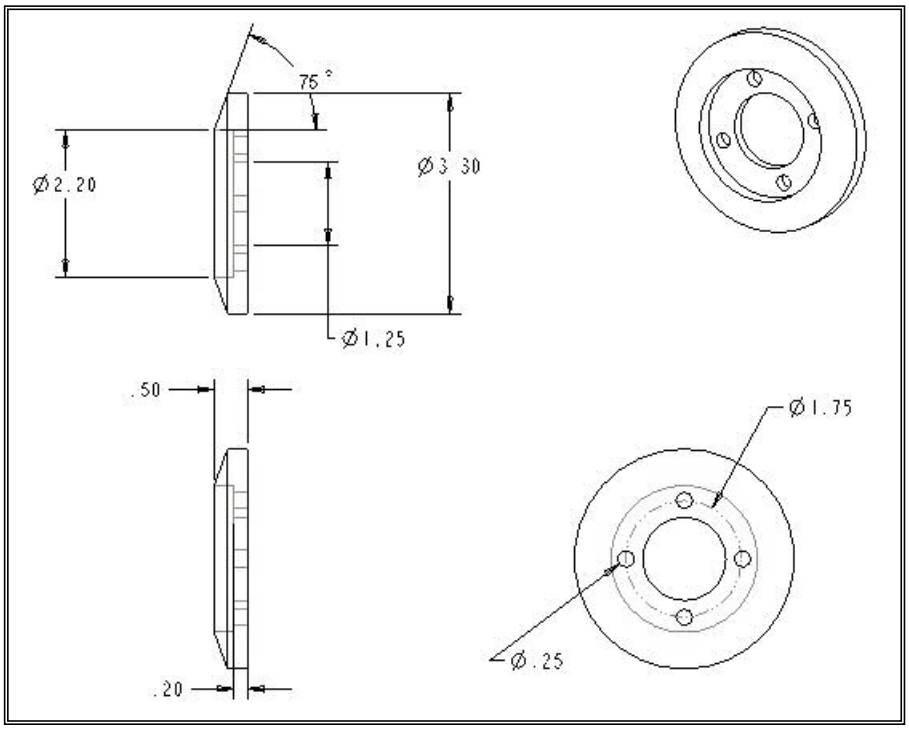

Figure 6.1.7 Multiview drawing of the spindle with dimensions

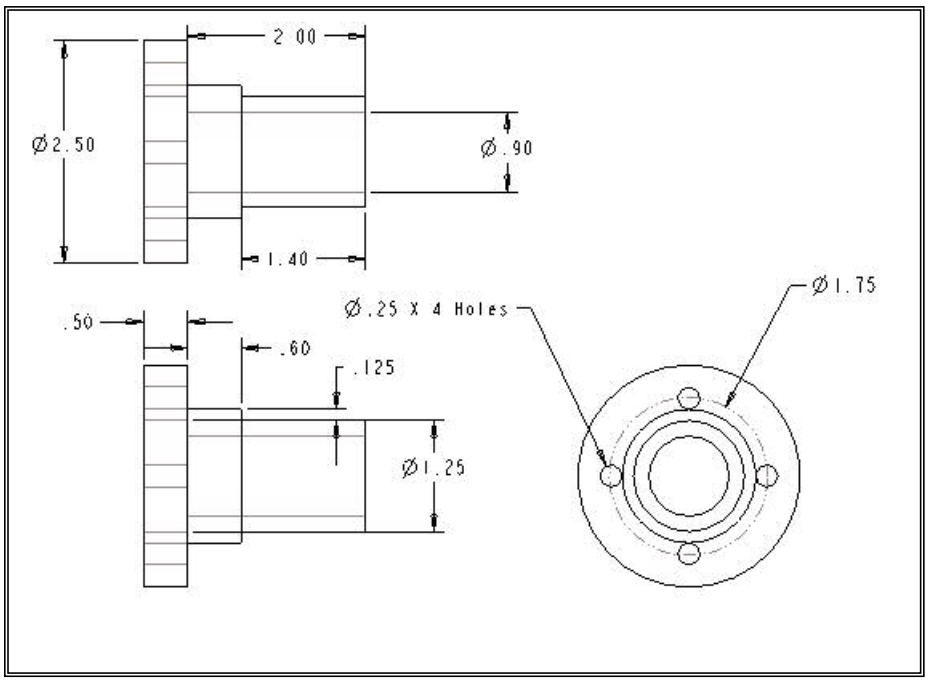

Figure 6.1.8 Multiview drawing of the spindle flange with dimensions

6.1.4 SPINDLE DRIVE ATTACHMENT

Spindle drive attachment provides drive force required to rotate the spindle at the desired speed. Drive attachment is made of two parts; 1) lathe carriage attachment and 2) motor and adjustable speed drive.

1. Lathe carriage attachment

As the name indicates, the attachment was mounted on the lathe carriage and fabricated using aluminum plates, bronze pipe (drive shaft) and bearings. All the components of the attachment have to be perfectly aligned co-axially to the spindle and the chamber. Misalignment can lead to vibration and bearing wear, there by affecting the sphericity of the balls. Figures 6.1.9 (a) and (b) are photograph of the attachment used in the present study.

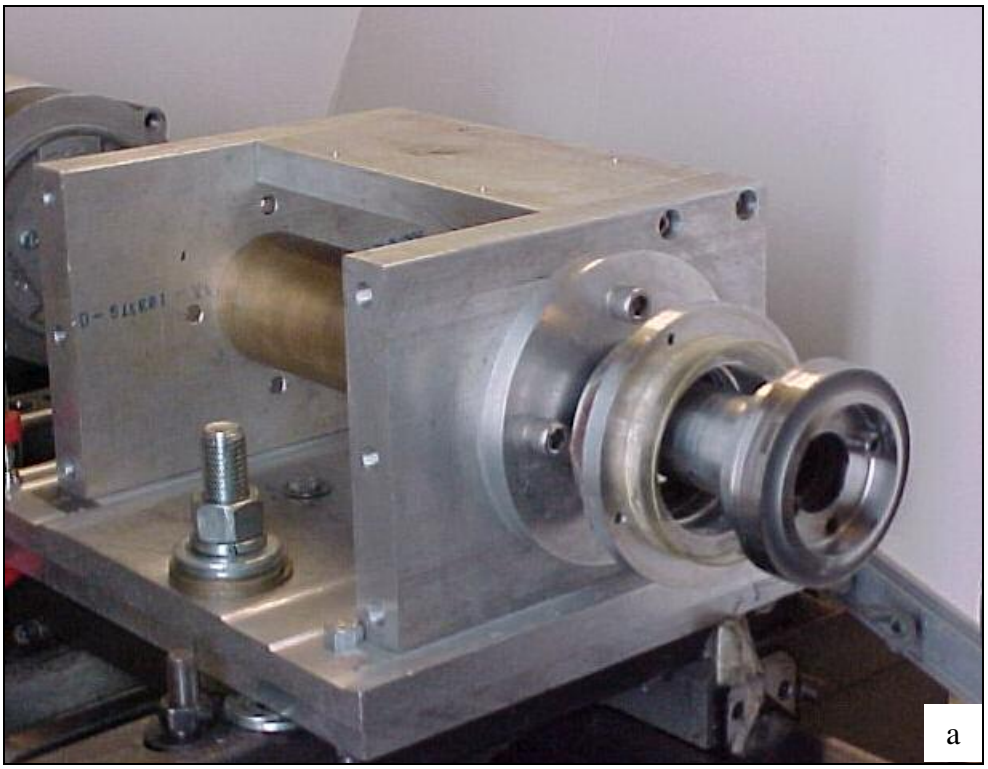

a

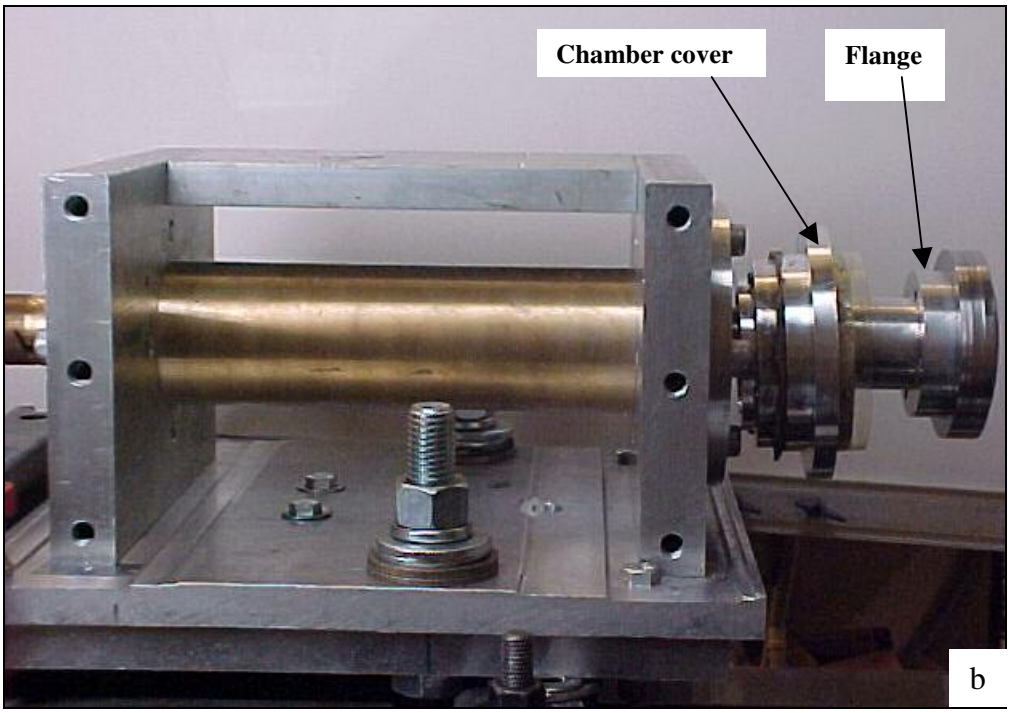

Figure 6.1.9 (a) front view and (b) side view photographs of the attachment connected to the flange and the spindle

2. Motor and Adjustable speed driver

Motor and adjustable speed driver were the source for transmitting rotational motion to the spindle through the drive shaft. Motor used in the study was BALDOR D.C. motor with maximum rpm rating of 1750. The motor was mounted on the base plate. The motor shaft was connected to one end of the drive shaft using spider coupling. Spider coupling serves two purposes: 1) to reduce vibration and 2) Nullifies slight misalignment between the motor and the shaft. BALDOR adjustable speed driver was used. It is capable of adjusting the speed from 0 to 100% of the rated motor speed. It also has a feature to adjust rotational direction, i.e. the motor can be rotated either in clockwise or in counter

clockwise direction. Figure 6.1.10 shows a photograph of motor and adjustable speed driver.

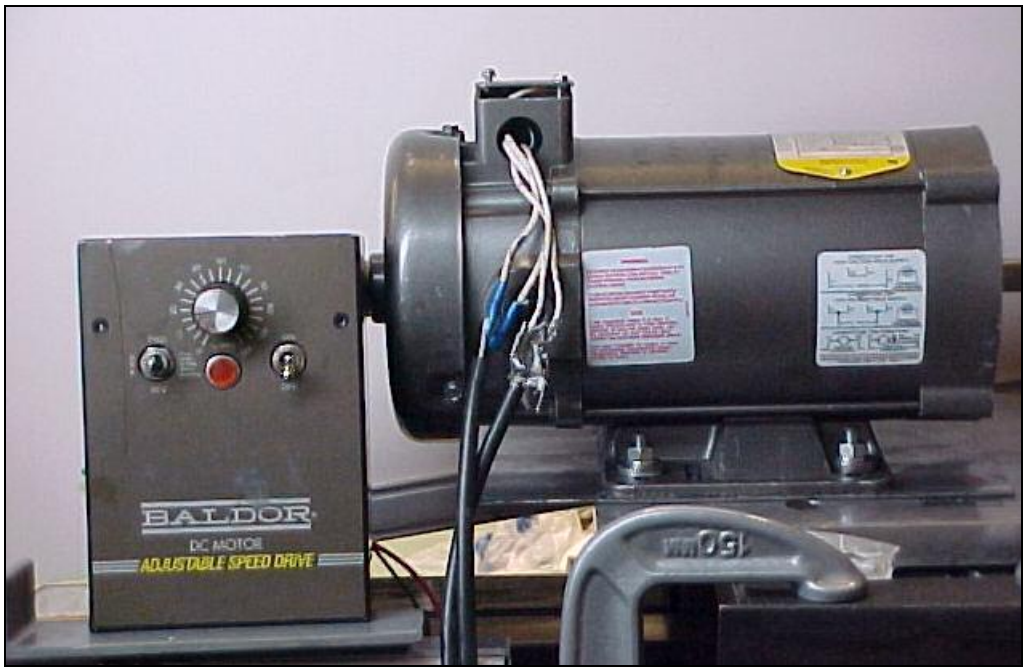

Figure 6.1.10 Photograph of the motor and adjustable speed driver mounted on the carriage

6.1.5 SPRING

MFP uses expensive magnetic fluid to generate the gentle polishing load (magnetic buoyancy force) but the current setup uses a spring to generate the required polishing load. The spring dimension was approximately equal to 0.75 times of acrylic polishing plate diameter. Table 6.1.1 gives the dimensions and loading capability of the spring used in the present study.

Table 6.1.1 Dimensions and properties of spring

Outer diameter (in.)	2.5
Free length (in.)	2.8
Inner diameter (in.)	2.174
Wire diameter (in.)	0.163
Spring rate	27.65 lbs/in. (123 N/in.) 4.842 N/mm
Number of coils	4.5
Spring material	Stainless steel
Ends	Closed and grounded

6.1.6 MAGNET LAYOUT

In this study 14 Nb-Fe-B type magnets with average intensity values of 4.85 KGauss were used. They were arranged in the radial direction on the inner surface of a steel pipe with alternate N and S Poles. Cubical polymer spacers were used to separate the two magnets along the perimeter of the steel pipe. FEM analysis confirmed that this arrangement would yield maximum field with ½ in^3 magnets. Figure 6.1.11 shows the layout of the magnets, with intensities and polarity.

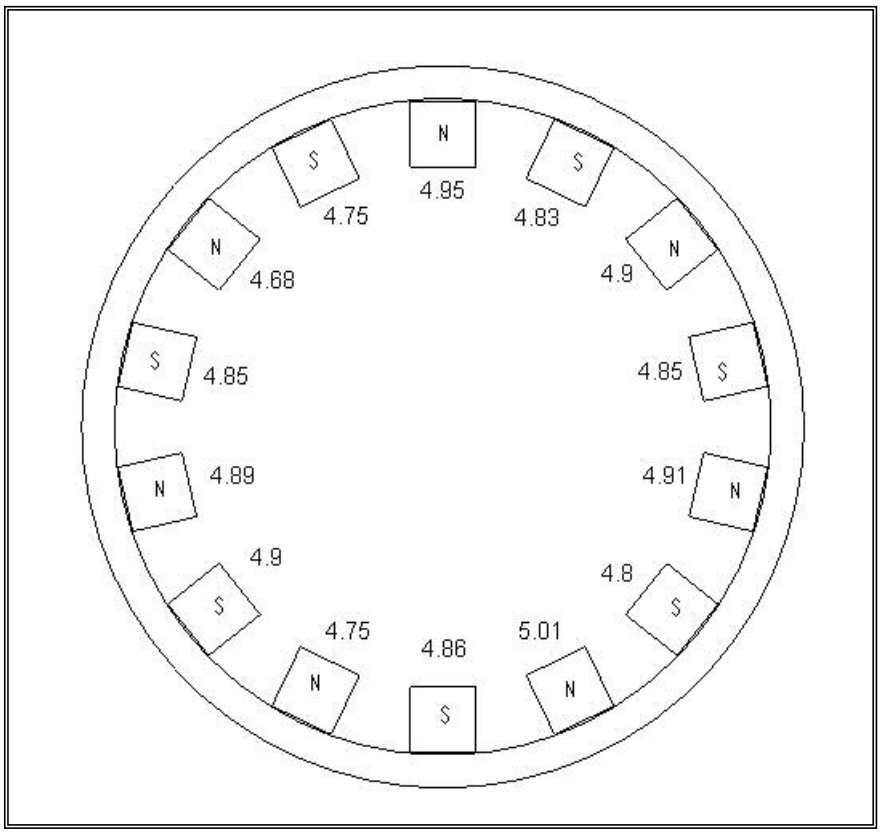

Figure 6.1.11 Magnetic flux distribution of magnets layout
(Average flux: 4.85 KGauss)

6.2 APPARATUS ASSEMBLY AND ALIGNMENT

Once all the components were machined to the desired dimensions, the next step was to assemble and develop a complete apparatus. Apparatus development includes the following:

- Carriage attachment installation
- Chamber Assembly and alignment

6.2.1 CARRIAGE ATTACHMENT INSTALLATION

First step was to fix six square steel tubing on lathe carriage in order support 24 in. long aluminum base plate. This plate serves as base for drive

attachment and motor. It was very important to insure that plate was leveled and fixed on sufficient supports, so as to keep vibrations low. Then drive attachment was fixed on the base plate and aligned co-axially with the lathe spindle axis. Similarly, with the help of 'tail stock dead center', motor was mounted and aligned coaxially with the lathe axis and drive attachment. One end of the drive shaft was connected to motor with the help of spider coupling; and the other end was pressure fitted with flange, on which spindle was to be mounted. Before the flange was fitted to the bronze shaft, the chamber cover was pushed on the shaft.

6.2.2 CHAMBER ASSEMBLY AND ALIGNMENT

Assembly starts with pressure fitting of spring holder co-axially with chamber. Then the chamber was fixed in a 4-jaw chuck by adjusting each chuck separately. Next step is to align each component of the apparatus to maintain co-axiality with the lathe axis. The components consisted of bronze shaft, flange, spindle and chamber. There are three critical alignments, namely, (1) the alignment of polishing chamber with the lathe axis (2) Alignment of polishing spindle with the drive shaft and flange (3) Alignment of polishing chamber and spindle. The alignments should be handled with care to obtain consistent and meaningful results. The instruments used in this alignment setup were Dial indicator (resolution: 0.0001 in.), Pneumo-Centric 5500 system, Pick-up probe and Probe holder. The Pneumo-Centric 5500 system was actually a roundness profiler (an older model of TalyRond 250 was used in this investigation). Figure 6.2.1 shows the photograph of alignment system used in this study.

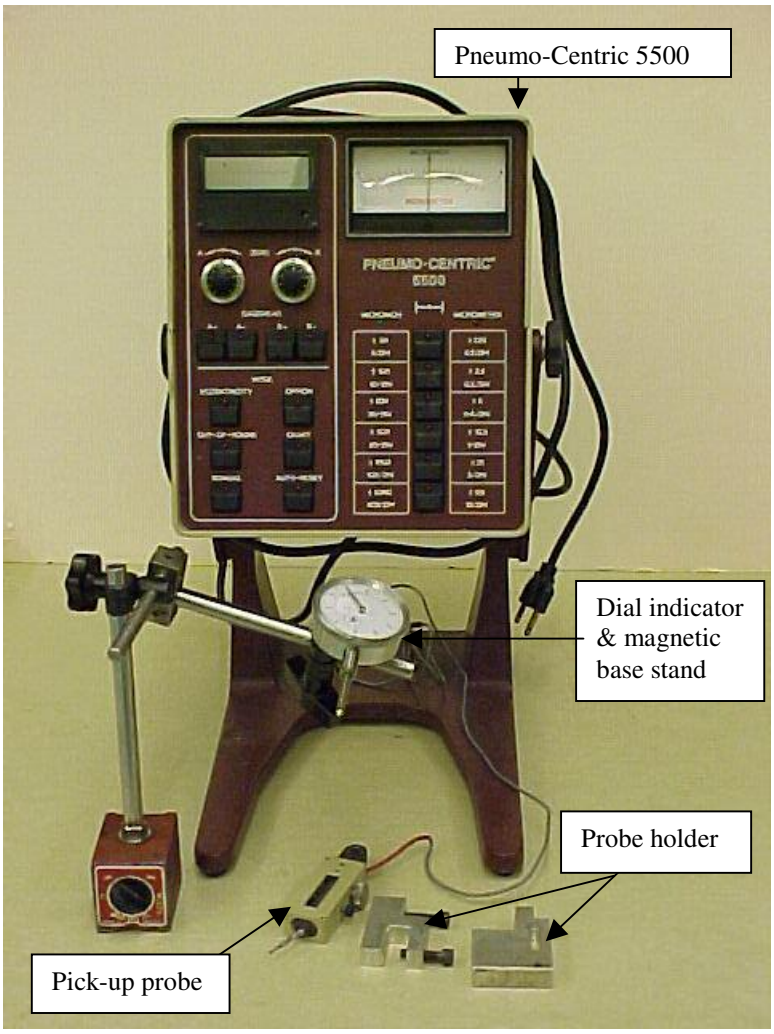

Figure 6.2.1 Photograph ofthe alignment system

Figures 6.2.2 (a) – (f) show the procedures used for the first alignment of polishing chamber. The details of the procedure are listed below:

1. Secure the polishing chamber on 4-jaw chuck, as shown in Figure 6.2.2 (a).
2. Make sure that lathe chuck is rotating accurately using dial indicator.
3. By adjusting each chucks separately, make sure that chamber rotation read zero deflection on dial indicator, as shown in Figure 6.2.2 (b).
4. Use pick-up probe and Pneumo-Centric 5500 for precise alignment of chamber.

5. Plug in pick-up probe to port A at the back of the Pnuemo-Centric system and turn on the power.
6. Select the sensitivity of the system to be 25 μm per division.
7. Fix the pick-up probe to portable stand with magnetic base and locate the tip of the pick-up probe to the outer surface of the polishing chamber, as shown in Figure 6.2.2 (c).
8. Apply gentle pressure to the tip of the pick-up probe through contact against the wall of the polishing chamber.
9. Adjust the 4-jaw chuck until the deflection on Pnuemo-Centric reading is in the range of ± 4 divisions at multiple locations.
10. Similarly, measure the inner surface of the chamber in the range of ± 4 divisions at multiple locations, as shown in Figure 6.2.2 (d).

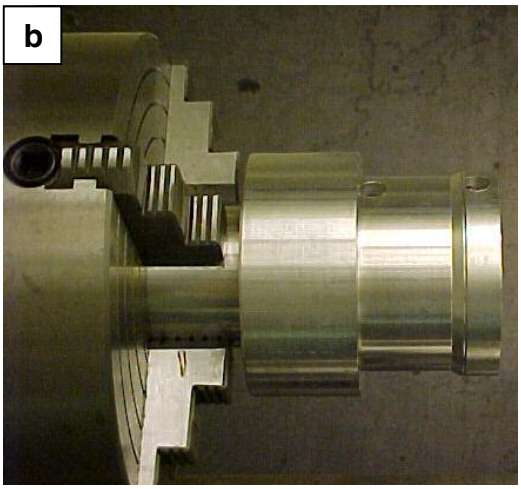

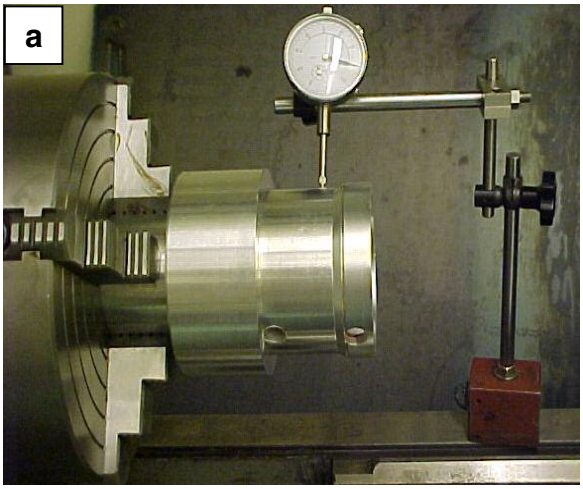

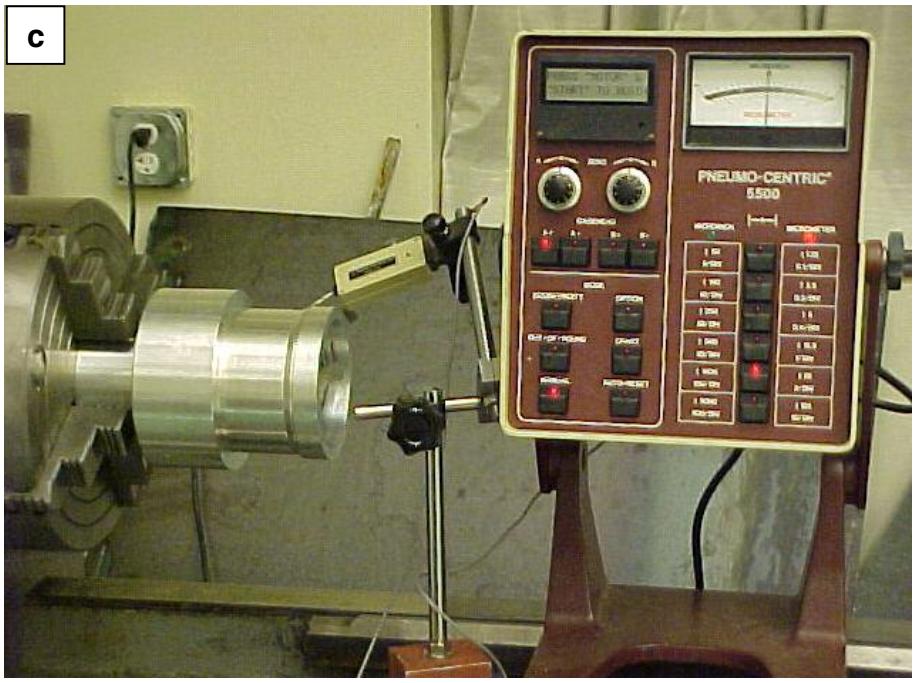

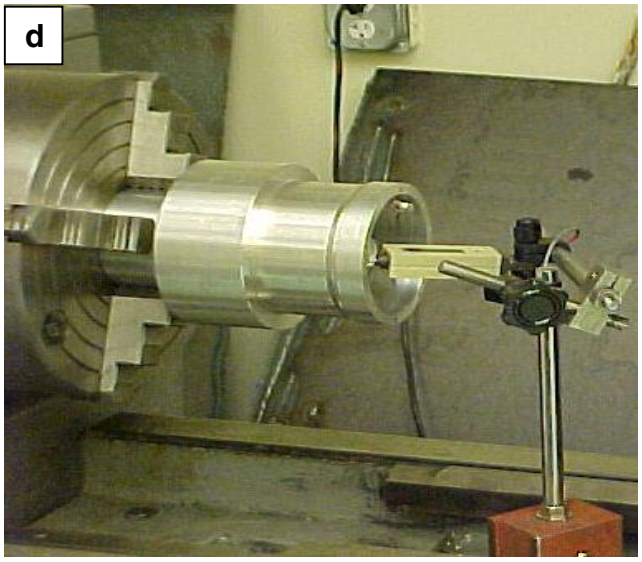

Figures 6.2.2 (a) – (d) Photographs of the chamber alignment procedure

Figures 6.2.3 (a) – (b) show the procedures for the alignment of polishing spindle. The details of the procedure are listed below:

1. Check the roundness of the drive shaft and flange at different points using the dial indicator.

2. Secure (not tightly) the polishing spindle to the flange with 4 socket headed screws.
3. Use the dial indicator for rough adjustment, use Pnuemo-Centric and pick-up probe for precise alignment of the polishing spindle.
4. Slowly rotate the drive shaft manually and now observe the deflection through the Pnuemo-Centric.
5. Adjust the 4 screws until the polishing spindle is properly aligned to the flange and the deflection of one full revolution of the drive shaft is within ± 4 divisions.
6. Relocate the tip of the pick-up probe to the bevel of the polishing spindle and repeat steps (3) – (5).
7. Finally, tighten the screws.

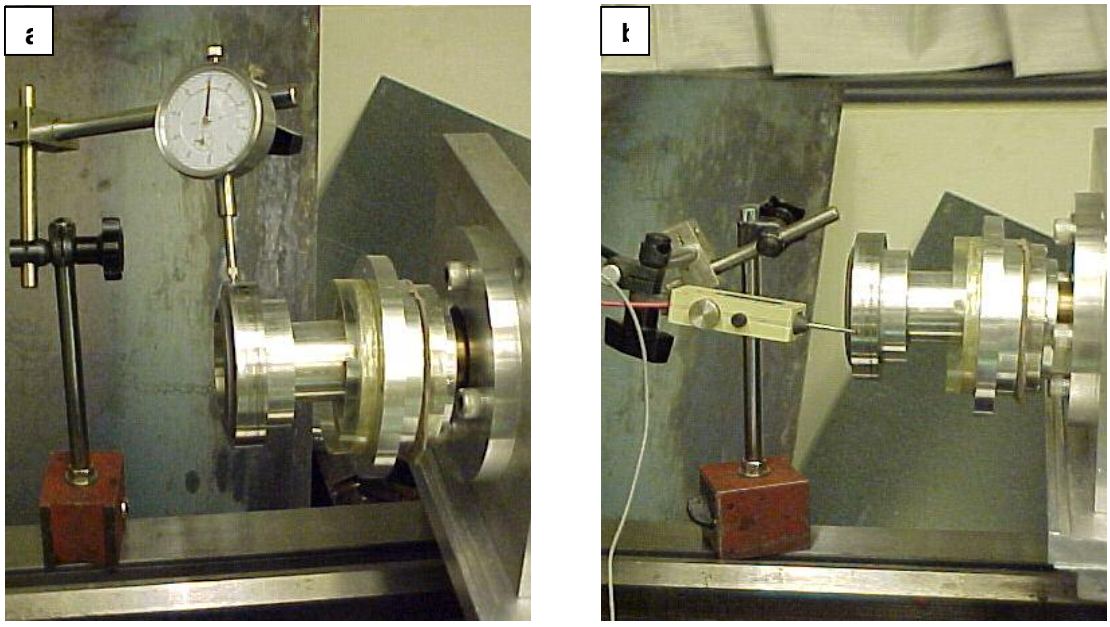

Figures 6.2.3 (a) – (b) Spindle alignment photographs

Figures 6.2.4 show the procedure for the alignment of polishing chamber and spindle. The details of the procedure are listed below:

1. Fix the probe to the probe holder and mount it on the chamber
2. Place the tip of the pick-up probe on the polishing spindle.
3. Apply gentle pressure at the tip of the pick-up probe through contact against the spindle.
4. Slowly rotate the drive shaft manually and observe the deflection through the Pnuemo-Centric.
5. Make sure that probe deflection is in the range of ± 4 divisions.

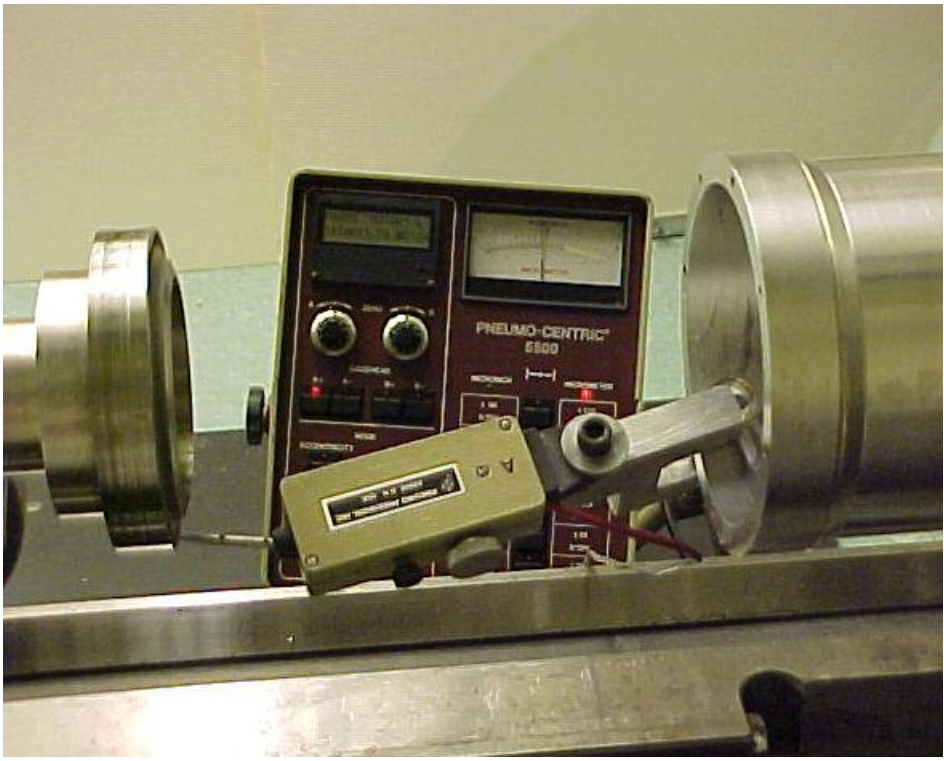

Figure 6.2.4 Photograph showing alignment of the polishing chamber and the spindle

CHAPTER 7

EXPERIMENTAL SETUP PROCEDURE AND METHODOLOGY

7.1 EXPERIMNTAL PROCEDURE

This Chapter provides detailed description of the steps involved in the experimentation process. The basic principle of UMAP apparatus is to establish 3-point contact of a ball between the spindle, the chamber wall and the acrylic polishing plate. It was later realized that the groove formed on the spindle bevel was beneficial for improving roundness profile. Reason for this improvement could be due to the fact that groove formation increases number of contact points during polishing. This causes the balls to rotate in such a way that their entire surfaces are uniformly polished. The abrasives cause the cutting action by acting between contact points, thereby fracturing or shearing the ball - on a micro scale. The parameters - spindle speed, chamber speed, polishing duration, spindle bevel angle and load - directly affect the output parameters.

In traditional magnetic float polishing apparatus, load is applied by moving the milling machine table upwards along with the chamber to contact the spindle. A dynamometer placed between the chamber and table measures the exact load. For large batch MFP the chamber is set on top of a platform which is mounted with four linear bearings and has only vertical motion. This

platform is attached to a counter-weight system that causes it to be lifted upward and comes in contact with the spindle. The amount of counterweights used determines the loading [Gerlick, 2004]. In both type of magnetic float polishing techniques, the set up time varies from 30 - 45 minutes. At the same time care has to be taken in order to maintain alignment of the polishing spindle and the chamber. In the present setting, the load is applied by moving carriage carrying spindle against the polishing plate supported by the spring. Linear distance traveled by carriage was used to calculate load applied. This corresponds to the amount of spring deflection.

Earlier studies have shown that in order to obtain best results while finishing a spherical object, the chamber must be aligned exactly co-axial with the spindle. This was one of the most significant factors affecting the results, and has proved to be the most challenging aspect of the entire process in the case of magnetic float polishing. The advantage of the present apparatus is it requires only one time alignment of the spindle and the chamber. Due to the use of a lathe, the operator does not have to be concerned with the alignment until a batch of balls is polished. Chamber and spindle being horizontal, they can be cleaned *in-place* without the need to take the chamber out for cleaning. This not only keeps the alignment intact but also reduces the unaccounted polishing time.

Though, this apparatus proves to be alignment-free still the initial alignment of the spindle and the chamber is a critical factor in obtaining good results. If the spindle and the chamber are not co-axial, unequal loading which results in bad sphericity due to higher material removal rates at areas of higher

loading. Also, this unequal loading is a source of vibrations, which again has the same effect.

The detailed procedure for polishing silicon nitride balls using UMAP apparatus is shown in Figures 7.1 (a) – (k), and the details listed following:

1. Fix the polishing plate to the plate holder as shown in Figure 7.1 (a). Increase the polishing load if necessary, by using an extra plate.
2. Slide spring into the plate holder as shown in Figure 7.1 (b).
3. Fit the polyurethane liner inside the chamber as shown in Figure 7.1 (c).
4. Push the spring along with the plate holder and the plate on the spring holder, until the plate is seen parallel to the inner edge of the ball inlet opening. Make sure that key way provided on the plate holder is aligned with the key to prevent any misalignment during polishing process as shown in Figure 7.1 (d).
5. Move the spindle at a convenient distance to the polishing plate such that loaded balls make a 3-point contact with the spindle, the chamber and the polishing plate as shown in Figure 7.1 (e).
6. Load the balls with gentle spring force between the plate and the spindle as shown in Figure 7.1 (f). Also, Figure 7.1 (g) shows the loaded balls.
7. Apply the desired load by moving the lathe carriage against the spring as shown in Figure 7.1 (h). Distance moved by the carriage is used to calculate the load applied on the balls.
8. Open end of the chamber is perfectly closed using chamber cover and 4-screws. View of the complete setup can be seen in Figure 7.1 (i).

9. Close the ball inlet tightly with the rubber cork.
10. Steel pipe carrying magnet arrangement is mounted on the chamber such that the magnets are placed on the polishing zone. Then, pipe is secured tightly on to the chamber using duck tape, as shown in Figure 7.1 (j).
11. Finally unbonded abrasive mixture, non-magnetic fluid and rust inhibitor are introduced into the chamber and the abrasive opening is tightly secured with another rubber cork.
12. Spindle is turned on first and speed is slowly increased to 200 rpm (15 – 20%) and then the lathe is turned on at 32 rpm.
13. After 5 minutes, spindle speed is slow increased to the desired speed. Noise level and vibration of the apparatus was monitored while increasing the spindle speed.
14. Finally, compressed air is forced on the polishing zone in order to keep the heat generated under control. Complete setup of the apparatus can be seen in Figure 7.1 (k).
15. Once the experiment is completed, spindle speed is slowly reduced to zero and at the same time, lathe also is turned off. Steel pipe is taken out from the chamber. Then chamber cover is carefully removed and the carriage is moved outside.
16. Chamber, chamber cover, and spindle were cleaned on the machine tool without disturbing their alignment.
17. *In-place* cleaning not only reduces cleaning time but also maintains the alignment and accuracy of the apparatus.


a

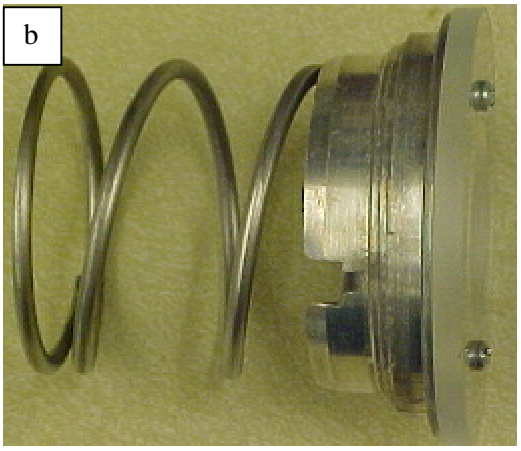
b

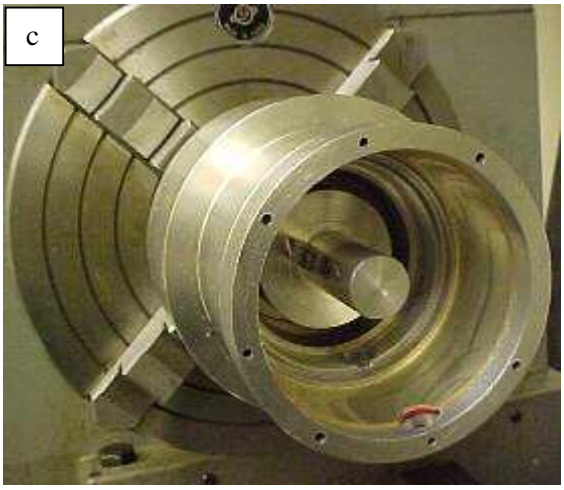
c

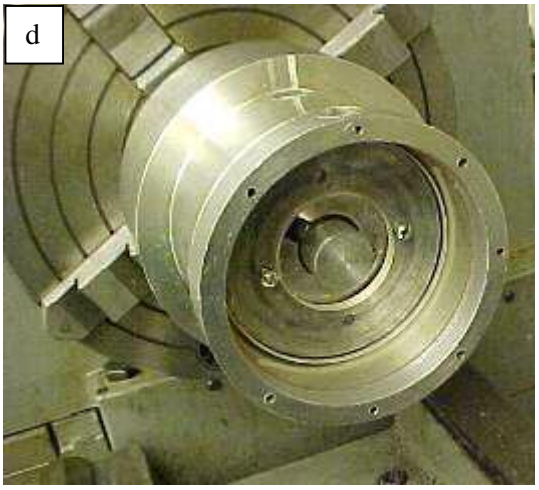
d

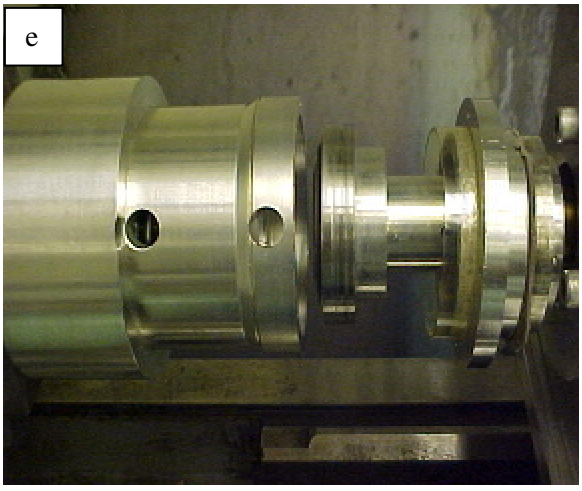
e

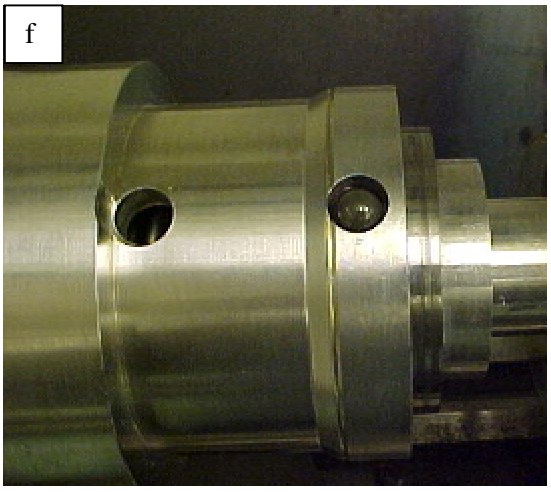
f

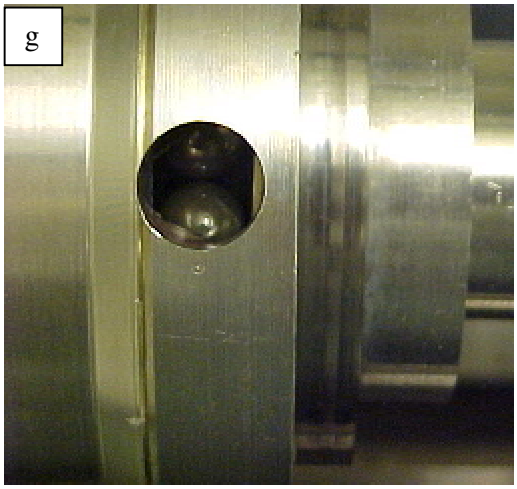

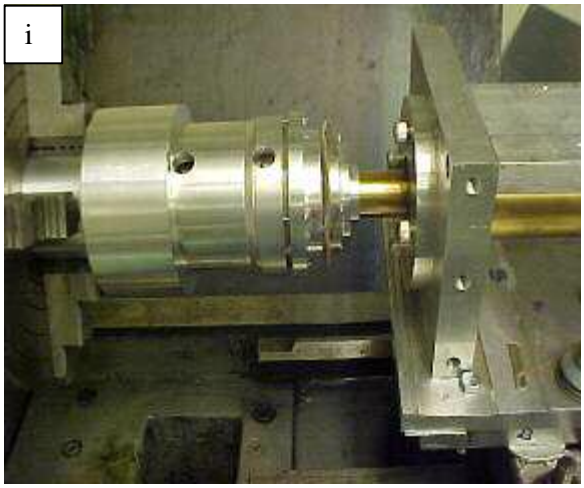

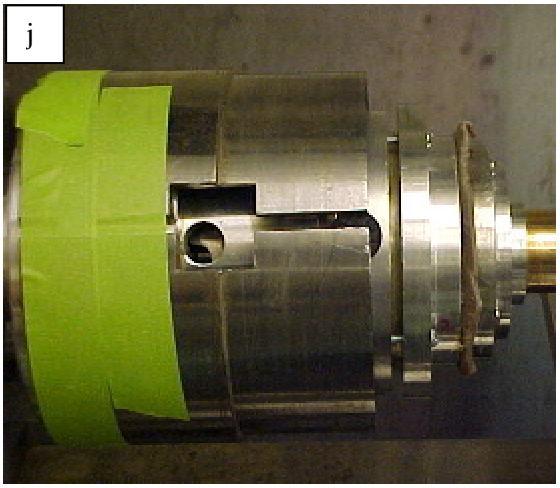

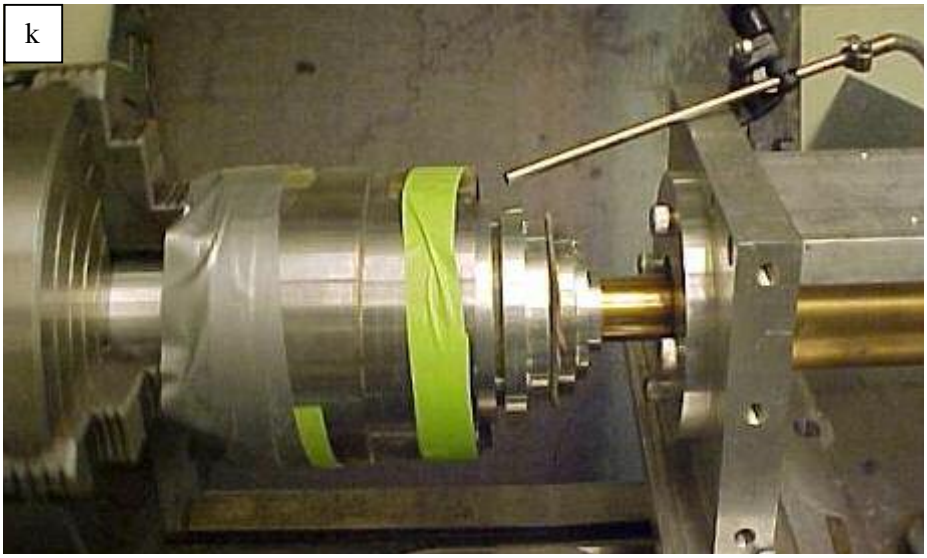

Figures 7.1 (a) – (k) Steps involved for the setup of the apparatus for UMAP polishing process

7.2 METHODOLOGY

Three output parameters, namely, diameter, sphericity, and surface finish are of interest in finishing the silicon nitride balls for bearing applications. Mechanical polishing followed by chemo-mechanical polishing were the steps to be followed to achieve these outputs. Mechanical polishing starts with use of harder and coarser abrasive with high-loads for higher material remove rates. As mechanical polishing progress lower hardness and finer grain size abrasive are used with controlled loading to maintain the removal at reduced rate and slowly improve the roundness. Finally, good sphericity and superior surface finish with minimal subsurface defect are achieved by polishing with finer abrasive, followed by chemo-mechanical polishing with CeO_2. Hence, polishing methodology can be summarized in three steps:

1. Initial roughing stage to obtain high MRR (0.6 – 1.10 μm/min) with loads ranging from 3-6 N/ball.
2. Semi-finishing stage to control diameter and improve roundness.
3. Final stage to achieve superior finish and good sphericity.

Boron carbide (B_4C)-500 grit and Silicon carbide (SiC)-600 grit abrasives harder than workmaterial are used during the initial polishing stage. This stage yields high material removal rates and slow improvement in ball shape as polishing runs proceeds. Under these conditions material removal as high as 1.15 μm/min is possible. Further material removal is controlled using SiC-600 grit abrasive. Iron powder varying from 44 – 297 μm is used at this stage. It is necessary to continue with the groove formed on the spindle right from the first

run until the batch of balls is finished. The groove not only helps in improving roundness of balls but also works fine during final finishing stage. Figure 7.2.1 shows a photograph of the groove formed on the bevel of the spindle, which assists in improving the roundness profile.

During the second stage of polishing, comparatively finer abrasives such as SiC-1200 grit and iron powder of 44 - 297 μm size are used. This stage facilitates controlled MRR, sphericity improvement, and good surface finish.

Kirtane [2004] reported that during finial finishing stage, machining the spindle groove is necessary to improve surface finish rapidly. But in the present study rapid surface finish was obtained without machining the spindle groove. Hence, this point towards some unexplored parameters which needs to explored in future study. During this stage MMR is very low. Fine SiC-8,000 and 10,000 grit abrasives are effective in improving the surface finish. Finally cerium oxide (CeO_2) (< 5 μm) is used to obtain very good surface finish. The parameters used in this investigation are listed in Table 7.2.1.

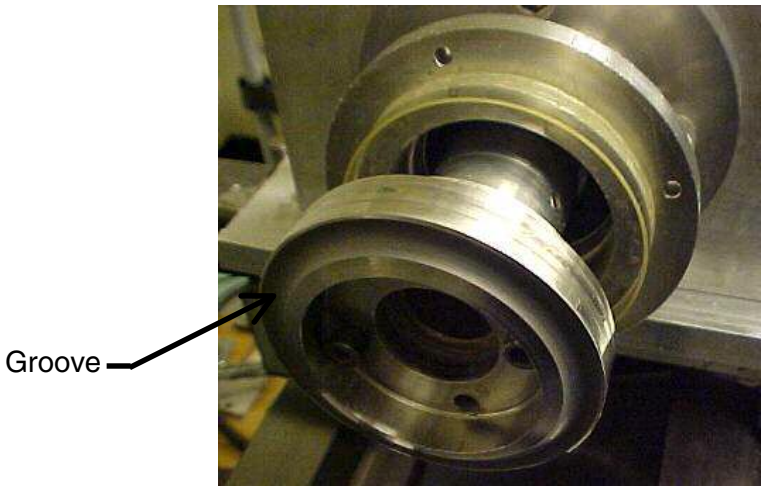

Figure 7.2.1 Photograph of the groove formed on the bevel of the spindle attachment during polishing

Table 7.2.1 Parameters used

Stage	Abrasives	Iron powder	Load (N/ball)
I	Boron carbide (B_4C) - 500 grit (12 μm) Silicon carbide (SiC) - 600 grit (10 μm)	Fe-114 (200-300 μm) Fe-112 (125 μm)	3 - 6
II	Silicon carbide (SiC)-1200 grit (2.1 μm)	Fe-112 (125 μm)	2 - 4
III	Silicon carbide (SiC)-8,000 and 10,000 grit (0.5 μm) Cerium oxide (CeO_2) - (< 5 μm)	Fe-112 (125 μm) Fe 102 (-325 mesh)	2.5-3.5

As-received 17, half-inch balls with average diameter of 0.52886 in. are used in this investigation. Motor speed 700 – 900 rpm and lathe spindle speed of 32 rpm of are used in each test run. Lathe which rotates chamber and plate was rotated at 32 rpm, because higher speeds lead to dispersion of magnetic abrasive due to centrifugal force. Approximately 20 ml of glycerin and 20 – 30 ml of de-ionized water are used, along with 2 – 3 ml of rust inhibitor (Cool Mist) for most of the experiments. Compressed air is continuously sprayed on the outer surface of the chamber to prevent over heating of chamber during polishing. During the initial polishing runs, once in 30 to 40 minutes, water with rust inhibitor was sprayed on chamber to reduce the heat generated. Apart from the actual polishing time, a set-up and cleaning time of approximately ~ 30 - 40 min. and characterization time of ~ 60 min. are required.

7.3 BALL CHARACTERIZATION INSTRUMENTS

In this study three balls were picked randomly for measuring the diameter and sphericity, and surface finish after each run. Each ball was measured in 3-planes. Following are the instruments used to characterize the finished balls:

- Micrometer (resolution: 0.00001 in.) was used to measure ball diameter.
- TalyRond 250 (Filter: 2CR, cut-off: 50 upr): To measure sphericity of the balls
- TalySurf 120L (Filter: ISO 2CR, Cut-off 0.08 mm, Evaluation length 4 consecutive cut-off) was used to measure surface finish
- The material removal rate was calculated by reduction in the weight of the balls by measuring the weight before and after each polishing run, using a precision balance (resolution: 0.1mg).
- Brinkmann precision balance was used to weigh batch of balls before and after the polishing run. Thus, the material removal rate (MRR) in mg/min/ball is determined.
- Gauss/Tesla meter was used to measure the magnetic field intensity.

CHAPTER 8

RESULTS AND DISCUSSION

This Chapter presents the results of all the test runs conducted in this investigation of unbonded magnetic abrasive polishing of silicon nitride balls. These results enable analysis of different parameters that controls the in polishing process. In order to obtain best results on the setup used, a logically approach is developed by conducting a series of test runs. A first set of experiments was executed to find out the need for magnetic field in this process. Next sets of experiments determine optimum speeds and polishing duration to pursue good sphericity. Similarly, test runs were carried out to study parameters required to obtain good surface finish.

Two sets of 17, half-inch silicon nitride (CERBEC NBD-200 from Norton Advanced Ceramics) as-received balls were used in the present study. Each set of balls were finished in two stages until they were completely finished by chemo-mechanical polishing. These four batches were named 1A, 1B, 2A and 2B; test runs performed under each batch were tabulated and are listed in Tables 8.1 to 8.4. This reflects the influence of different parameters on MRR, sphericity and surface finish.

The best average sphericity for a batch was 0.77 μm (0.5 – 1 μm), with a standard deviation of 0.175 μm. For a single ball, the best results obtained was a sphericity of 0.5 μm and a surface finish of 10.6 nm Ra, as shown in Figures 8.3 and 8.5, respectively, along with the as-received sphericity profile in Figure 8.2 and as-received surface finish profile in Figure 8.4. Photograph of the as-received and finished balls are included in Figures 8.1 (a) and (b).

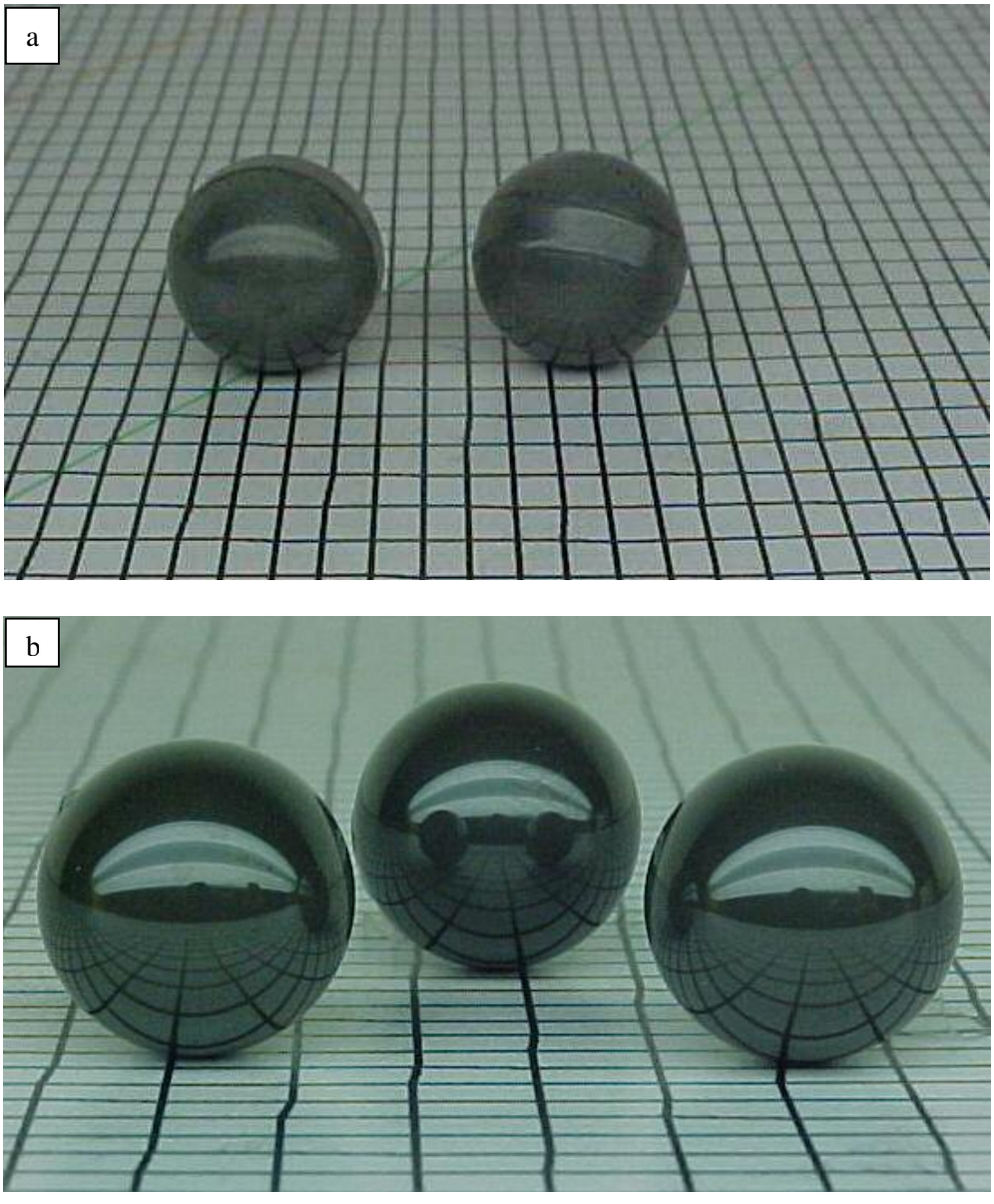

Figures 8.1 Photographs of (a) as -received and (b) finished Si_3N_4 balls

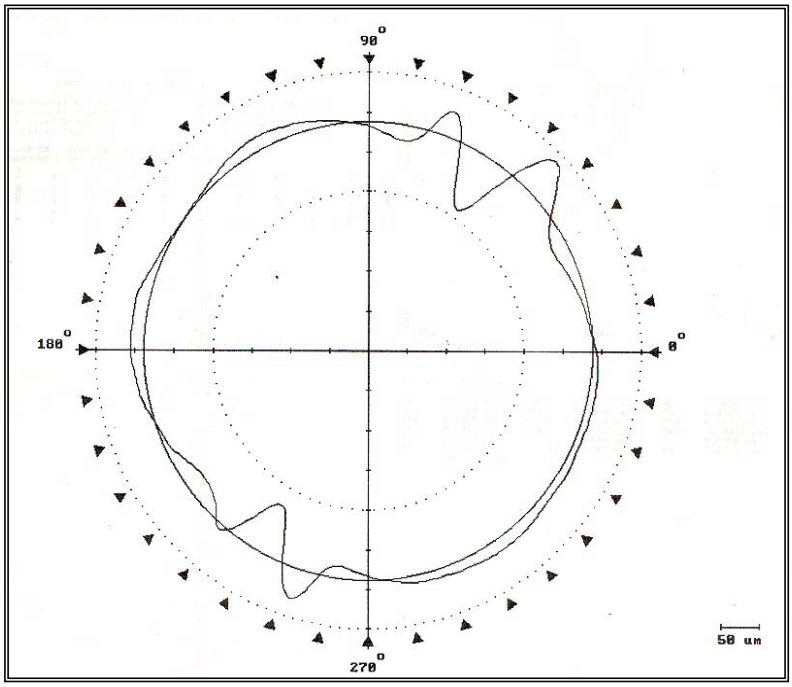

(Roundness: 128.48μm)
Figure 8.2 TalyRond roundness profiles of as-received Si_3N_4 ball

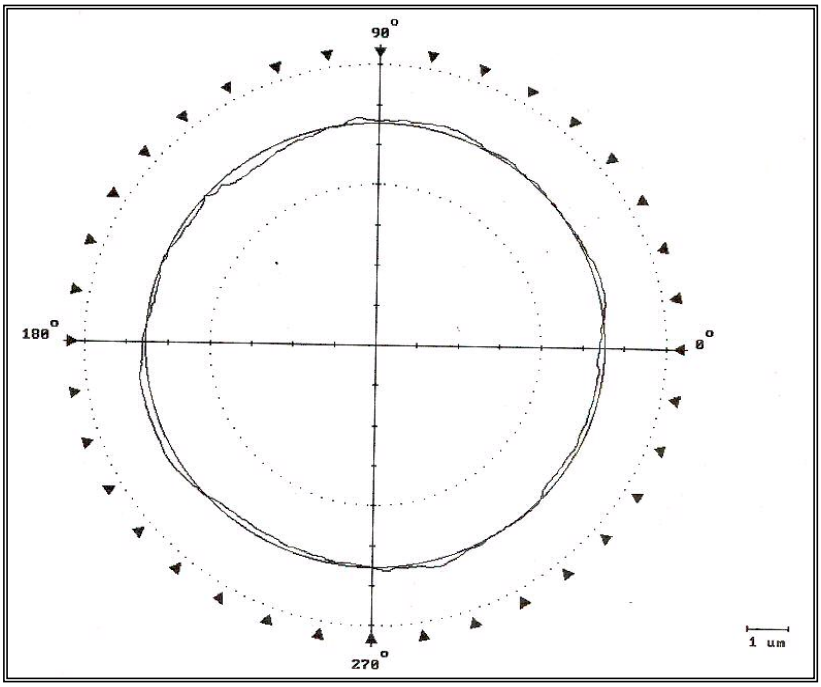

(Roundness: 0.5 μm)
Figure 8.3 TalyRond roundness profiles of finished Si_3N_4 ball

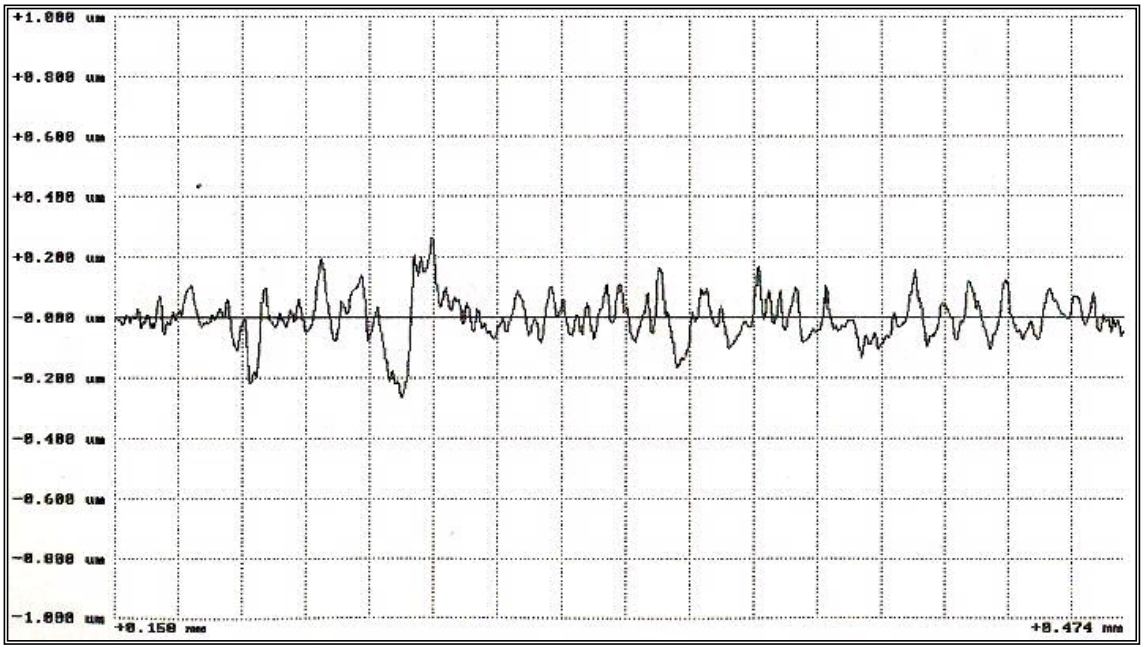

(Ra: 54.6 nm, Rt: 0.5356 μm)
Figure 8.4 TalySurf surface roughness profile of as-received Si_3N_4 ball

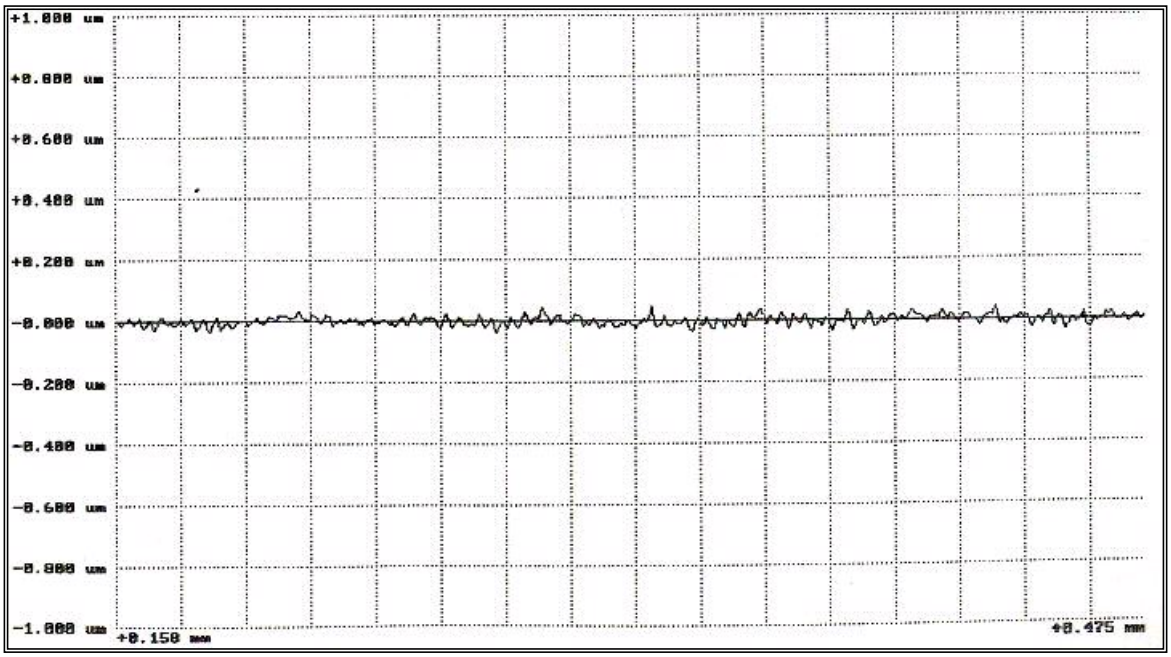

(Ra: 10.6 nm, Rt: 0.087 μm)
Figure 8.5 TalySurf surface roughness profile of finished Si_3N_4 ball

Table 8.1 Results of batch 1A

Run No.	Abrasive Type	Iron powder Type	Load (N/ball)	Abra. (ml)	Iron Powder (ml)	Glycerin (ml)	Water (ml)	Time (Min)	Speeds		Results					
									Lathe (rpm)	Motor (rpm)	Rd. (µm)	Ra (nm)	Rt (µm)	Dia. (inch)	MRR/ ball (mg/ min)	MRR/ ball (µm/ min)
1	B_4C-500	FE-112	3	20	20	10	25	45	32	1475	---	---	----	0.51099	0.041	0.062
2	B_4C-500	FE-112	4	20	20	10	25	45	32	1475	---	---	----	0.51087	0.05	0.068
3	B_4C-500	FE-112	5	20	20	10	25	45	32	1475	---	---	----	0.51047	0.17	0.22
4	B_4C-500	112+114	5	20	20	10	25	45	32	1475	---	---	----	0.51025	0.113	0.12
5	B_4C-500	112+114	5	20	20	10	25	45	64	1475	---	---	----	0.50995	0.152	0.17
6	B_4C-500	FE-114	4	20	15	10	20	45	64	1475	---	----	----	0.50981	0.086	0.074
7	B_4C-500	FE-112	5	20	15	25	20	45	32	1625	3.07	----	----	0.50858	0.5670	0.697
8	B_4C-500	FE-112	5	20	20	25	20	80	32	1550	1.8	----	----	0.50610	0.68	0.787
9	B_4C-500	FE-112	5	20	20	10	15	60	32	1375		----	----	0.50298	0.58	0.85
10	---	---	---	---	---	---	---	---	---	---	---	---	---	---	---	---
11	SiC-600	FE-112	5.8	15	12	10	20	75	32	1375	2.33	----	----	0.50001	-----	----
12	B_4C-500	FE-112	5.8	10	10	10	20	45	32	1375	5.91	----	----	0.49850	0.58	0.838
13	B_4C-500	FE-112	4	15	15	30	20	45	32	1475	6.45	----	----	0.49789	0.34	0.330
14	B_4C-500	FE-112	4.5	15	20	30	20	60	32	1630	5.39	----	----	0.49616	0.62	0.711
15	B_4C-500	FE-112	4.5	15	20	30	20	60	32	1650	1.95	----	----	0.49469	0.46	0.61
16	B_4C-500	FE-112	5.8	15	20	30	15	45	32	1650	1.6	80	0.627	0.49291	0.76	0.995
17	SiC-600	FE-112	5.8	15	20	30	20	60	32	1650	3.5	97	.8273	0.49057	0.76	0.965
18	SiC-600	FE-112	5.8	15	20	30	20	45	64	1650	11.24	110	1.042	0.4884	0.96	1.219
19	SiC-600	Fe-114	5.8	20	15	40	20	45	64	1630	7.03	89.78	0.669	0.48642	0.96	1.118
20	SiC-600	Fe-114	6	20	15	40	30	30	64	1630	3.67	133.4	1.022	0.48469	0.89	1.468
21	SiC-600	Fe-114	5.8	20	15	40	30	45	64	1630	6.44	121.7	0.897	0.48308	0.61	0.909
22	SiC-600	Fe-114	6.5	20	15	30	20	45	00	1630	3.22	96.6	0.845	0.48037	1.16	1.53
23	SiC-600	Fe-114	6.5	20	15	25	25	60	00	1630	2.54	101	0.821	0.47724	1	1.325
24	SiC-600	Fe-114	6	20	15	30	25	60	00	1630	5.175	100.1	0.8	0.47475	0.75	1.054
25	SiC-600	Fe-112	6	20	15	20	25	45	00	1630	3.8	----	----	0.47321	0.67	0.869
26	SiC-600	Fe-112	6	20	15	20	40	30	00	1630	3.055	----	----	0.47158	0.93	1.380
27	SiC-600	Fe-112	5.5	20	15	25	30	30	00	1630	1.9	----	----	0.47039	0.79	1.008
28	SiC-600	Fe-112	5	18	12	20	25	30	00	1630	1.89	----	----	0.46942	0.52	0.821
29	SiC-600	Fe-112	4	20	10	20	15	50	00	1630	4.36	----	----	0.46865	0.27	0.391
30	SiC-600	112+114	4	20	15	20	15	30	00	1630	3.61	----	----	0.46809	0.34	0.474
31	SiC-600	112+114	4	20	15	25	15	60	00	1630	5.03	----	----	0.46676	0.38	0.563
32	SiC-600	112+114	4	20	15	20	15	30	00	1630	4.17	----	----	0.46534	0.85	1.202
33	SiC-600	112+114	5.8	20	15	20	15	30	32	1630	4.98	----	----	0.46393	0.83	1.194
33a	B_4C-500	112+114	4.5	20	15	30	20	45	32	1630	3.93	----	----	0.46268	0.48	0.706
34	B_4C-500	112+114	5	20	15	30	20	45	32	1630	5.26	----	----	0.46107	0.62	0.909

Table 8.2 Results of batch 1B

Run No.	Abrasive Type	Iron powder Type	Load (N/ ball)	Abra. (ml)	Iron Powder (ml)	Glycerin (ml)	Water (ml)	Time (Min)	Speeds		Results					
									Lathe (rpm)	Motor (rpm)	Rd. (µm)	Ra (nm)	Rt (µm)	Dia. (inch)	MRR/ ball (mg/min)	MRR/ ball (µm/ min)
1	B_4C	112+114	5.8	20	15	25	15	60	32	1475	7.89	---	---	0.45893	0.63	0.89
2	B_4C	112+114	6	20	15	25	15	45	32	1630	6.5	---	---	0.45661	0.91	1.301
3	B_4C	112+114	6	20	15	25	15	40	32	1630	4.12	---	---	0.45474	0.76	1.186
4	B_4C	112+114	5.8	17	12	25	25	40	32	1630	3.79	---	---	0.45317	0.67	0.99
5	B_4C	FE-114	5.8	20	15	20	25	40	32	1630	3.55	---	---	0.45169	0.59	0.94
6	B_4C	FE-114	5.5	18	12	20	20	120	32	1000	1.34	132.3	1.012	0.4477	0.54	0.84
7	B_4C	114+112	5.5	20	12	20	20	120	32	1000	.8	107.5	.8772	0.44358	0.55	0.87
8	SiC-1200	114+112	5	20	12	20	20	130	32	970	.59	61.37	.5341	0.44166	0.25	0.38
9	SiC-8000	114+112	5	20	12	20	25	130	32	945	.58	25	.2364	0.44128	0.037	0.07
10	SiC-8000	FE-112	5	20	12	20	30	180	32	870	.62	30.93	.289	0.44091	0.037	0.05
11	SiC-10000	FE-114	5	20	8	20	20	105	32	970	.95	15.76	.1424	0.44085	0.024	0.01
12	SiC-10000	FE-102	5	20	8	20	20	105	32	990	.92	18.67	.1606	0.44067	0.020	0.04
13	SiC-8000	---	5	28	---	25	20	105	32	945	.82	13.61	.1386	0.44063	0.006	0.01
14	SiC-8000	---	5	25	---	20	20	105	32	945	.84	15.93	.1398	0.44058	0.006	0.01
15	SiC-10000	Fe_2O_3 + $Fe3O_4$	5	15	15	17	25	105	32	990	.81	12.85	.1274	0.44046	0.014	0.03
16	CeO_2	Fe_2O_3	5	15	15	12	25	120	32	945	.75	11.9	.1272	0.44038	0.002	0.017
17	CeO_2	---	5	15	---	15	25	120	32	1075	**.79**	**11.6**	.1192	0.44043	--	--

Table 8.3 Results of batch 2A

Run No.	Abrasive Type	Iron powder Type	Load N/ball	Abra. (ml)	Iron Powder (ml)	Glycerin (ml)	Water (ml)	Time (Min)	Speeds		Results					
									Lathe (rpm)	Shaft/ Spindle (rpm)	Rd. (µm)	Ra (nm)	Rt (µm)	Ball Dia. (inch)	MRR/ ball (mg/min)	MRR/ball (µm/ min)
Initial	As received condition with band															
1	B_4C-500	FE-114	5.4	15	7	20	30	105	32	1070	N/A	N/A	N/A	0.52886	0.40	N/A
2	B_4C-500	FE-114	5.8	15	7	20	30	105	32	1070	N/A	N/A	N/A	0.52350	1.04	0.91
3	B_4C-500	FE-114	5.8	15	7	25	25	105	32	1070	N/A	N/A	N/A	0.51999	0.90	1.10
4	B_4C-500	FE-114	4	15	7	25	25	105	32	1070	N/A	N/A	N/A	0.51865	0.32	0.33
5	B_4C-500	FE-114	5	17	8	20	25	105	32	1070	N/A	N/A	N/A	0.51597	0.54	0.64
6	B_4C-500	FE-114	5.5	18	8	20	20	105	32	1070	3.10	N/A	N/A	0.51249	0.71	0.84
7	B_4C-500	FE-114	4.3	17	7	20	25	105	32	950	3.65	N/A	N/A	0.51068	0.38	0.44
8	B_4C-500	112+114	4.75	15	10	20	20	110	32	970	2.27	114	0.88	0.50752	0.604	0.73
9	SiC-600	Fe112	5	15	8	15	20	105	32	900	2.8	114	0.88	0.503833	0.747	0.89
10	SiC-1200	Fe112	4	15	8	20	15	150	32	1050	2.97	58	0.45	0.502706	0.145	0.19
11	SiC-1200	Fe112	4	16	8	17	15	145	32	850	3.65	57.6	0.45	0.500944	0.256	0.31
12	SiC-1200	114+112	3.5	15	10	12	20	150	32	735	2.86	N/A	N/A	0.50010	0.15	0.2

Table 8.4 Results of batch 2B

Run No.	Abrasive Type	Iron powder Type	Load N/ball	Abra. (ml)	Iron Powder (ml)	Glycerin (ml)	Water (ml)	Time (Min)	Speeds		Results					
									Lathe (rpm)	Shaft/ Spindle (rpm)	Rd. (µm)	Ra (nm)	Rt (µm)	Ball Dia. (inch)	MRR/ ball (mg/min)	MRR/ball (µm/min)
1	B_4C-500	114+112	5.8	15	10	15	20	120	32	745	3.6	N/A	N/A	0.49605	0.66	0.857
2	B_4C-500	FE-114	5.5	15	10	15	20	120	32	850	2.65	N/A	N/A	0.49307	0.51	0.63
3	B_4C-500	FE-112	3.95	15	10	15	20	150	32	625	2.13	N/A	N/A	0.49127	0.23	0.31
4	B_4C-500	FE-112	2.8	12	8	15	20	165	32	625	1.93	N/A	N/A	0.49022	0.11	0.16
5	B_4C-500	FE-112	2.8	15	8	15	20	110	32	745	1.78	N/A	N/A	0.48760	0.48	0.6
6	B_4C-500	FE-112	2.8	12	8	15	20	100	32	745	1.97	N/A	N/A	0.48627	0.26	0.35
7	B_4C-500	FE-112	3.2	15	8	15	20	110	32	745	1.56	N/A	N/A	0.48386	0.43	0.56
8	B_4C-500	Fe-112	2.8	12	8	15	20	110	32	600	1.54	N/A	N/A	0.48306	0.14	0.18
9	B_4C-500	112+114	3.2	12	8	15	20	110	32	850	1.28	N/A	N/A	0.48089	0.38	0.5
10	B_4C-500	112+114	5.5	15	8	15	20	120	32	850	1.4	N/A	N/A	0.47687	0.63	0.85
11	B_4C-500	112+114	6	15	8	15	20	120	32	825	1.6	102.5	0.8702	0.47230	0.69	0.98
12	SiC-600	112+114	3.5	12	8	15	20	110	32	850	1.43	N/A	N/A	0.47039	0.31	0.44
13	SiC-600	112+114	3.25	12	8	15	20	110	32	850	1.44	99.6	0.8357	0.46856	0.29	0.42
14	SiC-1200	FE-112	2.2	12	7	15	20	80	32	850	1.32	61.8	0.5412	0.46834	0.06	0.07
15	SiC-1200	FE-112	2	15	8	15	20	90	32	750	0.9	57.3	0.5121	0.46821	0.04	0.04
16	SiC-8000	FE-112	2.2	18	8	15	20	90	32	735	0.97	16	0.152	0.46800	0.015	------
17	SiC-10000	FE-112	2.5	15	8	20	20	110	32	750	0.93	19.4	0.1925	0.46800	0.012	------
18	CeO_2	FE-112	3	10	8	20	25	120	32	735	0.77	12.2	0.119	0.46800	---	------

8.1 DISCUSSION OF BATCH 1A

This set of experiment served as the basis for the establishment of alternate and cost effective technology for finishing ceramic balls. Prior to this, three apparatus were designed, fabricated and experimented; in search of a new method for finishing large batches of ceramic balls. These apparatus was designed using 'Ball Screw'. Load application, wear of screw and nut were major concerns in these studies towards this study. The next two apparatus were based on a similar principle of ball screw, but the screw was replaced by a pulley made of two beveled steel plates with spring loading and the nut was replaced by a tube. Balls were loaded between these plates and tube inner surface, thereby establishing 3 point contact polishing. Stability, vibration and requirement of large amount of abrasive mixture were major concerns with these two apparatus.

Table 8.1 shows the parameters and results for first set of experiments. The first, objective was to identify the effect of magnetic field on the material removal rate (MRR). Test runs 1 to 6 were conducted without the magnetic field and the MRR values obtained were very low as compared to values with the magnetic field. This clearly shows that magnetic field aids in concentrating abrasive particles in the polishing zone, which leads to high MRR. Without out magnetic field there was every possibility of abrasive particles getting scattered. Figure 8.1.1 and Figure 8.1.2 are the photographs taken after test run, which clearly shows the impoundment of abrasive slurry around the balls due to magnetic field. Figure 8.1.3 show the graph of MMR with and without magnetic field. From test

run number 7 onwards a clear increase in MRR can be seen, this was because of the fact that magnetic field was used from 7th run onwards.

Figure 8.1.1 Full view photograph ofthe balls after the test run

Figure 8.1.2 Photograph of balls immersed in abrasive slurry after the test run

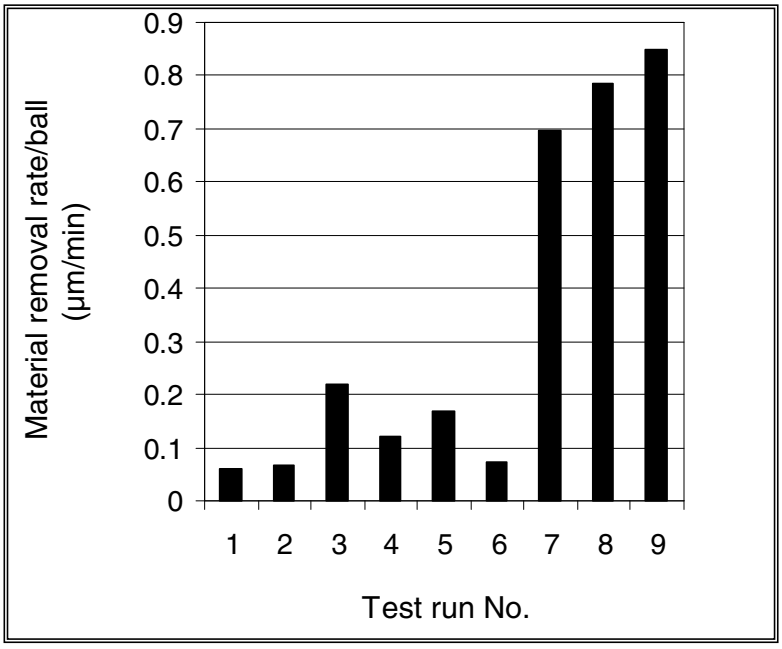

Figure 8.1.3 Variation in MMR with (7-9) and without the magnetic field (1-6)

Test runs from 7 to 17 and 33 to 34 were conducted at a lathe spindle speed of 32 rpm, test runs from 18 to 21 were carried out at lathe spindle speed of 64 rpm, and finally runs from 22 to 33 were conducted with only shaft rotating and lathe being still. These test results were conducted to determine optimum lathe spindle speed. In other words rotating speed of the acrylic polishing plate and the chamber to obtain good sphericity and high MRR. Table 8.5 shows the sorted test data of MMR for three different lathe spindle speeds (polishing plate) and at constant load. Sorted data of sphericity with three speeds are given in Table 8.1.2.

Table 8.1.1 Values of MRR for three different lathe spindle speed at a constant load of 5.8 N/ball

Load (N/ball)	Lathe Speeds (rpm)	Values of MRR/ball (μm/min)
5.8	0	1.01, 1.19, 1.38
5.8	32	0.84, 1, 0.97, 1.19
5.8	64	0.91, 1.12,1.22

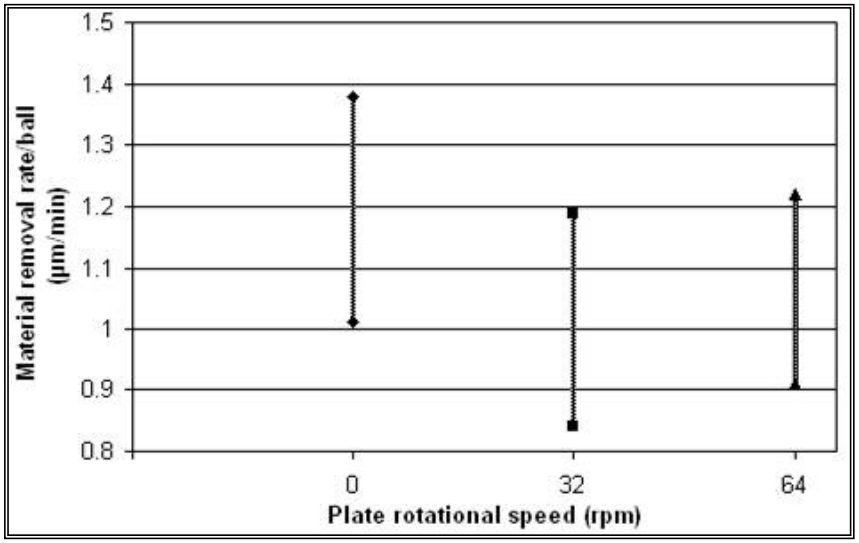

Figure 8.1.4 Variation in MRR with polishing plate speeds

Table 8.1.2 Values of sphericity for three different lathe spindle speeds

Lathe spindle speed (rpm)	Values of sphericity (μm)
0	2, 2.1, 2.54, 3.1, 3.22, 3.61, 3.8, 4.17, 4.36, 5.03, 5.75
32	1.6, 1.8, 1.95, 2.33, 3.5, 5.39, 5.9, 6.45
64	3.76, 6.44, 7.03, 11.24

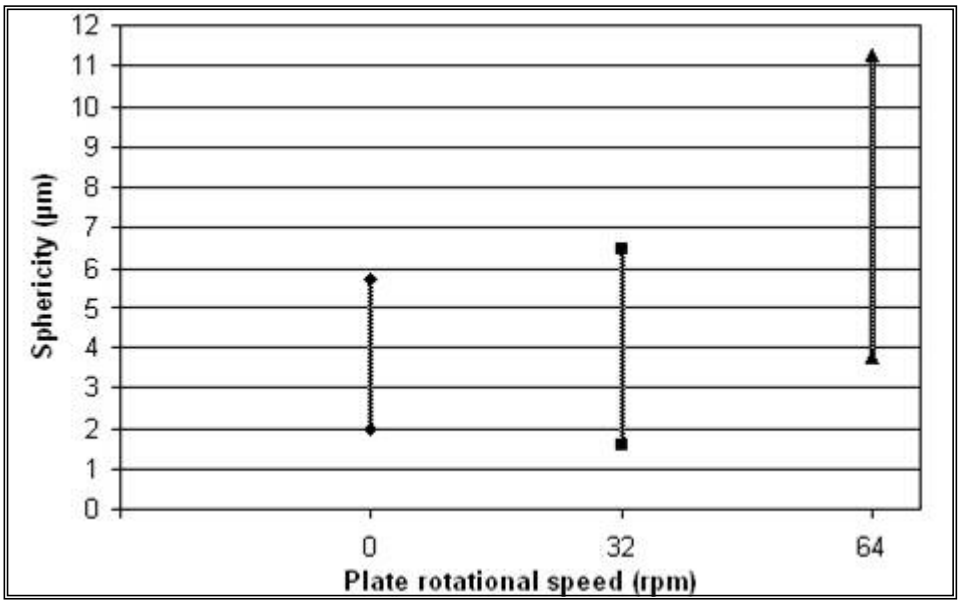

Figure 8.1.5 Variation in sphericity with polishing plate speeds

For the sorted values from Table 8.1.2, we can conclude that all three lathe spindle speeds provide close values of MRR, but 32 rpm helps in improves sphericity. Hence 32 rpm of lathe spindle speed is used in further experiments. Also, *in-situ* observation helped to conclude that lathe spindle speed should be maintained at 32 rpm.

To summarize, the investigation of batch 1A helps to conclude that magnetic field plays an important role in polishing and lathe spindle speed of 32 rpm yields considerable MMR and good sphericity.

8.2 DISCUSSION OF BATCH 1B

The apparatus was refitted with spindle being re-machined with 30˚ bevel. In order to prevent minor leaks, slight modifications were made to the apparatus keeping the basic design unaltered. These modifications facilitated in increasing

the polishing duration. One such example was continuous supply of compressed air near to the polishing zone to cool the chamber Also, an oil seal is introduced to prevent leaks. The average sphericity for the batch was 0.79 μm, with a standard deviation of 0.12 μm. For a single ball, the best results obtained were a sphericity of 0.5 μm and a surface finish of 10.4 nm Ra. Table 8.2.1 gives a outline of the polishing conditions, results, and general remarks for each of the runs for this batch. For the entire test runs lathe spindle speed was maintained at 32 rpm.

From the analysis of this batch, it was concluded that, though the spindle groove helps in improving sphericity, if groove exceeds the limit then it can become a hindrance for further improvement of sphericity. Two solutions can be considered to overcome this situation, one, is *in-situ* machining of the spindle and the other is to reduce the spindle bevel angle to ≤ 25˚. This aspect will be studied in the next batch. With groove on the spindle, still surface finish can be improved to 11 nm.

Table 8.2.1 Summary of polishing conditions and results for 1B batch

Run No.	Polishing conditions	Results	Remarks
	Initial measurements	Dia. 0.46107" Sphericity 5.26 µm Ra 133 nm	
1-5	B_4C-500, 5.5 - 6.0 N/ball, spindle- 1474 - 1630 rpm, 40 - 60 mins.	Dia. 0.45169 MRR- 0.89 – 1.3 µm/min/ball, Sphericity 3.55 – 7.89 µm Ra 133 nm	Due to machined bevel surface sphericity initially increases and than slow goes down with groove formed on spindle. Ra continues to be same due to B_4C-500 abrasive.
6 & 7	B_4C- 500, 5.5 N/ball, Spindle 1000 rpm, 120 mins.	Dia. 0.44358 MRR- 0.85 µm/min/ball, Sphericity 0.8 – 1.34 µm Ra 107 nm	A sharp improvement in sphericity due to decrease in speed to 1000 rpm and increase in polishing duration
8	SiC-1200, 5 N/ball, 970 rpm, 130 mins.	Dia. 0.44166 MRR- 0.38 µm/min/ball, Sphericity 0.59 µm Ra 61 nm	Sharp decrease in surface finish
9 & 10	SiC-8000, 5 N/ball, 870- 945 rpm, 130 – 180 mins	Dia. 0.44091 MRR- 0.05 – 0. 07 µm/min/ball, Sphericity 0.58 – 0.62 µm Ra 25 - 30 nm	No significant change in the sphericity. Decrease in surface finish due to use of softer abrasive
11 & 12	SiC-10000, 5 N/ball, 970- 990 rpm, 105 mins	Dia. 0.44067 MRR- 0.01 – 0. 04 µm/min/ball, Sphericity 0.92 – 0.95 µm Ra 15 - 18 nm	It was realized that due to a deep groove on spindle, ball sphericity was going bad. Hence, edges were smoothened off using a sand paper and a hand file, keeping spindle in place. Decrease in surface finish.
13 & 14	SiC-8000, 5 N/ball, 945 rpm, 105 mins	Dia. 0.44058 MRR- 0.01 µm/min/ball, Sphericity 0.82 – 0.84 µm Ra 13 - 15 nm	Improvement in sphericity. No iron powder and magnetic field was used. Hence, decrease in MRR can be seen.
15	SiC-10000, 5 N/ball, 990 rpm, 105 mins $Fe_2O_3 + Fe_3O_4$	Dia. 0.44046 MRR- 0.03 µm/min/ball, Sphericity 0.81 µm Ra 13 nm	As alternative iron oxide was used instead of iron powder, no significant improvement was seen.
16 & 17	CeO_2, 5 N/ball, 945 - 990 rpm, 120 mins Fe_2O_3	Dia. 0.44038 MRR- 0.017 µm/min/ball, Sphericity 0.75 – 0.79 µm Ra 11. 6 nm	Chemo-mechanical polishing improved sphericity to 0.79 µm and surface finish to 11.6 nm

8.3 DISCUSSION OF BATCH 2A

Last two batches of polishing confirm that spherical objects can be successfully polished using unbonded magnetic abrasive and spring loading. Several changes were necessary to maintain reliability of the process keeping both the set up time and cleaning time as low as possible. Though this time is not accounted for the total processing time, it adds up to a significant value by the end of complete polishing of a batch. In the apparatus used for the last two batches, it was difficult to control loading. Hence, this was taken care in this design and the last criterion was to use less abrasive powder by designing compact chamber.

Present apparatus was a result of these considerations. Hence, several changes to the original design and new batch of balls were taken for the study. This is the reason for the variation in results from different runs with identical run parameters.

Third batch of as-received half-inch balls were used for this study. Table 8.3 provides details of all the runs conducted to confirm MRR and sphericity during initial roughing stages. But, due to misalignment of spindle and chamber axis the desired sphericity value was not obtained. Hence, spindle was realigned and next set of experimentations were carried out as shown in Table 8.4. The third batch of polishing showed that MRR close to 1 μm/min/ball can easily be achieved.

8.4 DISCUSSION OF BATCH 2B

Except for the realigning of the spindle and the chamber, no other changes were made to the apparatus. However, the groove formed during polishing of batch 2A was continued. By now it was clear that higher loads will yield higher MRR during the roughing stage. In this batch, most of the test runs were conducted at lower loads and their effect on sphericity was identified.

Table 8.4.1 gives an outline of the polishing conditions, results, and general remarks for each test runs of batch 2B. For the entire test runs, lathe spindle speed was maintained at 32 rpm. It was also found that a, mixture of FE-112 (44-149 μm) and FE-114 (149-297 μm) iron powder would yield better removal rate and FE –112 should be used with softer abrasive.

Table 8.4.1 Summary of polishing conditions and results for 2B batch

Run No.	Polishing conditions	Results	Remarks
	Initial measurements	Dia. 0.49605", Sphericity 2.86 µm Ra 58 nm	
1-2	B_4C-500, 5.5 – 5.8 N/ball, spindle- 745 - 850 rpm, 120 mins.	Dia. 0.49307 MRR- 0.63 – 0.9 µm/min/ball, Sphericity 2.65 µm	Due to realignment of spindle and chamber, during first run sphericity shouted up from 2.86 µm to 3.6 µm, and then next run brought sphericity back to 2.65 µm.
3 - 9	B_4C- 500, 2.8 – 4 N/ball, Spindle 600 - 850 rpm, 100 - 120 mins.	Dia. 0.48089 MRR- 0.18 – 0.56 µm/min/ball, Sphericity 1.28 µm	A gradual improvement in spherity was observed during these runs. Hence it can be concluded that reduced loading helps in improving sphericity.
10 & 11	B_4C-500, 5.5 - 6 N/ball, spindle 825- 850 rpm, 120 mins	Dia. 0.47230, MRR- 0.38 µm/min/ball, Sphericity 1.4 -1.6 µm Ra 102 nm	The aim was to see what happens if load is increased at this stage? The conclusion made regarding reduced loading holds good.
12 & 13	SiC-600, 3.25 – 3.5 N/ball, 850 rpm, 110 mins	Dia. 0.46856 MRR- 0.42 – 0.44 µm/min/ball, Sphericity 1.43 – 1.44 µm Ra 100 nm	Again, due to reduced loading sphericity improves
14 & 15	SiC-1200, 2.2 N/ball, 750 - 850 rpm, 80 - 90 mins	Dia. 0.46821, MRR- 0.04 – 0. 07 µm/min/ball, Sphericity 0.9 µm Ra 57 nm	Significant improvement in sphericity from 1.4 to 0.9 µm
16 &17	SiC-8000 & SiC-10000, 2.2 -2.5 N/ball, 735 – 750 rpm, 90 -110 mins	Dia. 0.46800 Sphericity 0.93 – 0.97 µm Ra 16 - 19 nm	There was no change in diameter due to low loads; this may be because only 3 balls average measurement was taken. Significant improvement in surface finish even with groove.
18	CeO_2, 3 N/ball, 735 rpm, 120 mins	Dia. 0.46800 Sphericity 0.77 µm Ra 12.2 nm	Chemo-mechanical polishing resulted in good sphericity and surface finish as expected even with groove. This confirms taper ≤25˚ prevents machining of groove during final stage.

8.5 EFFECT OF DIFFERENT PARAMETERS ON SPHERICITY, MRR, AND SURFACE FINISH

This section deals with a comprehensive analysis of results obtained from all the polished batches. Analysis will include effect of different parameters and polishing conditions on sphericity, removal rate, and surface finish. Finally, typical polishing conditions for polishing of Si_3N_4 balls by UMAP are given, based on the output obtained from this study.

8.5.1 FACTOR EFFECTING SPHERICITY

Good sphericity is an important and essential output of the polishing process, especially for ball bearing applications. ASTM specification F 2094 – 03a is related to the standard specification for silicon nitride bearing balls. The tolerances by grade for individual balls and lots of balls are given in Tables 8.5.1 and 8.5.2. The letter C indicates in this case ceramic silicon nitride. In this batch, we were able to achieve best sphericity of 0.5 μm, which falls in the 24C grade. However, the Grade 24C is not adequate for the applications of high-speed spindle and high-precision machine tools. But, this study being first of its kind, future effort should be made to make this nascent technology into a matured process.

This section analyzes different factors effecting sphericity, based on the experimental apparatus used and test runs carried out during this study. Some of the aspects can be broadly classified and linked to the apparatus, setup, machine tool, and process parameters.

Table 8.5.1. Tolerances by grade for individual balls μm (μin.)
[ASTM F2094-03a, 2005]

Grade	Allowable Ball Diameter Variation (V_{dws})	Allowable Deviation from Spherical Form (R_W)	Maximum Surface Roughness Arithmetical Average (Ra)
2C	0.05 (2)	0.05 (2)	0.004 (0.15)
3C	0.08 (3)	0.08 (3)	0.004 (0.15)
5C	0.13 (5)	0.13 (5)	0.005 (0.20)
10C	0.25 (10)	0.25 (10)	0.006 (0.25)
16C	0.40 (16)	0.40 (16)	0.009 (0.35)
24C	0.61 (24)	0.61 (24)	0.013 (0.50)
48C	1.22 (48)	1.22 (48)	0.013 (0.50)

Table 8.5.2. Tolerances by grade for ball lots μm (μin.)
[ASTM F2094-03a, 2005]

Grade	Allowable Lot Diameter Variation	Nominal Diameter Tolerance	Allowable Ball Gage Deviation	
			High	Low
2C	0.08 (3)	± 0.51 (± 20)	+ 0.51 (+ 20)	- 0.51 (- 20)
3C	0.13 (5)	± 0.51 (± 20)	+ 0.51 (+ 20)	- 0.51 (- 20)
5C	0.25 (10)	± 0.76 (± 30)	+ 0.76 (+ 30)	- 0.76 (- 30)
10C	0.51 (20)	± 2.54 (± 100)	+ 1.27 (+ 50)	- 1.02 (- 40)
16C	0.80 (32)	± 2.54 (± 100)	+ 1.27 (+ 50)	- 1.02 (- 40)
24C	1.22 (48)	± 2.54 (± 100)	+ 2.54 (+ 100)	- 2.54 (- 100)
48C	2.44 (96)	N/A	N/A	N/A

8.5.1.1 Factors associated with apparatus fabrication.

1) Ball circulation or motion during polishing depends on chamber and spindle rotations. It is important to make sure that both are fabricated on a precision machine tool. Imperfect machining leads to chamber or spindle tilt, thus causing slight angle with each axis. This gives rise to elliptical contact and improper ball circulation.
2) Spindle is held on a flange connected to the shaft mounted on a carriage. Carriage fixture should be perfectly mounted and held on the carriage base.

Failure to do so will led to vibration. Present carriage fixture was mounted on hallow steel square tubing, which resulted in offset of ± 4 divisions on the dial indicator (resolution of 0.0001 in.). This offset can be eliminated by using solid aluminum 2 in. thick plate.

3) Efforts were made to ensure that the carriage attachment was fabricated precisely but there were some human errors which led to misalignment of the chamber and the shaft.

4) Taper angle on the spindle plays very important role in maintaining sphericity during the finishing stage. It was found that taper angle ≤ 25 ˚ will help in forming a wide groove and helps in maintaining ball sphericity during the finishing stage. Figure 8.5.1 shows the variation of sphericity with taper angle and Figure 8.5.2 show the groove formed on 30˚ and ≤ 25˚ spindle taper, respectively.

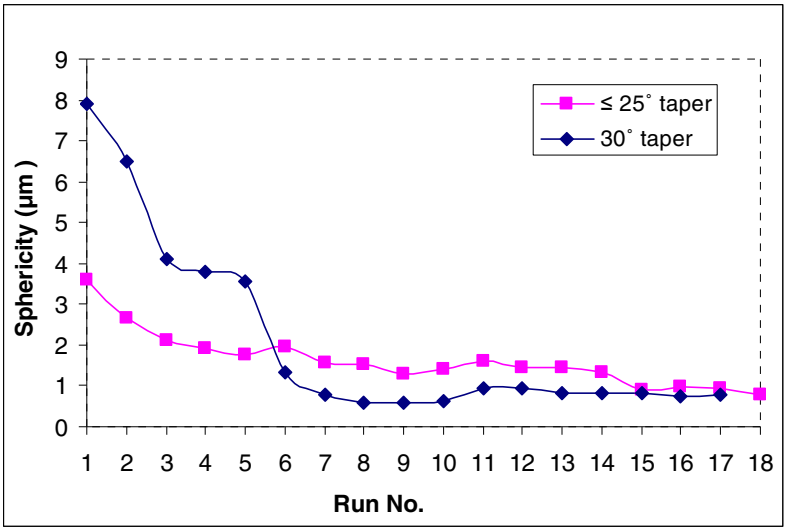

Figure 8.5.1 Variation of sphericity with polishing runs for ≤ 25˚ and 30˚ taper on the spindle

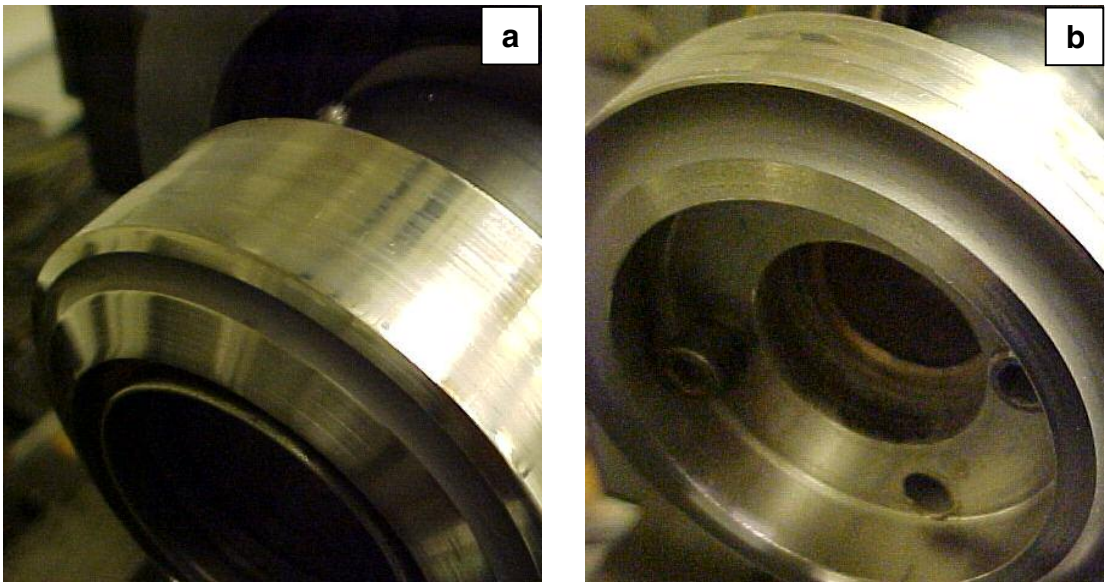

Figures 8.5.2 Groove formed on the spindle with (a) 30˚ taper, and (b) ≤ 25 ˚ taper

8.5.1.2 Factors associated with the setup.

Maintaining coaxiality between the rotating axis of the polishing spindle and the chamber inner surface is very important. Misalignment between the spindle and chamber axis can lead to non-uniform application of load on the balls, which may consequently lead to non-uniform removal of material resulting in bad sphericity. Hence, it is very important to follow the steps discussed in Section 6.2.2.

8.5.1.3 Factors associated with the machine tool

Machine tool on which the apparatus is mounted should be precise. But the lathe on which the present apparatus is mounted is off-centered by ± 4 divisions on the dial indicator (resolution of 0.0001 in.). This may lead to random motion of the chamber mounted on lathe chuck which can be aggravated at higher speeds. In this study the spindle of the machine tool is rotated at very low-speed of 32

rpm. Hence, this effect is assumed to be negligible. However, further study has to be carried out to determine its effect on sphericity.

Vibration due to machine tool can be another concern on sphericity. Again, this effect can be neglected due to low machine tool speed.

8.5.1.4 Factors associated with the polishing process

1. Abrasive wear on the spindle

Abrasive wear occurs on the polishing spindle, the polishing plate, and the polyurethane liner during polishing. The wear on the liner is negligible; however significant wear occurs on the plate and the spindle. The plate is replaced after two runs because both the surfaces are used; where as the liner is replaced after every polishing run.

A groove formed on the bevel of the spindle was found to be advantageous for improving sphericity. Severe abrasive wear occurs on the spindle forming deeper and deeper grooves as polishing progresses. This results in increased contact area. This increases the number of polishing contact points. This can change the 3-point contact polishing process to more than 3-point contact polishing process. Therefore, a groove is favored in achieving uniform polishing.

The groove formed on the spindle is such that its center will correspond to the center of the drive. Such wear is known as run-in wear. It is a well know fact that. In any mechanical system initial run-in wear rate of rotating or moving components shoots is very high (though the wear is small or negligible) and then stabilizes subsequently. Similarly, the run-in will be completed depending, on the spindle wear, which in turn depends on the eccentricity, speed, abrasive type,

and size. This eccentricity and vibration will be almost eliminated, thereby helping the process to improve sphericity. It should be noted that there will be a limit on the eccentricity between the spindle and the chamber axis, beyond which groove can not compensate. This is evident from batch 2A, where the amount of eccentricity was beyond the point of tolerance. Hence, sphericity could not be improved beyond certain point.

2. Spindle speed

Any rotating equipment or apparatus has a critical operating speed. Beyond the critical speed, equipment begins to vibration or cause noise, which affects the output. Similarly present polishing apparatus has a critical speed range beyond which speed affects sphericity. This critical speed depends on the accuracy of fabrication, machine tool and alignment accuracies. However, MRR can be achieved beyond this critical speed but at the expense of ball out-of-roundness. At the same time due to high-speed the chamber gets hot in ~40 - 50 min of polishing, thus making it impossible to run the experiment beyond 1 min. Hence, it was important to come up with optimum speed to improve sphericity and at the same achieve reasonable MRR. By analyzing the data sorted in Table 8.5.3 from all polishing batches, spindle speed in the range of 800-1100 rpm was found to be optimum to achieve good sphericity, MRR and long polishing time with less heat generation.

Table 8.5.3 Test results sorted from all batches to determine optimum spindle speed.

Batch	Run No.	Abrasive Type	Load (N/ball)	Time (Min)	Motor (rpm)	Rd. (µm)	MRR/ball (mg/min)	MRR/ball (µm/min)
1A	9	B_4C-500	5	60	1375		0.58	0.85
1A	16	B_4C-500	5.8	45	1650	1.6	0.76	0.995
1A	17	SiC-600	5.8	60	1650	3.5	0.76	0.965
1A	33	SiC-600	5.8	30	1630	4.98	0.83	1.194
1A	34	B_4C-500	5	45	1630	5.26	0.62	0.909
1B	1	B_4C-500	5.8	60	1475	7.89	0.63	0.89
1B	2	B_4C-500	6	45	1630	6.5	0.91	1.301
1B	4	B_4C-500	5.8	40	1630	3.79	0.67	0.99
1B	5	B_4C-500	5.8	40	1630	3.55	0.59	0.94
1B	6	B_4C-500	5.5	120	1000	1.34	0.54	0.84
1B	7	B_4C-500	5.5	120	1000	.8	0.55	0.87
2A	2	B_4C-500	5.8	105	1070	N/A	1.04	0.91
2A	3	B_4C-500	5.8	105	1070	N/A	0.90	1.10
2A	6	B_4C-500	5.5	105	1070	3.10	0.71	0.84
2B	1	B_4C-500	5.8	120	745	3.6	0.66	0.857
2B	2	B_4C-500	5.5	120	850	2.65	0.51	0.63
2B	10	B_4C-500	5.5	120	850	1.4	0.63	0.85
2B	11	B_4C-500	6	120	825	1.6	0.69	0.98

3. Polishing plate speed

From Tables 8.1.1 and 8.1.2 and Figures 8.1.4 and 8.1.5, It can be seen that all three lathe spindle speeds provide close values oi MRR, but 32 rpm plate speed provides best value of sphericity. Hence lathe spindle speed of 32 rpm, which rotates the plate, was selected for all experiments. Also, *in-situ* observation helped in concluding that lathe spindle speed should be maintained at 32 rpm.

4. Polishing Load

It can be seen from Table 8.5.3 that among the loadsused in the range of 2.5 – 5.8 N/ball higher load yield higher MRR and lower loads better sphericity.

Therefore, depending on the output requirements and the stage of the polishing process, loads can be selected.

5. Polishing duration

Polishing duration depends on the spindle speed. Unlike in MFP there is no concern about degradation of the abrasive slurry. From Table 8.5.3, it can be seen that polishing duration in the range of 100 – 180 minutes is appropriate. However, other factors such as MRR required, abrasive type, and speed should be considered while deciding on the polishing duration.

8.5.2 MATERIAL REMOVAL RATE (MRR)

The parameters affecting MRR are load, spindle speed, polishing duration, and abrasive type.

1. Load

Higher the polishing load, higher is the MRR. However, Kang *et. al.* [2005], concluded in case of lapping there is critical load beyond which MRR starts to decrease proportionately. Such study was not conducted in this investigation. Maximum load tested on this apparatus was 6.5 N/ball and the highest MRR achieved was 1.53 µm/min/ball. This confirms that higher load will yield higher MRR, at the same time other parameters have to be considered while deciding the load.

2. Spindle speed

Similarly higher speed will yield higher MRR, but at the expense of sphericity. By analyzing the data sorted from all the polishing batches in Table 8.5.3, spindle speed in the range of 800-1100 rpm was found suitable for

achieving moderate MRR while maintaining good sphericity. Other factors to be considered while deciding on the spindle speed are load, abrasive type, and polishing duration.

3. Polishing duration

Unlike in the case of MFP, there is no consideration of magnetic fluid getting degraded. Polishing can be carried out until the abrasive particles are completely used up. However, future studies should analyze the wear debris to determine optimum polishing duration. From the data gathered from 90 – 180 minutes was the good rangefor the present study.

4. Abrasive

Harder and coarser abrasive yields higher MRR. Depending on the stage at which polishing is in progress, abrasive are selected. Table 8.5.4 gives the abrasives-type to be used at different stages and corresponding removal rates.

Table 8.5.4 MRR corresponding to abrasive type and load

Stage	Abrasives	Load (N/ball)	MRR (μm/min/ball)
I	Boron carbide (B_4C) - 500 grit (12 μm) Silicon carbide (SiC) - 600 grit (10 μm)	3 - 6	0.3 - 1.2 0.3 - 0.9
II	Silicon carbide (SiC)-1200 grit (2.1 μm)	2 - 4	0.05 – 0.2
III	Silicon carbide (SiC)-8,000 and 10,000 grit (0.5 μm) Cerium oxide (CeO_2) - (< 5 μm)	3 – 3.5	0.01 – 0.03 Max 0.01

8.5.3 SURFACE FINISH

Jaing [1998d] identified three parameters affecting surface finish, namely, load, spindle speed, and abrasive concentration. Jaing and Komanduri [1997] used Taguchi's method and showed that higher load, higher speed, and lower

abrasive concentration yield good surface finish and sphericity. In case of UMAP where groove was used during the finishing stage, in addition to load, speed and abrasive concentration spindle bevel angle also plays an important role. It was observed that taper angle of ≤ 25˚ is required to achieve good surface finish with a groove. It is also recommended that last or second CMP test should be run without magnetic particles. This facilitates improvement of surface finish at a faster rate.

8.6 TYPICAL PROCESSING CONDITIONS FOR FINISHING HALF-INCH SILICON NITRIDE BALLS

Based on the data gathered from initial experimentation, the following processing conditions are proposed to finish 17, ½ in. silicon nitride balls using UMAP. Table 8.6.1 gives run by run procedure for polishing ½ in. balls. An average sphericity of 0.7 μm and surface finish of 10 nm can be expected by following the procedure outlined.

If the carriage attachment base plate was mounted on the solid aluminum plate. Instead of hallow square tube and by designing a better spindle holder can definitely improve the results.

For all the polishing runs the following parameters should be maintained constant : lathe spindle speed of 32 rpm, abrasive of 15 – 20 ml, iron powder of 8- 10 ml, glycerin 20 – 25 ml, de-ionized water 25 – 30 ml, and a few drops of water soluble rust inhibitor (except the last run).

Table 8.6.1 Typical conditions for polishing 17, ½ in. silicon nitride balls

Run No.	Abrasive Type	Iron powder	Load N/ball	Abra. (ml)	Time (Min)	Spindle (rpm)	Ball Dia. (D)	ΔD (in.)
1	B_4C-500	114+112	5.2 -5.5	20	180	700 -750		0.005-0.007
2	B_4C-500	114+112	5	15	180	750-800	0.52315	0.006-0.007
3	B_4C-500	114+112	5	15	150	750-800	0.51615	0.005-0.006
4	B_4C-500	114+112	4.5	15	120	750-800	0.51015	0.0035-0.0045
5	SiC-600	114+112	4.5	15	120	750-800	0.50615	0.003-0.0035
6	SiC-600	114+112	3.5	15	120	750-800	0.50265	0.002
7	SiC-1200	112	3	15	120	750-800	0.50065	0.00025-0.0003
8	SiC-1200	112	2-2.5	15	120	750-800	0.50035	0.0002
9	SiC-8000	112	2.5-3	15	120	750-800	0.50015	0.0001
10	SiC-8000or 10000	112	2.5-3	15	120	750-800	0.50005	0.00005
11	CeO_2	112	3	15	100	750-800	0.50000	----
12	CeO_2	-----	4	20	90	850 - 1000	0.50000	-----

CHAPTER 9

CONCLUSIONS AND FUTURE WORK

9.1 CONCLUSIONS

1. In this investigation a cost effective polishing technology, namely, unbonded magnetic abrasive polishing (UMAP) was developed by combining the principles of MAF, MFP and V-groove lapping.

2. This process uses neither expensive diamond abrasive nor costly magnetic fluid.

3. Childs and Moss [2001] identified the three functions of the magnetic fluid. They are: 1) viscous drag on the balls resulting in sliding between shaft and ball, 2) compliant loading system of balls on shaft due to magnetic force and 3) loose abrasive grit levitation. These functions were replaced by 1) using a mixture of glycerin and de-ionized water, known as, non-magnetic fluid [Chang and Childs, 1998] to achieve viscous drag on balls, 2) mechanical compression spring as the loading system for balls on the polishing spindle, 3) unbonded magnetic abrasive (loose abrasive grit and iron powder) so as to suspend the loose abrasive in the polishing zone by magnetic action.

4. A two batch of 17, half-inch balls have been finished with average sphericity of 0.79 and 0.77 μm (0.5 – 1 μm) and average surface finish R_a, of 11.6 nm

(10.6 – 12.5 nm). High material removal rate up to 1.2 μm/min/ball has been achieved.

5. A systems approach involving principles of MAF, MFP, and lapping, magnetic field analysis (FEM), design and construction of apparatus, identifying optimum polishing conditions and process modeling was used for the development of the technology.

6. Basic apparatus design beganwith geometric design of the components based on ball diameter, required magnet size and approximate chamber diameters (based on the knowledge from previous apparatus design). Most of the components used in UMAP apparatus were similar to that of MFP. Hence, same materials used in MFP were selected for UMAP components. Once the dimensions of all the parts were decided. Each component was modeled and machined *in-house* to a tolerance of ± 0.0004 in.
7. FEM analysis confirms that 14 magnets of ½ in^3 each arranged radially on the periphery of a 5 in. ID steel pipe with alternate N and S poles, separated by non-magnetic spacer, generates maximum radial magnetic flux and field in the polishing zone.
8. The balls can be finished from the as-received condition to finished stage in one operation by changing the abrasive type, abrasive size, load, iron powder size, abrasive concentration and speed. Hence, it is not necessary to change the machine or method from initial roughing to final finishing.
9. Lathe is used as the machine tool. The equipment was mounted on the horizontal axis. This facilitates clean up of the apparatus *in-place* without

pulling out the chamber or spindle. *In-place* cleaning not only reduces unaccounted cleaning time but also maintains spindle and chamber alignment, which increases accuracy of machining. It also reduces significant time consumed in setting up of experiment for the next polishing run.

10. Due to simple setup and operating procedure, least supervision is needed to operate the UMAP equipment. Operator's attention is needed only during first 15 – 30 min of the test. Unlike in other ball polishing apparatus there is no need to check the fluid level or vibrations until the experiment is completed.
11. UMAP equipment can be easily mounted on commercially available lathe without the need for heavy capital investment on a precision machine tool
12. This technique can be used to polish fewer ceramic balls in one batch. Unlike the conventional technique where a large number (1000 – 10,000) of balls required to maintain alignment and accuracy.
13. The three-stage (roughing, semi-finishing, and final finishing) polishing procedure established for MFP has been successfully implemented for UMAP technique. Initial roughing was carried out using B_4C (500 grit) and SiC (600 grit) to achieve high material removal. Semi-finishing was carried out using finer SiC abrasive (1200 grit) to improve sphericity. Finishing was carried out using SiC abrasive (10,000 grit) followed by chemo-mechanical polishing using CeO_2, to improve the surface finish and sphericity.
14. The groove formed on the spindle bevel helps in improving and maintaining the sphericity at all stages of polishing. Significant amount of time spent on machining spindle groove was saved by continuing the groove till the batch of

balls was finished. It was reported by Kirtane [2004] that machining of spindle groove was necessary to improve surface finish during finishing stage in MFP. However by reducing taper angel to ≤ 25˚, required surface was achieved without the need for machining the spindle groove, thereby eliminating machining and aligning times.

15. In addition to increased load, increased polishing speed and decreased concentration, taper angle on the spindle plays important role in achieving good finish.
16. Recommended iron powders
    - Mixture of Fe-114 and Fe-112 for first and second stages
    - Fe -112 for final finishing stage
    - Last CeO_2 run out without magnetic particles

9.2 FUTURE WORK

1. Further research needed for superior results (better sphericity and finish)
2. Efforts are being made to polish large number of balls without increasing the chamber size. This can be achieved by recalculating the balls between the plate and the spindle through a plastic tube.
3. Efforts should be made to use bonded type abrasive to study its effect on the output parameters.
4. Before any future experimentation is carried out on this apparatus, it is advisable to change steel hallow plate supporting base plate on carriage by a solid support. Also, spindle support has to be more robust and vibration free

by aligning co-axially with the lathe spindle, as to increase the critical speed range of the spindle. This will further help in achieving good sphericity and surface finish close to 4 nm.

5. Ball surface analysis after polishing with different abrasive has to be carried out. In order to investigate the extent of damage caused during mechanical polishing on the surface.
6. Wear debris analysis has to be carried out to study material removal mechanisms and the chips formed during mechanical polishing.
7. There are large numbers of parameters in case of UMAP. Further studies have to be carried out to study the effect of each parameter on sphericity and MRR.
8. Design of experiment, such as Taguchi's method has to be used to improve MRR and sphericity.
9. This process can be further extended to finish other advanced ceramics, such as zirconia balls, alumina balls for flow control applications.
10. Present study uses concentric alignment of polishing plate and spindle; efforts should be made to design eccentric UMAP machine.
11. Study the effect of different viscous liquids instead of glycerin or with different proportions of glycerin and do-ionized water on MRR, sphericity, and finish.
12. It was confirmed from this study and previous studies that groove on the polishing spindle helps in improving sphericity. Effort should be made to study the effect of groove on the polishing plate and the spindle on sphericity, MRR, and surface finish.

13. The material of the polishing plate should be changed and study its effect on the output parameters.
14. Finish larger diameter balls the size of the magnets have to be changed and analysis has to be carried out to arrive at the optimum conditions.
15. Different magnet layouts should be simulated to concentrate maximum field at the polishing contact point. This helps in improving the MRR.

REFERENCES

Agrawal, K., "Magnetic abrasive finishing (MAF) of non-magnetic rollers," M.S. thesis, Mechanical and Aerospace Engineering, Oklahoma State University, Stillwater, OK, (1994).

ASTM F 2094-03a, "Standard specification for silicon nitride bearing balls," Annual Book of ASTM Standards, 1.08 (2005) 497-504.

Atlantic Equipment Engineers (AEE), Website (www.micronmetals.com/iron.htm).

Bhagavatula, S., "Chemomechanical polishing of silicon nitride with chromium oxide abrasive," M.S. thesis, Mechanical and Aerospace Engineering, Oklahoma State University, Stillwater, OK, (1995).

Bhagavatula, S. R. and R. Komanduri, "On chemomechanical polishing of Si_3N_4 with Cr_2O_3," Philosophical Magazine A, 74 (1996) 1003-1017.

Buijs, M., Korpel-Van Houten, K., "Model for lapping of glass," Journal of Materials Science, 28 (1993) 3014-3020.

Chandrasekar, S., and Farris, T.N., "Machining and surface finishing of brittle solids," Sadhana: Acad. Proc. Eng. Sci., 22 (1997) 473–481

Chang, G. W., Yan, B. H., Hsu, R. T., "Study on cylindrical magnetic abrasive finishing using unbonded magnetic abrasives," Int. Journal of machine tools & manufacture, 42 (2002) 575-583.

Chang, F. Y. and Childs, T. H. C., "Non-magnetic fluid grinding," Wear, 223 (1998) 7–12.

Childs, T. H. C. and H. J. Yoon, “Magnetic fluid grinding cell design,” Annals of the CIRP, 41 (1992) 343-346.

Childs, T. H. C., Mahmood, S. and H. J. Yoon, “The material removal mechanism in magnetic fluid grinding of ceramic ball bearings,” Proceedings of the I Mech E Part B, Journal of Engineering Manufacture, 208 (1994a) 47-60.

Childs, T. H. C., Jones, D. A., Mahmood, S., Zhang, B., Kato, K. and N. Umehara, “Magnetic fluid grinding mechanics,” Wear, 175 (1994b) 189-198.

Childs, T. H. C., Mahmood, S. and H. J. Yoon, “Magnetic fluid grinding of ceramic balls,” Tribology International, 28 (1995) 341-348.

Childs, T. H. C. and D. J. Moss, “Wear and cost issues in magnetic fluid grinding,” Wear, 249 (2001) 509-516.

Coats, H. P., “Method and apparatus for polishing containers,” US Patent No. 2,196,058 (April 2,1940).

Fox, M. J., “Magnetic abrasive finishing of non-ferromagnetic rolling elements,” M.S. thesis, Mechanical and Aerospace Engineering, Oklahoma State University, Stillwater, OK, (1994).

Fox, M., Agrawal, K., Shinmura, T., Komanduri, R.,”Magnetic abrasive finishing of rollers,” Annals of CIRP 43 (1) (1994) 181-184.

Gerlick, E., R., “Polishing of ¾ in. silicon nitride balls using the large batch magnetic float polishing,” M.S. thesis, Mechanical and Aerospace Engineering, Oklahoma State University, Stillwater, OK, (2004).

Hou, Z. B. and R. Komanduri, “Magnetic field assisted finishing of ceramics - Part I: Thermal model,” Transactions of the ASME, Journal of Tribology, 120 (1998a) 645-651.

Hou, Z. B. and R. Komanduri, “Magnetic field assisted finishing of ceramics - Part II: On the thermal aspects of magnetic float polishing (MFP) of ceramic balls,” Transactions of the ASME, Journal of Tribology, 120 (1998b) 652 659.

Hou, Z. B. and R. Komanduri, “Magnetic field assisted finishing of ceramics - Part III: On the thermal aspects of magnetic abrasive finishing (MAF) of ceramic rollers,” Transactions of the ASME, Journal of Tribology, 120 (1998c) 660-667.

Jiang, M. and R. Komanduri, “Application of Taguchi method for optimization of finishing conditions in magnetic float polishing (MFP),” Wear, 213 (1997) 59-71.

Jiang, M., Wood, N. O. and R. Komanduri, “On chemo-mechanical polishing (CMP) of silicon nitride (Si_3N_4) workmaterial with various abrasives,” Wear, 220 (1998a) 59-71.

Jiang, M., Wood, N. O. and R. Komanduri, “On the chemo-mechanical polishing (CMP) of Si_3N_4 bearing balls with water based CeO_2 slurry,” Transactions of the ASME, Journal of Engineering Materials and Technology, 120 (1998b) 304-312.

Jiang, M. and R. Komanduri, “On the finishing of Si_3N_4 balls for bearing applications,” Wear, 215 (1998c) 267-278.

Jiang, M., “Finishing of advanced ceramic balls for bearing applications by magnetic float polishing (MFP) involving fine polishing followed by chemo-mechanical polishing (CMP),” Ph.D. thesis, Mechanical and Aerospace Engineering, Oklahoma State University, Stillwater, OK, (1998d).

Kann, L. W., “Appling abrasive materials,” US Patent No. 588,441 (August 17, 1897).

Kang, J., Hadfield, M. and R. Cundill, “The consequences of aggressive lapping processes on the surface integrity of HIPed silicon nitride bearing balls,” Proceedings of the International Conference on Tribology in Environmental Design 2000, Bournemouth UK, (2000) 227-234.

Kang, J. and M. Hadfield, “Parameter optimization by Taguchi methods for finishing advanced ceramic balls using a novel eccentric lapping machine,” Proceedings of the I Mech E Part B, Journal of Engineering Manufacture, 215 (2001a) 69-78.

Kang, J. and M. Hadfield, “A novel eccentric lapping machine for finishing advanced ceramic balls,” Proceedings of the I Mech E Part B, Journal of Engineering Manufacture, 215 (2001b) 781-795.

Kang, J. and M. Hadfield, “The effects of lapping load in finishing advanced ceramic balls on a novel eccentric lapping machine,” Proceedings of the I Mech E Part B, Journal of Engineering Manufacture, 219 (2005) 505-513.

Kirtane, S., T., “Finishing of silicon nitride(Si_3N_4) balls for advanced bearing applications by large batch magnetic float polishing,” M.S. thesis, Mechanical

and Aerospace Engineering, Oklahoma State University, Stillwater, OK, (2004).

Komanduri, R., Umehara, N. and M. Raghunandan, "On the possibility of chemo-mechanical action in magnetic float polishing of silicon nitride," Transactions of ASME, Journal of Tribology, 118 (1996b) 721-27.

Komanduri, R., Hou, Z. B., Umehara, N., Raghunandan, M., Jiang, M., Bhagavatula, S. R., Noori-Khajavi, A. and N. O. Wood, "A gentle method for finishing Si_3N_4 balls for hybrid bearing applications," Tribology Letters, 7 (1999a) 39-49.

Komanduri, R. and M. Jiang, "Magnetic float polishing processes and materials therefor," US Patent No. 5,931,718 (August 3, 1999).

Komanduri, R. and M. Jiang, "Magnetic float polishing of magnetic materials," US Patent No. 5,957,753 (September 28, 1999).

Lee, Kok-Loong, "Investigation of "Hidden" polishing parameters in magnetic float polishing (MFP) of silicon nitride (Si_3N_4) balls," M.S. thesis, Mechanical and Aerospace Engineering, Oklahoma State University, Stillwater, OK, (2005).

London, C. L., "Apparatus for low stress polishing of spherical objects," US Patent No. 4,965,967 (October 30, 1990).

Morgan Advanced Ceramics, (http://www.morganadvancedceramics.com/about ceramics.htm)

Raghunandan, M., "Magnetic float polishing of silicon nitride balls," Ph.D. thesis, Mechanical and Aerospace Engineering, Oklahoma State University, Stillwater, OK, (1996).

Raghunandan, M. and R. Komanduri, “Finishing of silicon nitride balls for high-speed bearing applications,” Transactions of the ASME, Journal of Manufacturing Science and Engineering, 120 (1998) 376-386.

Reddecliff, J. M., Valori, R., “The performance of a high-speed thrust bearing using silicon nitride balls,” Journal of Lubrication Technology, 10 (1976) 553-563.

Saint-Gobain Ceramics Website (www.cerbec.com).

Sato, C., “Ball lapping machine,” US Patent No. 5,301,470 (April 12, 1994).

Shinmura, T., Takazawa, K., Hatano, E. and M. Matsunaga, “Study on magnetic abrasive finishing,” Annals of the CIRP, 39 (1990) 325-328.

Shinmura, T., Hatano, E., and Takazawa, K., “The development of magnetic abrasive finishing and its equipment by appling a rotating magnetic field,” Bulletin of JSME, 29 (1986) 4437-4443.

Shinmura, T., and T. Aizawa, “Study on magnetic abrasive finishing process,” Bull. Japan Soc. Of Prec. E., 23 (1989) 236-239.

Shinmura, T., “A study on polishing mechanism of magnetic abrasive polishing and development of the apparatus,” PhD thesis, Utsunomiya University, Japan (1987).

Takazawa, K., Shinmura, T., and Hatano, E., “Development of magnetic abrasive finishing and its equipment,” MR 83-678. Proc. of the SME’S 12th Deburring and Surface Conditioning Conference, Orlando, (1983) 8-10.

Tani, Y. and K. Kawata, “Development of high-efficient fine finishing process using magnetic fluid,” Annals of the CIRP, 33 (1984) 217-220.

Thomas, V., “Magnetic abrasive finishing of internal surfaces,” M.S. thesis, Mechanical and Aerospace Engineering, Oklahoma State University, Stillwater, OK, (1997).

Umehara, N., “Research on magnetic fluid polishing,” PhD thesis (in Japanese), Tohuku University, Sendai, Japan (1990).

Umehara, N. and K. Kato, “Principles of magnetic fluid grinding of ceramic balls,” Applied Electromagnetics in Materials, 1 (1990) 37-43.

Umehara, N. and K. Kato, “Fundamental properties of magnetic fluid grinding with a floating polisher,” Journal of Magnetism and Magnetic Materials, 122 (1993) 428-43.

Umehara, N. and K. Kato, “Magnetic fluid grinding of advanced ceramic balls,” Wear, 200 (1996) 148-153.

Yasunaga, N., Obara, A. and O. Imanaka, “Study of mechanochemical effect on wear and its application to surface finishing, Journal of JSPE, 44 (1978) 77-83 (in Japanese).

Yuan, J. L., Lu, B. H., Lin, X., Zhang, L. B. and S. M. Ji, “Research on abrasives in the chemical-mechanical polishing process for silicon nitride balls,” Journal of Materials Processing Technology, 129 (2002) 171-175.

Ziegler, G., Heinrich, J., and G. Wotting, “Review - relationships between processing, microstructure and properties of dense and reaction-bonded silicon nitride,” Journal of Materials Science, 22 (1987) 3041-3086.

VITA

Anand Uplaonkar

Candidate for the Degree of

Master of Science

Thesis: EXPERIMENTAL INVESTIGATION OF UNBONDED MAGNETIC ABRASIVE POLISHING (UMAP) OF SILICON NITRIDE BALLS

Major Field: Mechanical Engineering

Biographical:

Personal Data: Born in Gulbarga, Karnataka, India, on August 2, 1977, the son of Shivasharanappa and Vijaylaxmi Uplaonkar

Education: Received Bachelor of Engineering degree in Mechanical Engineering from P.D.A College of Engineering, Gulbarga University, Gulbarga, India, in December 1999.
Completed the requirements for the Master of Science degree with a major in Mechanical and Aerospace Engineering at Oklahoma State University in December 2005.

Experience: Graduate Research Assistant in Mechanical and Aerospace Engineering Department, Oklahoma State University, Stillwater, Oklahoma, January, 2003 – present.
Graduate Assistant in Bio-system and Agricultural Engineering Department, Oklahoma State University, Stillwater, Oklahoma, May 2004 – December 2004.
Project Assistant, Instrumentation Department, Indian Institute of Science (IISc.), Bangalore, India.
Student Intern, Hindustan Aeronautics Limited (HAL), Bangalore, India.

Professional Memberships: ASME student member

Name: Anand Uplaonkar Date of Degree: December, 2005

Institution: Oklahoma State University Location: Stillwater, Oklahoma

Title of Study: EXPERIMENTAL INVESTIGATION OF UNBONDED MAGNETIC ABRASIVE POLISHING (UMAP) OF SILICON NITRIDE BALLS

Pages in Study: 141 Candidate for the Degree of Master of Science

Major Field: Mechanical Engineering

Scope and Method of Study: New polishing technique know as "Unbonded Magnetic Abrasive Polishing (UMAP)" was designed and built *in-house*, to investigate polishing of Si_3N_4 balls in an economical way. UMAP is based on the combination of underling principles of magnetic float polishing (MFP), magnetic abrasive finishing (MAF) and V-groove lapping. Balls to be finished were loaded between an acrylic polishing plate and a beveled top plate attachment to the spindle by spring action. This set up was placed in a non-magnetic chamber mounted horizontally on a lathe. The chamber was filled with a mixture of loose abrasive grit, iron powder, and non-magnetic viscous fluid (a mixture of glycerin, de-ionized water and rust inhibitor). Magnetic field gradient generated around the balls concentrates abrasive particles in the polishing region. Polishing action was achieved by the motion of the balls around the inner surface of the chamber. This action occurs due to relative movement of the polishing plate and the spindle rotating in opposite directions.

Findings and Conclusions: A bevel of ≤ 25˚ with the groove was essential for improving the sphericity. Also, the surface finish improves rapidly without the need for machining this groove. Material removal rate (MRR) upto 1.2 μm/min/ball with an average sphericity of 0.77 μm and a surface finish of 11.6 nm were obtained. The best ball measurements achieved were 0.5 μm sphericity and 10.4 nm surface finish.

ADVISER'S APPROVAL: Dr. Ranga Komanduri